UNIVERSIDAD NACIONAL AUTONOMA DE MEXICO

FACULTAD DE MEDICINA
DIVISION DE ESTUDIOS DE POSGRADO
DOCTORADO EN CIENCIAS MEDICAS
INSTITUTO NACIONAL DE CARDIOLOGIA
"IGNACIO CHAVEZ"

ESPECTROCARDIOGRAFIA DE ALTA FIDELIDAD PARA EL DIAGNOSTICO DE CARDIOPATIA ISQUEMICA: VALIDACION DE UNA NUEVA PRUEBA DIAGNOSTICA.

T E S I S

QUE PARA OBTENER EL GRADO DE:

DOCTOR EN CIENCIAS MEDICAS

P R E S E N T A:

MARTIN ROSAS PERALTA

ASESORES DE TESIS:

DR. SERGIO PONCE DE LEON (MEXICO)

DR. ALVAN R. FEINSTEIN (USA)

RESPONSABLE DEL PROGRAMA DE MAESTRIA Y DOCTORADO SEDE SUR: DR. ALFREDO ULLOA AGUIRRE

2000

AMOR SCIENTIA QVE DESERVIANT CORDI

MEXICO

INSTITVTO·N·DE CARDIOLOGIA IGNACIO·CHAVEZ

MIEMBROS DEL JURADO ACADEMICO

Presidente: **DR. JOSE ANTONIO GONZALEZ HERMOSILLO**
Instituto Nacional de Cardiología.

Secretario: **DRA. FLORENCIA VARGAS.**
Instituto Nacional de la Nutrición "Salvador Zubirán"

1er. Vocal: **ALFREDO DE MICHELI**
Instituto Nacional de Cardiología "Ignacio Chávez"

2do. Vocal: **DRA. MARIA GARZA**
Instituto de Investigaciones Matemáticas Aplicadas a Sistemas.

3er. Vocal: **DR. STEPHAN MIHALESCU**
Instituto de Investigaciones Biomédicas, UNAM.

Suplente: **DR. ABDO BISTENI**
Instituto Nacional de Cardiología "Ignacio Chávez"

Suplente: **DR. SERGIO PONCE DE LEON ROSALES**
Instituto Nacional de la Nutrición "Salvador Zubirán"

DEDICATORIA

AL DR. ALVAN R. FEINSTEIN

" Maestro distinguido, guía y amigo. Sus enseñanzas me dejaron una profunda huella intelectual que demarcaron mi ruta académica."

AL DR IGNACIO CHAVEZ RIVERA

"Maestro: La presente tesis es tan solo un intento por corresponder a su apoyo y amistad, gracias por haberme dado su voto de confianza, hay cumplo a usted con respeto y cariño"

AL DR FAUSE ATTIE

" Los jóvenes entusiastas requerimos de la estructura y dirección que solo la experiencia con visión puede otorgar. Jamas olvidaré sus consejos ayuda y amistad sin las cuales difícilmente hubiese obtenido este logro."

AL DR JORGE KURI

"Piedra angular para la obtención de este grado, sus enseñanzas y consejos me hicieron valorar mas el humanismo y la clínica."

A MI ESPOSA SARA Y A MIS HIJAS ROXANA, LILIANA Y MARIANA.

"Por su tiempo amor y comprensión"

A MIS PADRES Y AMIGOS.

LUIS ROSAS
LILIA PERALTA

"Gracias por haberme dado el ser y enseñarme el camino de la honestidad dedicación y trabajo"

A MIS PACIENTES

Por su fé, su confianza y apoyo.

"El latido cardíaco es acompañado del desarrollo y propagación de corrientes iónicas a través del cuerpo que resultan en el establecimiento de potenciales eléctricos sobre la superficie corporal"

" Este flujo de corriente es consecuencia del movimiento iónico a través de de las membranas celulares de los miocitos y del subsecuente movimiento a través del espacio extracelular de los diferentes tejidos del cuerpo"

Wilson FN, 1933

Index

I. INTRODUCTION

Ischemic cardiopathy is the main cause of death in the adult population over 40 years old in the countries with atheroesclerosis propensity. Symptomatic coronary artery disease is present in more than 6 million people in the United States, and recent estimated costs of cardiovascular disease were $135 billion dollars per year (1). In Mexico around to 400,000 infarcts are expected from this year and close to 2000 day/hospital beds will be needed, a figure that exceeds by far the total capacity of all coronary units in our country (2). It is also known that a sudden death occurs approximately every minute, in which the coronary artery disease is the most common underlying disorder. Therefore, an identification as fast as to be possible of the high risk patients to develop coronary arteriosclerosis is one of the most important actions, because of this fact will provide the means for giving an opportune management of these patients, which is a keystone for survival (3).

Although several alternative paraclinical methods to make a diagnoses of ischemic heart disease with a high degree of sensitivity and specificity are available today, a risk stratification to develop myocardial ischemia usually will require of sophisticated, and costly medical equipment (treadmill, ergometric bicycle, echocardiography, gammagraphy, etc.). Thus, there is no doubt that as a public health problem, the coronary artery disease represents for our country a challenge, which needs a multi-disciplinary approach (4). Thus, any clinical or basic research aimed at contributing for detection, treatment and/or prevention of ischemic heart disease is justified by itself.

Despite the usefulness of the exercise ECG testing (conventional exercise testing) as a screening method, its use is limited. False negative responses are not rare in patients with a clinical suspect of coronary artery disease. In addition ECG-exercise has several limitations, such as: (i) High specificity but moderate sensitivity (95% and 75%, respectively), (ii) the patient must have no physical

incapacity to perform the test, (iii) absence of advanced disorders in rhythm and/or electrical conduction, and (iv); in the women, for reasons that are not clearly established yet, this method offers a lower sensitivity and specificity. Therefore its use in this last group is still controversial (5-6). One of the principal reasons for identifying an ischemic process in the myocardium by ECG-exercise test is the wide spectrum of changes on waves, segments and intervals of the ECG. The most common changes tat are considered as normal and abnormal are showed in appendix A. By consensus, a depression of the ST-segment with at least 80 ms of duration in a horizontal or downsloping form is classically considered of high probability for having an ischemic process.

Notably, most of the pathological process registered by the conventional surface ECG (12-leads) are detected using a top-filter of 100 Hz, this mean that all the information obtained from the ECG is limited to this maximum of frequency. Surprisingly, the use of filters becomes easier the interpretation of the ECG, it permitted the recognition of 'classical patterns' for identifying several underlying pathologies from heart. In other words, the filters did to the ECG one of the principal noninvasive methods to study the heart on the 1940-70's period. However, this restriction perhaps was also the beginning of the end. This restriction may mask important information from the electrical activity of heart.

The ECG-exercise needs a second type of filters in order to maintain 'stable' the recording on screen during the exercise. We believe that all these technical restrictions may be an obstacle to identify underlying heart disorders. In the Mexican school of electrocardiography this point has been proved.

These problems on ECG-exercise test, explain why the necessity of seeking other methods such as: stress echocardiography, nuclear medicine, and magnetic resonance to identify myocardial ischemia. However, the main limitation of these tests is their high cost (7-7a).

On the other hand, it is important to mention that the detection of myocardial ischemia is not only important during the pre-infarct period but also after the infarct because it permits stratify risk and prognostic implications, all of this has been well demonstrated (8-10). Therefore, the ideal screening method for ischemic cardiopathy would be one in which the degree of sensitivity and specificity were elevated, but also one that could be practiced not only at the high specialties' hospitals and of course, all at the lowest cost.

The conventional methods have related the myocardial ischemia with changes in the repolarization process of the cardiac cycle. Recently, the high resolution electrocardiography has been suggested as an alternative method for identifying pathological process of heart. However, all the current methods have been based only in the time domain analysis. The changes in the frequency domain (for example, spectral density of QRS complex) and its utility as a scrutiny method for detection of myocardial ischemia is unknown. Its theoretical advantages would be factibility, lower cost, and higher sensitivity and specificity.

HIGH FIDELITY ELECTROCARDIOGRAPHY.

High fidelity electrocardiography was a method that became popular at the 50's decade. The fundamental of this method was based on the elimination of all the filters on the electrical signal. Thus, the ECG recordings were obtained from the body surface to allow the recording of all the possible "slurs" or abnormalities inscribed into the QRS complex, which had been masked by the conventional filters (11).

Since most of the electrical heart diseases can be observed below 100 Hz, most of the filters used in the current commercially available equipment have been restricted to this frequency. As mentioned, most of the commercial equipment used for the exercise ECG-test have been provided with a double

system of filters in its algorithm of analysis. One for the QRS complex itself and the other one to maintain the signal level in an stable position on the screen, which is moved constantly due to the exercise. These circumstances may reduce the detection of fine disturbances within the QRS complex and, even worse, within the ST segment.

The new computational techniques have allowed better analyses of the electrical signals produced by the heart. Nowadays, it is common to keep the electrical signals for long periods of time, processing the signal from long distances (telemetry) or even defragment the QRS complex for identifying high frequency and low amplitude signals (termed "Late Potentials", LP) (12-13).

Recently, the frequency-domain analysis (Spectroanalysis) has gained much more interest, because it can provide a new possibility to analyze the quantitative as well as the qualitative features of the electrical signal. In addition it has been one of the aims into the research of the arrhythmogenic substrates ("late potentials") (14-15). The impacts of spectral temporal-mapping to determine changes due to ischemia are unknown yet. The present paper was aimed to evaluate the possible utility of a novel approach of analysis of the QRS complex using several techniques of process (spectral mapping, FFT and autoregressive model), evaluating if it is possible to identify myocardial ischemia, above all in adult patients without a previous infarct (phase I), with doubtful results from the conventional exercise-ECG (treadmill) or non conclusive results. Initially, all patients with a normal surface ECG taken at rest position. The gold standard chosen to validate our method was the cardiac gammagraphy with pharmacological testing (Dipyridamole).

II. ANTECEDENTS

II.1 EXCITATORY PROCESS OF THE NORMAL HUMAN HEART

In order to elucidate the fundamental of our method, will be necessary the knowledge and review of the time course as will as the instantaneous distribution of excitatory process to the normal human heart.

Knowledge of the time course and instantaneous distribution of the excitatory process in the normal human heart would be of value for an understanding of *QRS* complex (16). Studies about this process, during a surgical intervention for heart pulmonary disease was restricted to the epicardial surface and mostly only to those parts that were easily accessible. Some insight could be obtained about intramural excitation by the introduction of one or more intramural electrodes during surgical intervention. However, the data obtained in this way were of curse limited.

Durrer D., et al (17) demonstrated that three endocardial areas were synchronously excited 0 to 5 msec after the start of the left ventricular cavity potential: (A) an area high on the anterior paraseptal wall just below the attachment of the mitral valve, extending at least 2 cm toward the apex into the region of the anterior papillary muscle; (B) a central area on the left surface of the intraventricular septum; (C) the posterior paraseptal area at about one third of distance from apex to base.

These activated areas increase rapidly in size during the next 5 to 10 msec, becoming confluent at l4 to 20 msec after the onset of excitation. At this time the activation front envelops a great part of the ventricular cavity except for a posterobasal area, a middle lateral area and an apical anterior area. This movement around the cavity is much more rapid than the spread toward the epicardium. As activation continues individual variation from a general pattern increase. A nearly completely closed front is present after 30 msec, except at the

posterobasal area. At this time, excitation has already reached the epicardial surface of those sites overlaying the areas of earliest endocardial excitation. Activation continues to move to the epicardial surface in the other areas according to more or less concentric isochronic line. The latest part to be made active is the posterobasal area; in some hearts it is the posterolateral area.

II.1.1. Excitatory process of the Right Ventricle.

Endocardial activation starts near the insertion of the anterior papillary muscle about 5 to 10 msec after the onset of the left ventricular cavity potential, or slightly later. Then rapid invasion of the septum and the adjoining free right ventricular wall occurs results in epicardial breakthrough in the area pretrabecularis after about 20 msec. The isochrones are not concentric, but rather, activation continues in a regular, more or less tangential way, reaching ultimately the pulmonary conus (at 60 to 70 msec) and the posterobasal area (at 60 to 70 msec).

The intraventricular septum: Activation starts on the left septal surface in the middle third part, somewhat anteriorly, and at the lower third part at the junction of septum and posterior wall. Thus, activation continues from left to right, and in apical-basal direction. A right-to-left contribution is present in a varying degree, in the anterior half of the middle third part, activity a the right septal surface always being later than earliest activity a the septal surface. The crista supraventricularis is activated late; in the two hearts on which detailed information about the septal half of the crista supraventricularis can be given, excitation proceeded from the left side to the right, merging after about 45 msec with a front reaching the crista through the free wall of the right ventricle. **Figure** 1 illustrates the overall pattern of ventricular excitation, as it was determinate in one heart, based at 870 intramural terminals. The figure of below shows the horizontal electrode planes into which the heart had been sectioned. This is an

isochronic representation in which each color corresponds to a unique 5-msec interval.

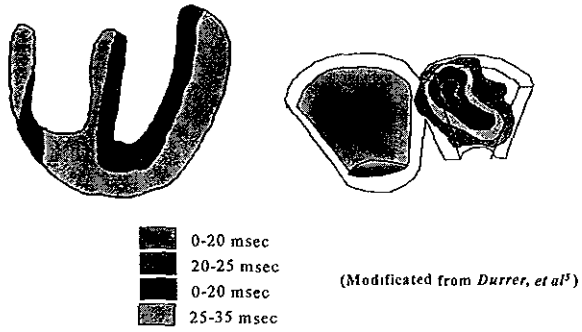

Fig. 1 **Pattern of Ventricular Excitation**

II.1.2. Epicardial excitation.

The epicardial excitation pattern reflects the movements of the intramural excitation wave. Early epicardial breakthrough occurred in the area pretrabecularis of the right ventricle in the 20 to 25 msec interval. From the area an approximately radial spread toward apex and base occurred, with latest excitation of the A-V sulks region and pulmonary conus. The latest part to be made active was the posterobasal area of the right ventricle. Three early points of epicardial breakthrough were found: (I) a small area on the anterior surface paraseptally close to the A-V sulks; (II) an anterior paraseptal area located halfway between apex and base, and (III) a posterior paraseptal area, about halfway between the apex and base. In some hearts a small area of early breakthrough was found near the posterior apex. The location of the latest made areas active differed. Generally, the posterobasal left paraseptal region was the last activated part; in some hearts, however, a more lateral location was found.

Intramural Conduction Velocity: In one heart, conduction velocity was determined by driving the heart by a short train of stimuli delivered first at the subepicardial and then at the subendocardial terminal of total of 22 multi-electrode needles. The stimuli were slightly suprathreshold; the frequency of stimuli was slightly above the rate of the spontaneous sinus rhythm. In the case of the intraseptal needles, the stimulating terminals were situated just below the right and left septal endocardial surface. In addition, spike Purkinje were recorded at a distance about 2 cm and the time interval was 10 msec, indicating that conduction velocity may be of the order of 2 m/sec, which agrees well with findings in the dog's heart (18).

Evidently total excitation studies of isolated hearts have many pitfalls. The removal of the heart about half an hour after death and the perfusion methods may lead to great changes in excitation pattern. In control experiments in canine hearts, in which the procedure of removal of the human heart simulated as closely as possible, the in situ excitation of the heart was compared with excitation during perfusion. The general pattern of excitation did no change after isolation of the heart. However, total excitation in perfused heart was completed earlier than in the in situ heart. Also, conduction velocity, determined by stimulating the heart at subepicardial terminals both in situ and during perfusion, increased upon isolation. The explication of an increase in conduction velocity and reduction in the voltage of complexes in isolation human heart is unknown Has been suggested that the latest parts of the heart to be made active are so small as to contribute but little to the peripheral *QRS* complex. Indeed, even the longest *QRS* measured in limb leads is shorter that the duration of total depolarization as measured in vectocardiograms (19). Data concerning the epicardial activation pattern of the left ventricle are in less agreement. Early activation has been reported to occur at the anterolateral surface near the left atrial appendage, at any level paraseptally, at anterior and posterior paraseptal zones, at the posterior part of the apex, and at the left paraseptal zone. The last

activated areas of the left ventricle are said to be the posterobasal area, the lateral half of the anterior surface and lateral surface, and the upper portion of the left border (19-20).

Thus, the sites of early epicardial breakthrough correspond to early made endocardial regions active: the area pretrabecularis of the right ventricle, the left anterior basal and middle paraseptal regions, and the left midposterior paraseptal region. The small area made active early at the epicardium near the apex which was sometimes found does not appears to correspond particularly to an early activated endocardial region but probably results from early activity in the lower posterior wall. It should be stated here that our data from intramural sites close to the apex are scant.

The initial deflection in left precordial leads is influencing by (A) septal excitation in the upper part of the anterior wall of the left ventricle proceeding toward the exploring electrode, and (B) by excitation in the posterior wall which is moving in the opposite direction. Five to ten milliseconds later, excitation continues through the free wall of the right ventricle and moves from right to left in the mid-anterior part to the septum. Data available from canine heart studies agree that earliest activity on the right septal surface is always later the on the left side.

II.1.3. Atrial Activation.

The atrial activity spreads more o less according to concentric isochronic lines over the atrial surface. Has been suggested a higher conduction velocity along the crest of the interatrial band, that is, along Bachmann's bundle In addition, activity went on from one terminal to the other at the same velocity of about 1 m/sec on the crest of the interatrial band earlier than the zones next to it.

Madison S. et al. (20) informed in a chimpanzee model the potential distributions during ventricular activation using body surface maps. The general sequence of epicardial changes was similar to that of the dog. Initially positive

potentials covered most of the ventricles except for negative potentials on the lateral left ventricle (LV). On the body surface this produced an anterior maximum and posterior minimum. Subsequently there were rapid changes due to right ventricular breakthrough that was apparent on the epicardium of approximately 5 msec before a saddle distribution. During the latter half of ventricular activation the epicardial patterns became complex due to multiple isolated excitation waves, and theses' complexities were not reflected in the same patterns on the body surface. Changes on the epicardial diaphragmatic surface produced little change on the body surface in the area of maximum and minimum but produced major changes in the distant low-level potentials, especially over the right lower torso.

Five msecs: On the epicardium a maximum was present over the septum anteriorly and a minimum at the LV base. The body surface pattern reflected this with an anterior maximum over the one on the epicardium and with a minimum on the back.

Eleven msecs: Epicardial positive potentials extended over the apex of the LV and a second maximum developed on the diaphragmatic surface. The minimum remained stationary. On the body surface the positive potential area expanded inferiorly while the minimum did not move.

Sixteen msecs: Negative potentials had developed on the anterior RV due the epicardial breakthrough that had occurred at 11 msec. The maximum on the LV increased in magnitude. On the body surface there was a saddle distribution with a minimum over the upper sternum where there had been positive potentials. The positive potential area had expanded inferiorly on the torso.

Twenty-eight msecs: Epicardial breakthrough on the diaphragmatic surface on the LV produced a minimum there, and the RV was enveloped in negative potentials. Positive potentials covered most of the LV on which there

was a single maximum. The body surface distribution was more simple. The minimum was over the lower sternum in front of the epicardial minimum, and the maximum was on the left precordium directly over the left ventricular epicardial maximum. Positive potentials formed a broad base around the lower torso.

Forty-four msecs: Two excitation waves produced isolated positive potential areas superimposed on a predominantly negative epicardial pattern. Scattered positive potentials due repolarization appeared. On the body surface the major change was development of negative potentials on the right lower torso with little change in the maximum and minimum.

Thereby, analysis of the potentials' distribution through body surface maps is a good method by evaluation of changes in the myocardial and allows to detection origin sites' arrhytmogenics.

II.2. Coronary Flow and its Influence on Electrogenesis: Role of Exercise Testing.

QRS complex recorded on *ECG* surface is an average vector that results from summarize all microvectors generated in the myocardial. By definition in the heart "cell that depolarize, cell that is living." Flow coronary reduction will reduce the energy supply that will originate high accumulation of calcium into the cell. Calcium elevated is a source of dysfunction diastolic and delay of front wave. Infralevel of *ST* segment is the first manifestation of lesion on conventional *ECG* that which indicate subendocardial suffering. In order to know better the sequence of ischemic injury and its impact into the electrogenesis we will need to review some topics of the coronary circulation.

II.2.1. Pathways of Ischemia.

As the malfunctioning of an industrial product can be due to the critical alteration of any of its basic components, so myocardial ischemia represents the final common pathway of the different morphologic and functional substrates. To have the coordinates to localize the pathways of ischemia, the normal heart can

be conveniently schematize in its three fundamental anatomic components, each one being a potential target of pathologic conditions leading to ischemia: epicardial coronary arteries, myocardium, and small coronary vessels.

II.2.1.1. Fixed Stenosis.

The human body incorporates a functional reserve which allows it to cope with the emergencies of physiology and the dangers of pathologic states. By exploiting its functional reserve, each organ can play - for a certain amount of time - much more demanding than its usual one, or -when a pathologic process develops- it can also maintain a normal function in resting conditions. The coronary reserve represents the capability of the coronary arteriolar bed to dilate in response to the increased cardiac metabolic demands. (21-22) It's is fully exhausted when maximal vasodilatation is reaching, corresponding to about four times the resting coronary blood flow in the normal subject. A fixed atheroesclerotic stenosis reduces the coronary reserve in a predictable way. In this curve four separated segments can be identified: (1) the hemodinamical silent zone, were stenoses ranging from 0% to 40 % do no affect the coronary flow reserve to any detectable extent; (b) the clinically silent zone, where stenoses ranging from 40% to 70% reduce the flow reserve without reaching the critical threshold required to provoke ischemia with usual stretches; the zone potentially capable of inducing ischemia, where stenoses exceeding the critical level of 70% elicit myocardial ischemia when exercise is applied, but not in resting conditions; (d) the zone provoking ischemia at rest, where tight stenoses (>90%) completely abolish the flow reserve and may critically reduce the coronary blood flow even in resting conditions.

II.2.1.2. Dynamic Stenosis.

From a theoretical viewpoint, dynamic stenoses may represent the consequence of three causes: the increase of tone at the level of an eccentric coronary plaque, complete vasoespasm due to local hyperactivity of the coronary smooth muscle

cells, and intravascular thrombosis. The first mechanism can significantly modulate the angina threshold in patients with chronic stable angina, the vasoespasm is responsible for variant angina, and all three mechanisms coexist in unstable angina, although their relative role in different patients and in different stages of the disease is difficult to establish. The biochemical mechanisms of coronary vasoconstriction still remain at least partially elusive; however, we know that coronary vasoconstriction can be superimposed on any degree of anatomic stenosis, and that functional and organic (fixed and dynamic) stenoses can be associated to a variable extent over time, transiently lowering the exercise tolerance in the individual patient. The organic stenoses determine the fixed ceiling of flow reserve which cannot be trespass without eliciting ischemia, whereas the dynamic stenoses can modulate the exercise capacity in the patient in a transient, reversible and unpredictable way

II.3. Mechanisms of Ischemia due to Organic Coronary Disease.

Tests exploring organic coronary stenosis can induce ischemia through two basic mechanisms: (a) an increase in oxygen demand, exceeding the fixed supply; (b) flow mistake, due to inappropriate coronary arteriolar vasodilatation triggered by a metabolic/pharmacological stimulus.

Both these mechanisms can provoke myocardial ischemia in the presence of a fixed reduction in coronary flow reserve due to organic factors (involving the epicardial coronary arteries and/or myocardium and/or microvasculature).

II.3.1. Increase in Demand.

This mechanism can be easily fitted into the familiar conceptual framework of ischemia as a supply-demand mismatch, deriving from an increase in oxygen requirements in the presence of a fixed reduction in coronary flow reserve. The different stresses can determine an increase in demand of different entity and through different mechanisms:

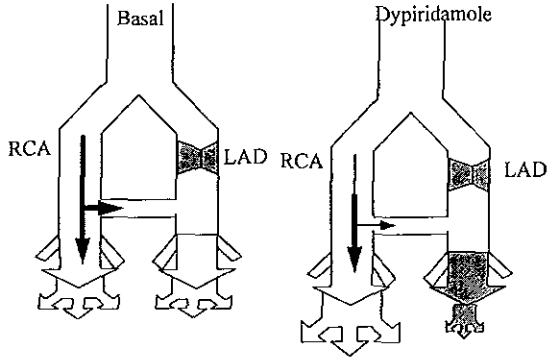

Fig Hydraulic model illustrating coronary horizontal steal The perfusion decrease by collaterals after stimulation with dipirydamol on normal circulation

In resting conditions, myocardial oxygen consumption is mainly dependent upon heart rate, inotropic state, and the parietal stress (which is proportional to the systolic blood pressure. Following dipyridamole or adenosine administration, a slight increase in myocardial function, a modest decrease in blood pressure, and mild tachycardia can be observed, overall determining only a trivial increase in myocardial oxygen demand.

During exercise, the increase in heart rate and to lesser extent, blood pressure and inotropic state account for the overall increase in myocardial oxygen consumption. Other stresses also increase, to a lesser extent, myocardial oxygen demand; during pacing, the increase is mainly due to the increased heart rate; with dobutamine, there is a marked increase in contractility and a relatively modest rise in heart rate.

II.3.2. Abnormal Distribution of Coronary Flow.

In the presence of coronary atheroesclerosis, and appropriate arteriolar dilatation can paradoxically exert detrimental effects on regional myocardial perfusion, determining an overperfusion of myocardial layers or regions already

well perfused in resting conditions at the expense of a region or layers with a precarious flow balance in resting conditions. In "vertical steal," the anatomic requisite is the presence of an epicardial coronary artery stenosis, and the *epicardium "stealing"* blood from the subendocardial layer. The mechanism underlying vertical steal is a fall in post-stenotic pressure secondary to the increase in flow across the stenosis. The flow increase is made possible by the existence of a depressuratization of *microcirculation induces a collapse* of subendocardial vessels, since extravascular resistance is higher in the subendocardium, thus causing an absolute reduction --compared to resting conditions-- of subendocardial flow.

The ***"horizontal steal"*** requires the presence of collateral circulation between two vascular beds; the victim of the steal is the myocardium fed by the more stenotic vessel. The arteriolar vasodilatadory reserve must be preserved -- at least partially-- in the donor vessel and abolished in the vessel receiving collateral flow. After vasodilatation, the flow in the collateral *circulation is* abolished in comparison to resting conditions, since the arteriolar bed of the donor vessel "competes" with the arteriolar bed of receiving vessel whose vasodilatadory reserve was already exhausted in resting conditions.

The stresses provoking that an abnormal distribution on flow act through a "reverse Robin Hood effect": thus, *unlike the British hero* who stole from the rich to give the poor, they steal from the poor (myocardial regions or layers dependent upon critically a stenosed coronary artery) and give to the rich (region or layers already well nourished in resting conditions). The biochemical effector of this hemodynamic mechanism is the inappropriate accumulation of adenosine, which is the main physiologic modulator of coronary arteriolar vasodilatation. Inappropriate adenosine accumulation can be triggered by a stimulus, which is either metabolic (such as exercise or pacing) or pharmacological (such as exogenous *adenosine or Dypiridamole*, which inhibits the cellular reuptake of endogenously produced adenosine). It is certainly difficult but this mechanism is

likely to play a key role in adenosine or Dypiridamole-induced ischemia and a relatively minor, although significant, role in exercise- or pacing-induced ischemia. Theoretically dobutamine agent might also induce flow misdistribution (of moderate entry?) by stimulating beta-adrenergic receptors which mediate coronary arteriolar vasodilatation.

II.3.3. The diagnostic "Gold Standard": Pure Gold?

Results of noninvasive diagnostic tests are usually compared to a "gold standard", which usually is the angiographically assessed coronary artery disease. This anatomic approach measures the sensitivity and specificity of the diagnostic test. *Although generally accepted, the gold standard has some limitations of both a theoretical and practical nature.*

First, the coronary stenosis is assessed by angiography, but the visually assessed percentage reduction oh the vessel lumen, which is commonly employed, can be considered a reliable index of severity only if two conditions are verified (in absence of a functionally important collateral circulation as well as of stenoses in series or a particularly long stenosis): (a) the vascular segment immediately proximal and distal to the stenotic segment is normal; (b) the lesion is concentric and symmetrical. Both assumptions are valid only in a very limited number of cases: the lumen reduction, and the most frequent-type of lesion is eccentric.

Second, coronary angiography is only a representation of the vessel lumen, an innocent bystander of atheroesclerotic disease, rather than of vessel wall, which is the real victim. Minimal, "nonsignificant" lesions at angiography can harbor a diffuse, severe atheroesclerotic process, which can be unmasked by epicardial or intracoronary ultrasound imaging. It is not surprising that the close correlation found in experimental animals between coronary stenosis and coronary flow reserve is replaced in the clinical setting by an *impressive scatter* of data which makes it virtually impossible to predict the physiologic meaning of a

stenosis provokes ischemia as a result of its hemodynamic consequences on the coronary reserve, but also a perfectly normal angiographic appearance of the coronary arteries and a markedly depressed flow reserve.

Thirdly. coronary angiography evaluates the anatomic component of myocardial ischemia, while stress tests can induce ischemia through mechanism which are totally different from the organic stenosis, such as dynamic vasoconstriction, and cannot be assessed by means of a purely morphologic, static evaluation of the coronary tree. Extracoronary factors, such as myocardial hypertrophy, can also reduce coronary flow reserve and therefore make the myocardium potentially vulnerable to ischemia during stress tests.

Finally, the visual and subjective assessment of the stenosis, which is the method commonly employed in clinical practice, is burdened by a marked intra- and interobserver variability, and arbitrary threshold criteria (such as the presence of a 50% stenosis in at least one major coronary vessel) are introduced to distinguish between "normal" and "sick" patients when, in fact, the severity of the atheroesclerotic disease ranges over a continuos spectrum.

II.3.3.1. Nuclear Medicine as a "Gold Standard"

We decided using as a "gold standard" to a Nuclear Medicine study (MIBI) because first of all, our principal endpoint by now is to determinate if it is possible to detect the presence of ischemia in the myocardium more than know if there are correlation between the level of interference coronary and spectral changes. In addition, is clearly known that may have myocardial ischemia without injury on the epicardial coronary arteries. However, since all patients whom the perfusion studies resulting abnormals are left to angiography coronary, this information will be registered by others aims, which will consist in trying to correlate the kind of changes in spectral turbulence with the zone of ischemia.

II.3.3.2. Maximum Oxygen Uptake.

When dynamic exercise begins, oxygen uptake by lungs quickly increases. After several minutes, oxygen uptake usually remains relatively stable (Steady state)at each intensity of exercise. During the steady state, heart rate (HR), cardiac output, blood pressure, and pulmonary ventilation are maintained at reasonably constants levels. Maximal oxygen consumption is the great amount of oxygen a person can use while performing dynamic exercise involving large components of total muscle mass and represents the amount of oxygen transported and used in cellular metabolism. It is convenient to express oxygen uptake in multiples of resting /sitting requirements. The metabolic equivalent is a unit of sitting/resting oxygen uptake (3.5 ml O_2 per Kg/min.) (ml Kg^{-1} min. $^{-1}$). Rather than determining each person's true resting oxygen uptake, one met is designated as this average, $V0_2max$ is significantly related to age, gender, exercise habits, heredity, and clinical cardiovascular status. Maximum values of VO2 max. occur among 15 and 30 years and decrease progressively with age.

II.4. Electrophysiological Basis of the High Fidelity Espectrocardiography

Interpretation of the conventional surface *ECG* usually relies on the recognition of grossly identifiable morphological alterations on the *QRS* complexes and T waves. Because these changes typically involve frequencies below 100 *Hz* the band width used in clinical electrocardiography is usually limited to 100 *Hz*. However, the higher frequency components are present in the *ECG* waveform, and notching within the *QRS* complex is caused by frequencies in both above and below 100 *Hz*. Hence in the past several years, the terms "high frequency", and "wideband electrocardiography" have been used by several investigators, (23-25) to refer to the process of *ECG*s recording with an extended band width of up to 1,000 *Hz*. The wide band *ECG* has been used to analyze the high frequency details in the *QRS* complex with the hope that

additional features seen in the *QRS* complex would provide information enhancing the diagnosis value of the *ECG*. Their analysis was based mainly on the temporal appearance of the notches and slurs in the conventional *QRS* complex, which correspond mainly to the frequency range of 40 to 150 *Hz* and the term "high-fidelity *ECG*" seems to be more accurate.

Although a different approach using averaging and filtering was used for selective recording of the high frequency *ECG*, the cathode ray oscillograph and the high speed camera were presented as a method for the more detailed study of electrocardiography patterns (26).

Monitorization with high frequency *ECG* in the coronary unit has been suggested by Sayers15. Goldberger et al (27), found that the root-mean-square (RMS.) voltages over the high frequency (80 to 300 *Hz*) were significantly greater in normal subjects than in patients with myocardial infarction, and that quantitative high frequency electrocardiography may be helpful in increasing the diagnostic accuracy of conventional *ECG*. Abboud S.(28-29), has analyzed of form extensive this insight, so, they found that ischemia can be detected with greater sensitivity by examining the high frequency QRS complex than by visual inspection of the standard ECG. This high frequency electrical activity is usually buried in random noise. Thus high again amplification, signal filtering, and averaging are necessary to improve the signal to noise ratio of the output signal. In addition they have suggested a computerized method of signal averaging for recording His' bundle activity and late potential using Fast Fourier Transform algorithm and a crosscorrelation function for averaging and filtering the ECG waveforms.

II.4.1. The Signal-Averaging Technique.

The ECG waveforms are stored on an FM recorder for later playback and analysis. During playback of the recorder high-fidelity low-pass anti-aliasing filter and the digitized by analogue -to-digital converter with a sample rate of 1,000 Hz.

The digitized waveforms are averaged together to reduce the relative contribution of uncorrelated noise. The ECG waveforms are averaged with the use of a cross-correlation function to reduce the relative contribution of noise. During the averaging process, accurate waveform alignment and elimination of artifacts are required. When a measurement of the similarity or of the relative time delay between two *ECG* waveforms is necessary, such correlation techniques are useful, permit rejection of synchronizing marks in the averaging process. That is, the point of maximum correlation for a waveform is taken as its fiducial point for averaging, and artifacts and abnormal complexes that cannot be correlated with the reference wave are eliminated. The fiducial points are then use to align the original waveforms for averaging. Before averaging, the candidate waveforms are first passed through a nonrecursive digital bandpass filter with a bandpass of 30 to 250 Hz as to maintain the high-frequency components in the *QRS* complex while reducing interference from the noise of equipment and low-frequency noise as the effects of a respiratory variation.

II.4.2. The filtering process.

Before the correlation procedure described previously, each of the ECG waveforms had been based through a nonrecursive digital bandpass filter using the fast Fourier transforms algorithm. The averaged waveform is the band-pass filtered with a low-frequency cutoff at 100 Hz and high-frequency cutoff at 250Hz

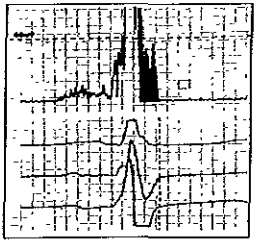

Fig. Amplification and filtration of QRS complex to X,Y,Z orthogonal leads.

The averaged, filtered high-frequency QRS complexes analysis to determine the boundaries or envelopes of the waveforms. The upper and lower boundaries of the envelopes were defined as the line segments connecting local maxim and minim, respectively. A local maximum, Ymax determination is locates at sample point ti if and only if the amplitude of high-frequency ECG, V (ti), at this point exceeded the amplitude of the three sample points preceding and following ti. A local minimum, Ymin is determining in similar fashion.

A reduced amplitude Zone (RAZ) within the envelope of the averaged high-frequency QRS is identifying if at least two local maxim of the upper envelope or two local minimal is present. So, RAZ is defining with the region lying between two neighboring maximal or minimal.

II.4.3. Effects of ischemia and Necrosis on the High Frequency QRS potentials.

Early studies have shown that an altered depolarization after myocardial infarction can be manifested as an increased number of notches and slurs within the QRS complex (30-31)[20-21] In contrast, spectral analysis revealed reduction of high-frequency energy in patients after myocardial infarction. Standard time-domain analysis is based on the idea of late ventricular potentials defined as high-frequency (usually above 25 Hz) low-amplitude potentials at the terminal 40 ms of the QRS complex. Late potentials are present in 21 to 44% of patients recovering from an acute myocardial infarction, and this finding is associated with a high risk of sustained ventricular tachycardia. However, since time-domain analysis is limited to the terminal QRS complex, late potentials may not be detected if the abnormal myocardial region is made active earlier during the QRS complex. (32) Furthermore, patients with bundle branch blocks are generally excluded from this analysis or modified criteria must be used.

II.4.3.1. Spectral analysis.

Spectral analysis was also used to search for unique frequency features that characterize late ventricular potentials and for the analysis of the entire cardiac cycle. However results of spectral analysis are difficult to reproduce since the basic requirement for the signal stationary is not fulfilled. More advanced techniques, such as spectrotemporal mapping and, in particular, turbulence analysis reduced some undesirable properties of spectral analysis. These dynamic techniques were found to be more sensitive than time-domain analysis for the detection of patients prone to the ventricular arrhythmia following myocardial infarction.

Novak, et al. (33) used time-frequency mapping based on the modified Winger distribution to study the QRS complex of patients with and without heart disease. Their findings verify abnormalities on QRS complex in patients with heart disease.

II.4.3.2. Concept of time-frequency Mapping.

The ventricular activity can be expressed in a two-dimensional plane where one axis is time and the second is frequency. The summed projection in the time axis is the QRS complex (more precisely, the square of the QRS complex), while the summed projection in the frequency axis is its spectrum. In other words, a square of the QRS complex at a chosen time instant is equal to the sum of all frequency components at the time. In Mathematical language:

$$\int P(t,f)df = |S(t)|^2$$

where **s(f)** denotes a spectrum of the signal s(t) and P(t,f) stands for a time-frequency distribution (t = time, f = frequency)

The duality between time and frequency is a basic concept of time-frequency mapping. The advantage of this approach is that it enables more detailed analysis of high-frequency components of the QRS complex than

standard Fourier methods. In addition, it eliminates the assumption of signal stationary.

Since only the time projection (e.g., the QRS complex) is know, the problem is to reconstruct the time-frequency plane from the QRS complex. In 1932, Wigner (34) described a function (Wigner distribution) that turned about to be a good candidate for reconstruction of the time-frequency plane from time *functions.*

However, undesirable properties of the basic definition of the basic definition of the Wigner distribution limited its applications to only simple monocomponent signals. If two or more frequencies are concurrently present in the signal, the Wigner distribution generates spurious peaks called cross terms. This spurious interference occurs between the signal frequencies. The relationship between the classical Fourier spectrum and Wigner distribution can be demonstrated on the time-frequency plane. When the frequency components do not change during the analyzing time interval, then the Fourier spectrum is equal to the sum of the frequency components along the frequency axis (over that time).

The source(s) of the high-frequency components detected on the body surface both in healthy and myocardial infarction patients remains to be clarified.

II.4.4. High-Frequency Electrocardiography in Dogs During a Coronary Artery Occlusion.

Similar to finding by *Abbout S. et al,* we in order to detect the changes on *QRS* by ischemic insult were studied Mongrel dogs. They were anesthetized with pentobarbital, artificially ventilated through a cuffed endotracheal tube, their *chest opened, pericardium* incised, and the left anterior descending artery exposed. A Balloon occluded was placed just distal to the first diagonal branch of the vessel and tested to determined the level of inflation required for complete occlusion. Ischemia was induced by a complete 5-minute occlusion. The chest

was closed and evacuee of air. The tree orthogonal derivations were recorded. (X, Y, Z) and its average. (Fig.3·).

The high-frequency QRS complex can be represented by multiplication of two sinusoidal waveforms . **(1)** a high-frequency component that simulated the rapid alterations and **(2)** a low-frequency component that represents the envelope of the high-frequency *QRS* complex . The *Fourier's transform* of a waveform separates the signal into a sum of sinusoids of two frequencies: FH+FL and FH-FL.. A broad-spectral peak is present at approximately 160 Hz. *Abbout et al.* studied the effects of angioplasty on high-frequency electrocardiogram, they informed that each patient, surface electrocardiographic leads I, **aVL** , and **V5** were continuously recorded during *PTCA* by means of a photographic multichanel oscillographic recorder. Bandpass filters of the *ECG* amplifiers were set at 0.01 to 100 Hz for leads I and **aVL**, but **V5** was recorded as a high-fidelity signal with bandpass filters among 0.01 to 500 Hz. Additionally, a unipolar intracoronary *ECG* from the dilated was obtained by positioning a standard *PTCA* guidewire and balloon catheter across the target stenosis and recording among 0.01 and 500 Hz. Before advanced of the guidewire and balloon catheter across the *LAD* (*Left Artery Descending*) stenosis, the three surface electrocardiographic leads were recorded continuously after the guidewiere and balloon catheter had been positioned across the stenosis and during subsequent balloon inflations and deflations. After completion of the dilation and withdrawal of both the guidewire and balloon catheter from *LAD*, another 10-minute recording of surface electrocardiographic leads was obtained.

The digitized data form surface lead **V5** were divided into three time segments: **(1)** the control period before advancement on the guidewire or balloon catheter across the target stenosis. **(2)** the last 30 seconds of initial balloon inflation and the 10-minute recording period at the conclusion of the procedure. Electrocardiopgraphic waveforms in each time segment were averaged together,

filtered among 150 and 250 Hz, and used to compute the root mean square *(RMS)* voltage of filtered *QRS* as well as its envelope. A computer algorithm was used to define the time of onset and termination of the *QRS complex* by searching between the *PR interval* and the *ST segment* for a signal with *RMS amplitude* greater than three times the *RMS* of a noise. The cross-correlation coefficient then returned to its control value within 20 beats after balloon deflation. During the control recording period high-frequency *RMS* voltage was 3.97 mcV and the envelope revealed a *reduced amplitude zone (RAZ)* after 30 seconds of balloon inflation associated with a reduction in the high frequency voltage (*RMS*, 2,26 mcV) and broadening of the *RAZ*. After balloon deflation and withdrawal of balloon catheter RMS increased *to 5,13 mcV and the RAZ X was less obvious*.

II.4.4.1. Exercise-Induced Ischemia.

The diagnostic usefulness of exercise electrocardiography is limited and false negative responses are frequent in patient with clinically suspected coronary disease. Conventional methods relate myocardial ischemia to changes in the repolarization process of the cardiac cycle. Preliminary studies from laboratories' Abbout, have suggested that the morphology of the high frequency QRS may provide useful information regarding the presence of myocardial ischemia during exercise testing. However, many patients relief still had *RAZ after PTCA* perhaps indicating nonrevascularized viable myocardium in the distribution of other no dilated diseased vessels or, alternatively, regions of prior infarction rather than ischemia.

II.5. Electrocardiographic Models of Myocardial Ischemic Injury.

The assessment of alterations in *ST* segment deflections obtained by electrocardiographic mapping of the epicardial or precordial surface remains a valuable experimental and clinical method of dynamically reflecting alterations in the metabolic status of ischemic myocardial cells. Consequently, considerable

interest has been focused a defining as specifically as possible the relationship between epicardial *ST* segment deflections and transmembranal potential (*TMP*) changes in the underlying region of ischemic cells.(35-36) Only in this way may *ST* segment deflections be realistically interpreted in terms of the cellular changes that they reflect. The predictors of previous models of myocardial ischemic injury, employing a solid angle analysis, have proven to be inconsistent with experimental observations regarding both the distribution of *TMP* changes within an ischemic region and the distribution of epicardial *ST* segment elevation (*ST*) overlying and ischemic region.

The origin of cardiac injury potentials, manifested as *ST* segment elevation, in the epicardial ECG, was initially formulated by Wilson et al.(37), Bayley(38), Sodi Pallares (39), de Micheli (40) and others (41-42). by the application of basic principles of field theory. Wilson proposed that solid angle theory could be used to predict the *ST* segment elevation at a given recording site from Knowledge of the geometrical configuration of a region ischemic injury. A solid angle analysis (see appendix C), is based on the assumption that *TMP* is uniformly altered throughout as ischemic region such that a difference in *TMP* exists only at the boundary has been represented as a polarized surface giving rise to injury potentials measured as *ST* segment elevation in the ECG, and we will therefore refer to models employing a solid angle analysis as "polarized surface" models. Polarized surface models predict that the *ST* segment elevation, observed at a given recording site is proportional to the solid angle subtended at that recording site by the polarize surface representing the boundary of ischemia. Holland and Brooks applied the principles developed by Wilson and Bailey to spherical heart model and in this way predicted the epicardial and precordial electrocardiographic alterations produced by ischemic regions of various geometrical configurations. Their theoretical findings provided the first thorough examination of a polarized surface model of ischemic injury and form the basis upon witch the validity of such a model may be assessed.

More recently, has been examined a polarized surface model by correlating the degree of *ST* segment elevation recorded at precise epicardial locations overlying a region of ischemic with solid angle measurements obtained from the ischemic region. The results led Richarson to conclude that the polarization giving rise to epicardial *ST* segment elevation is distributed over an ischemic border zone rather than a sharply defined polarized surface between ischemic and normal regions of myocardium, as had been initially proposed. Smith et al., demonstrated in a model in which polarization is distributed over the entire ischemic regions provides the most accurate model linking cellular alterations in *TMP* to the distribution of epicardial *ST* segment elevation. Such model was refereed as "polarized volume"(43).

II.5.1. Distribution of the epicardial *ST* segment elevation:

First, polarized surface models of ischemia predict that with transmural ischemia the highest *ST* segment elevation is expected to occur near the boundary of ischemia, while a progressive decrease in *ST* segment elevation is expected to occur approaching the center of the ischemic region (increasingly distant from the boundary of ischemia). This characteristic is a "keystone" in the distribution of *ST* segment elevation overlying a region of ischemia predicted by models of either Holland and Brooks or Richarson such as is illustrated in its computer generated 3-dimensional plots.

Secondly, there is a discrepancy between theoretical predictions derived from polarized surface models and experimental observations with regard to the directional changes which occur in *ST* segment elevation after an increase or decrease in the size of an ischemic region. A polarized surface model predicts that as the size of a transmural ischemic region is reduced, epicardial *ST* segment elevation overlying the region is decreased. However, experimental observations have shown that when the size of an ischemic region was increased by 1) hypoxemia, 2) isoproterenol, glucagon, bretylium or ouabain or

3) tachycardia or hypotension, epicardial *ST* segment elevation overlying this region increased. Also, when the size of ischemic region was reduced by 1) intra-aortic balloon counterpulsation 2) mannitol, 3) glucocorticoids, 4) increased oxygen inhalation or 5) nitroglycerin, epicardial *ST* segment elevation correspondingly decreased.

II.5.2. Distribution of Transmembrane Potential:

A third limitation of polarized surface models as applied to ischemic injury is that experimental observations have not supported the fundamental assumption of such models that the changes in *TMP* are uniform throughout the ischemic region. Several investigators have utilized intracellular floating microelectrode recordings to examine the spatial changes in *TMP* within a region of *ischemia. Prinzmental et al* (36)., Ratti and Sanna and Mittra have observed that the changes in *TMP* are, in fact, nonuniform, with the smallest changes occurring near the boundary of ischemia, and progressively greater changes approaching the center of ischemia. Bailey and Spach and Barr (38) have previously commented on inability of a polarized surface model to account for this nonuniformity of *TMP* alterations within the ischemic region; however, no suitable alternative analysis has as yet been proposed.

The failure on theoretical polarized surface models of myocardial ischemic *injury* to be corroborated by a number of experimental findings suggests that our current understanding of electrical events responsible for *ST* segment elevation is inadequate. In the present protocol, a model is developed which accounts for nonuniform changes in *ST* segment changes within the ischemic region and which conforms more closely to experimental observations regarding *ST* segment elevation than polarized surface models.

II.6. Development of a novel approach for High-fidelity ECG model.

II.6.1. Phase I.

The model that we proposed has the capability of representing polarization which is distributed throughout a QRS complex and thereby affords a method of accurately describing the nonuniformity in QRS changes witch occur within a region of ischemia. (Fig. Below)

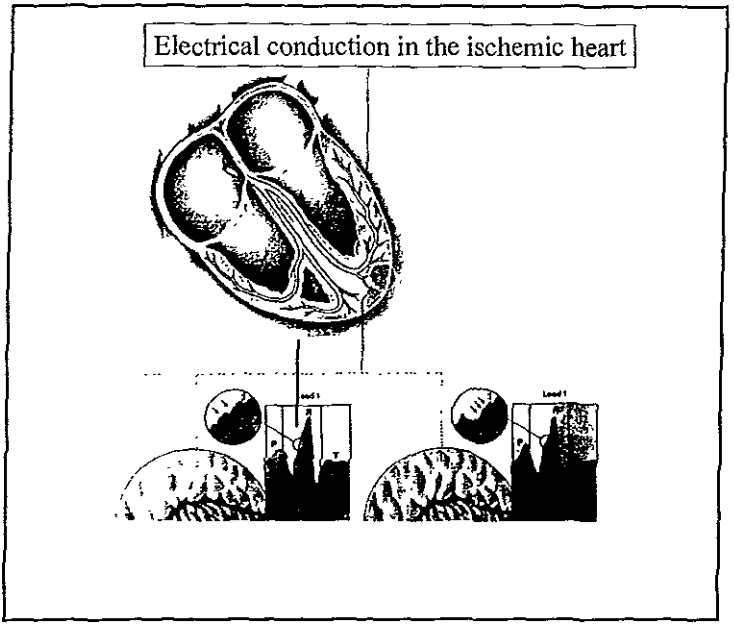

The development of our model began with a characterization of the polarization of any given QRS segment contained within the total ischemic zone. The correspondence rules were set forth by witch the '*ST*' segment changes at a given point on the epicardial surface may be defined in terms of the summated contribution of all such frequency-spectral zones. For simplicity a geometrical

model is employed similar to that introduced by Abbout et al., in which the ventricle is represented as a spectral-temporal mapping of QRS complex. A transmural Ischemia is defined as the reduction in both frequency and voltage of the *QRS* components. The size of the ischemic region is defined by angle (¢) which determines the angular extension of the ischemic boundary from the center (Isoelectric point)

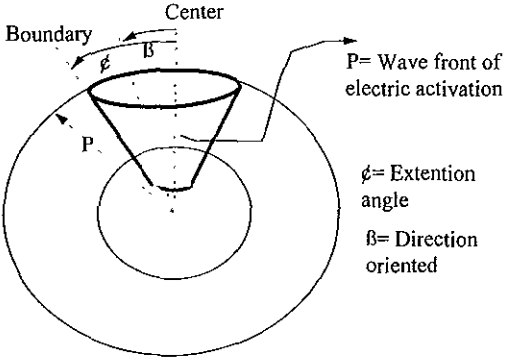

Fig. X Hipotetized model of ventricular activation, the sequentia, direction and orientation is despicted (P) = depolarization of endocardium to epicardium, and sametime of center to boundary .

This model includes the recording of three orthogonal derivation called "X,Y,Z", similar to vectocardiogram. Each derivation is analyzed in a separated form and also the averaged QRS complex. In order to reduce interpretation error by angle of analysis, the spectral mapping was divided into an arbitrary larger number of segments to analysis, so, each segment was correlated with its segment adjacent

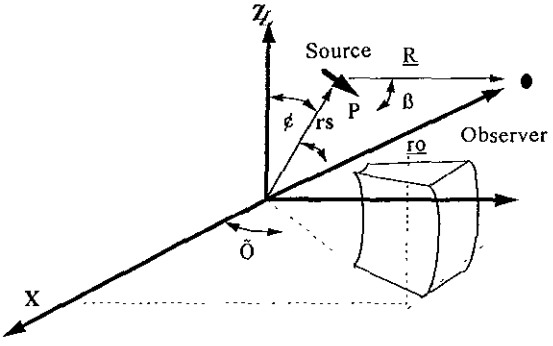

Hypotetized Model of perspective 3-dimensional of ventricular depolarization Its relationship between Source and Observer (electrode) during record of ECG.
P= Vector resultante, R= (r²source - r² observed - 2rs*ro cos &))/2 , &= angle between rs and ro , ß= angle between P and R , ƒ= is the conductivity of the extracellular space.

Limiting the region of interest. Once the QRS image had been established on the monitor, the starting mark was placed 25 msec before the start of the QRS complex (termed start mark or T1), and the ending mark was placed 100 msec after the end of the QRS complex (T2).

Spectrocardiographic calculations. In accordance with Kelen JG, calculation was performed independently for each orthogonal lead in the terminal region and in the whole QRS. The QRS complex was divided in 24-msec intervals between the T1 and T2 marks, each of these segments is separated from the next one by 2 msec, and the end of the last segment must coincide with the T2 mark.

Differentiation. Each 24-msec segment was differentiated according to the following formula

$$y(t) = ((x(t+1)) - (x(t-1)) + ((x(t+2)) - (x(t-2) - x(t-2)/8)$$

where **y(t)** is the new (differentiated) value of the signal at a given time; **X(t)** is the original amplitude of the signal from leads **X, Y, or Z** at a given time.

All calculations were made on the basis of the velocity and not the amplitude of the electrical wave front. Hence, each differentiation step is critical for the rest of the analysis. It should be noted that:

a) It is the clear drop (>30%) in the velocity of the wave front which is correlated to the possible presence of ischemia.

b)Differentiation allows to exchange frequency contents of the signal progressively following a precise mathematical path. Fourier analysis of relatively short segments provides sufficient frequency resolution to allow its use.

Mean Subtraction. The arithmetic mean of the differentiated signal segments was next calculated and subtracted from each (differentiated) data point to remove the effect of direct-current offset.

Window assignment. After differentiation and subtraction of the general mean from each 24-msec segment, these are each multiplied by a 4th-level Blackman-Harris window of equivalent duration. Window selection is based on the excellent concentration at its central lobe and low structure in the lateral lobe.

Fast Fourier transform. After window assignment, each 24-msec segment is placed on the beginning of the data arrangement at 64 points, zeros are used to fill from point 25 to 60, and then a fast Fourier transform is performed at a double precision to 64 points. The spectral power density of each frequency of harmonics is standardly calculated as the sum of the squares of the corresponding real and imaginary Fourier coefficients.

Normalization. After calculating separately the power of the spectral density for each segment of each of the orthogonal leads (X, Y, Z), the maximum spectral power density for any frequency at any lead is arbitrarily designated as

100% of power in decibels, and the rest of the frequencies are calculated in proportion to this maximal peak.

Graphic representation of the spectrum. The CEWS equipment's software generates automatically three dimensional plots for each lead, and due to the tridimensional nature of the spectral information multiple views can be obtained.

Numerical calculations. The power of the normalized spectral density for each segment in each orthogonal lead is recorded on a separate table, rows contain the spectral power density of the 24-msec segments, which varies with frequency. Columns contain the spectral power density at a given frequency which varies with time during the whole QRS complex. The corner stone of normality is that time transition is generally homogeneous from one segment to the

next. Calculations are based on the correlation of spectral power density among the different segments.

We chose four spectral turbulence parameters to identify the different variations in abnormality observed visually on the spectrocardiogram. In some subjects spectral turbulence is very intense but with a relatively short duration, whereas in others it might be not as intense but more prolonged. The four spectral turbulence parameters are: 1) Mean interslice correlation (MISC), that is, the average level at which one segment correlates with the preceding one. 2) Standard deviation of the interslice correlation (SDISC). 3) Low interslice correlation rate (LISCR) corresponding to the percentage of paired segments that correlated below 0.985; 4) Spectral entropy (SE), which is the mean discordance (1 - correlation coefficient) of each segment with respect to a mean imaginary segment, multiplied by 100. The average segment by which each actual segment is correlated corresponds to the arithmetic mean of the spectral power density for each frequency over the entire QRS complex. Our hypothesis was based on the

assumption that a crossed correlation index, measured through a determination coefficient (r) > 90%, must be kept when comparing the basal state vs. the pharmacological challenge.

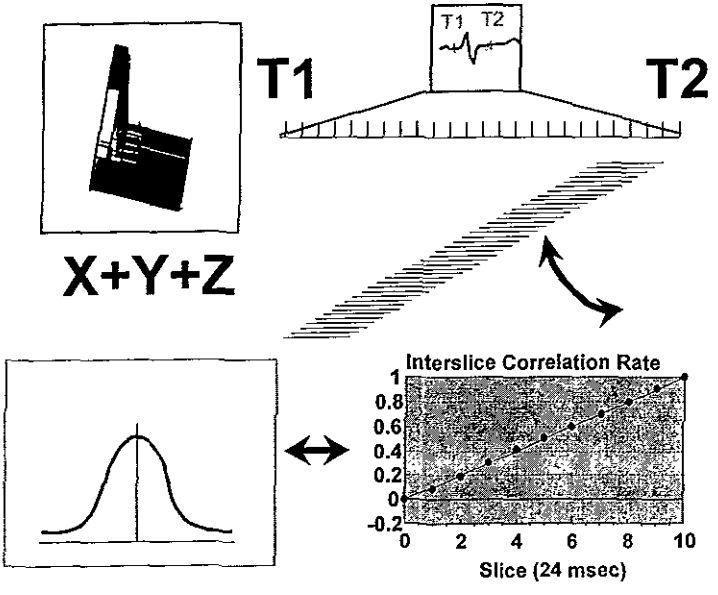

Fig. Graphic representation of the analysis form and construction of *a spectral* t mapping. X+Y+Z; tridimentional plot of vector magnitude according to spectral (slices

II.6.2. Phase II

After the analysis of the overall outcome we detected several limitation in this model. The principal limitation was the size of slice (24 msec) and the signal overposition because of the change step by step of each segment. Of course

when the zone of ischemia was large the manifestation was clearly identified. Another problem was the difficult to define what frequency band was involved.

The phase two of our system was done to develop a model in which the analysis of any selected band were possible. First the signal of each averaged ortogonal lead was recovered directly from the computer, then we developed a software to convert the original file into the ASCII code. An extraordinary characteristic of our algorithm was the opportunity to rescue from the averaged file each ortogonal lead. (appendix F)

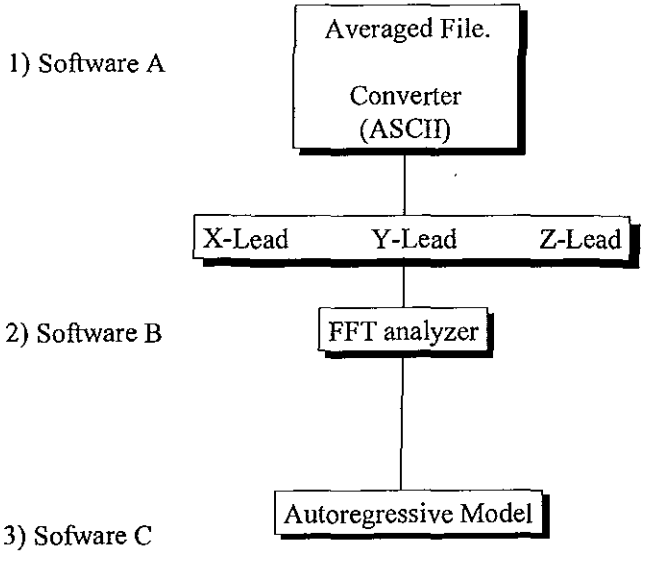

This software was made using Turbo C++ language package for PC.

Although for that time several authors had been proposed that the ischemic insult gave alterations principally into the width band of 120-250, we probed several intervals using as gold standard cases in which the evidence of ischemia was incontrovertible.

Thus we confirm that the best width band was 160-250 Hz. Each orthogonal lead in both time and frequency domain (FFT) were graphically presented and a correlation coefficient was available at screen.

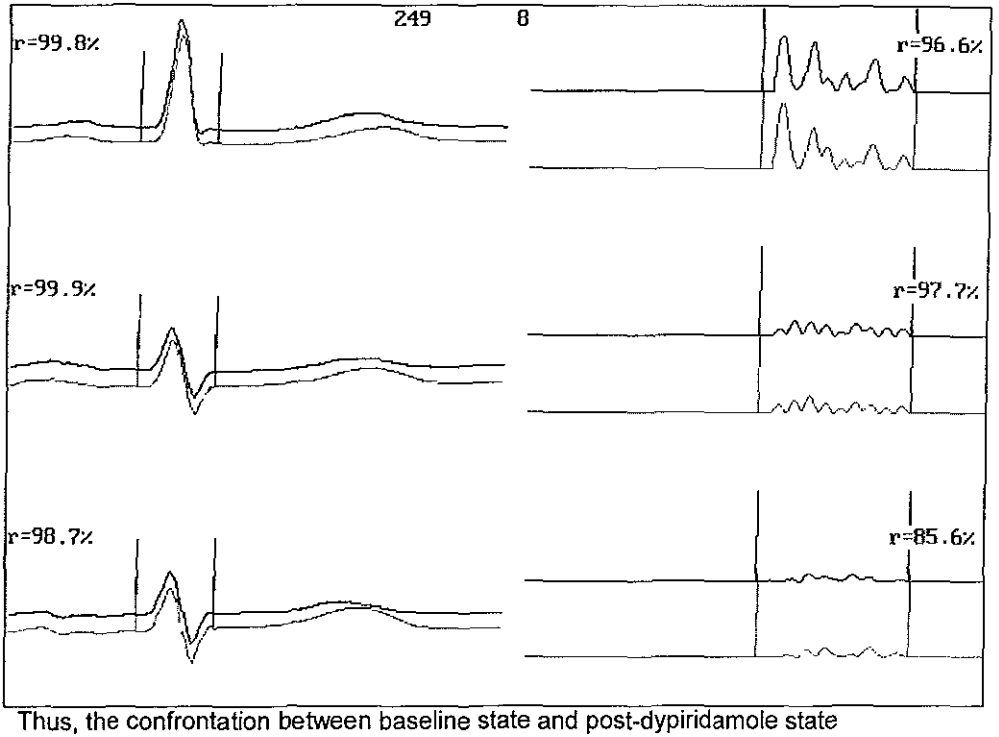

Thus, the confrontation between baseline state and post-dypiridamole state was possible and correlation coefficients were collected.

II.6.3. PHASE III

Applications of Fourier analysis were expected to improve the detection of abnormal activation patterns. However, the implicit assumption of the signal stationary is in contrast with real situations and this discrepancy could explain the controversial reports that use Fourier-based analysis. An elegant way to reduce the requirement on the signal stationary is to compute the successive spectra over shorter segments (spectrotemporal mapping) using Fast Fourier Transform (FFT) algorithm or autoregressive model. [Harbel R, Jilge G, Steinbeck G: Spectral Mapping of the electrocardiogram with Fourier transform or identification of patients with sustained ventricular tachycardia and coronary artery disease. Circulation 1990;82: 1183.] These techniques showed that high frequency components of the terminal QRS complex could be present in both patients with and without ventricular tachycardia. Dr. Novak (Ontario, Canada) did a strong criticism to our system. He said that our system not solve the main limitation of Fourier-based analysis (the assumption of the signal stationary). The FFT generates spurious peaks even for very short segments if the frequency content within this data segment changes. Furthermore, the resulting frequency resolution for such short segments is very low.

Therefore, we developed a system to overcome these limitations of FFT by means of more adequate signal processing method. It focuses on the time-frequency characteristics of ventricular activation in normal subjects and in myocardial ischemic patients. We use a novel signal processing approach, already successfully applied for the analysis of heart rate variability, AUTOREGRESSIVE MODEL. Our method was based on the distribution of frequency populations into the QRS complex using the Borg's method which can classify subgroups of PSD according with its frequency content. The main implications of our new system were: (1) High frequency components of the QRS complex can be reliably detected and traced in frequency by means of Power Spectral Density (msec2/Hz); (2) High frequency components are present

throughout normal ventricular activation; (3) these components are increased in patients after an ischemic insult and they are not limited to the terminal QRS complex; and (4) the results of time-frequency components are no influenced by QRS duration, and thus patients with conduction defects do not have to be a priori excluded.

Burg's Model.

Parametric power spectral estimators such as Burg, Yule-walker, and covariance are based on time series models. The real problem in parametric power spectral estimation is to find the time series model. Once the time series model is found, it is easy to find the power spectrum vía DFT. The model assumed for burg is termed autoregressive. The autoregressive model derives the current sample of a sequence from the weighted sum of previous sequence sample values and a zero mean noise term:

$$X[n] = a_1x\,[n-1]+a_2[n-2]+.....+a_px(n-p) + \varepsilon\,[n]$$

By convention the coefficients are actually the negative of the above, so that:

$$X[n]+a_1x[n-1]+a_2x[n-2]+.....+ a_px[n-p]= \varepsilon\,[n]$$

a_1 ..... a_p are termed the autoregression coefficients or parameters of the model, hence the word "parametric" in parametric power spectral estimation.

Burg's method is similar to the covariance method in that the error filter is kept on the data [Burg JS: Maximum Entropy Spectral Analysis, A New Analysis Technique for time Series Data, Modern Spectral Analysis, D.G. Childers, ed., IEEE Press, New York, 1978.] Additionally, Burg's method runs the data throughout the error filter in the forward and reverse directions which stated another way is minimizing the sum of the forward and reverse error powers. An algorithm for calculating the autoregressive coeficients by Burg's method is given by Andersen [Andersen N: On the calculation of Filter Coefficients for Maximum Entropy Spectral Analysis, Geophysics, 1974; 39: 69-72. Reprinted in Modern

Spectral Analysis, D.G. Childers, ed., IEEE Press, New York, 1978.] High frequency (above of 100 Hz) are lead dependent, but their spatial distribution on the body surface did not correlate with the site of ischemia, This is true only if not exist a way to determine the source of them. We hypothesized that if it is possible to create an inverse autoregressive model like anti-FFT we could know where the frequency signals are produced. This point will require further studies.

Sequence of analysis using Burg's Method.

Once the averaged signal was obtained, each file was converted to ASCII language by the method described in phase II. Then all ASCII values at each orthogonal lead were read and converted into TXT file to be analyzed. A new file for each orthogonal lead before and after Dypiridamole testing were obtained and pooled in specific directories of PC. Then, each file was read and processed in a computer program for time and frequency domain. The specific autoregressive analysis (Burg's Method) was done using the SACALC (signal analysis calculator) program developed by William T. Hardy. Three specific steps summarize our work.

First step: Template of both signals to be confonted. (see Fig. Below)

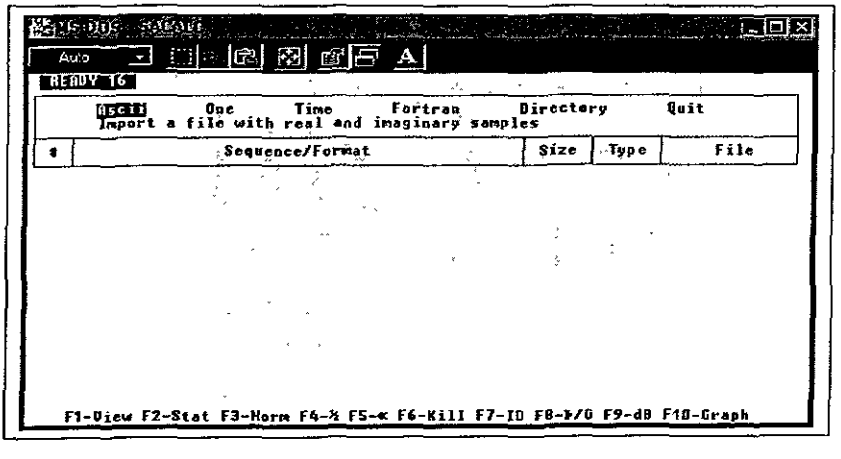

1)Each signal was read using a sample rate of 512 Hz, and a polynomial order of eleven.

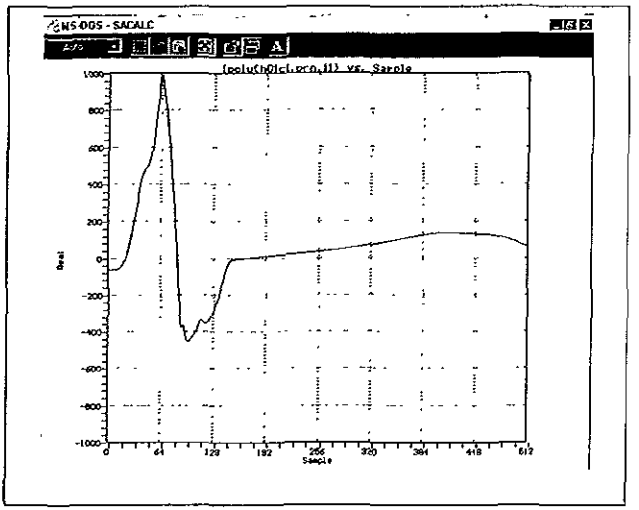

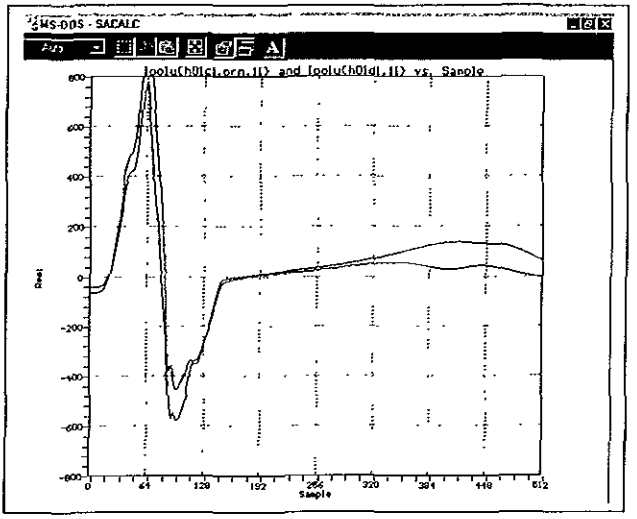

2). Selection of QRS complex: Sacalc program permits cut an specific interval for analysing.

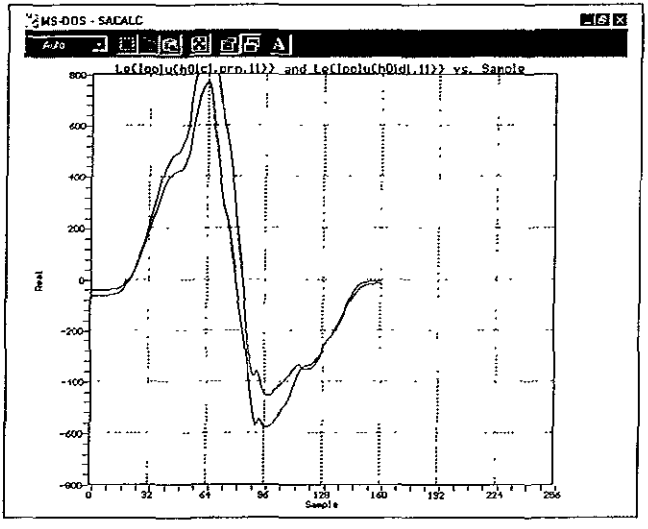

3. Filtering. Both signal were filtered using a High pass filter of .005 to eliminate DC effect.

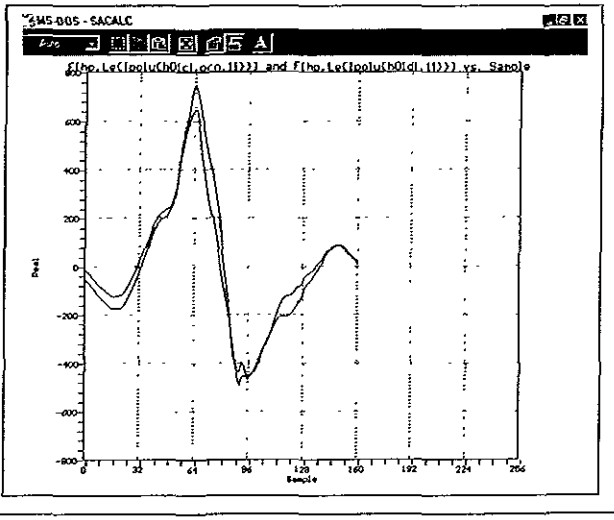

4. Borg's method. A parametric model analysis was applied using Borg's method. We selected a polynomial of 20th order because graphically demonstrated to be the best to evidence the changes provoked by ischemia. Then we selected the interval from 100 to 250 Hz. Both signals were graphically showed.

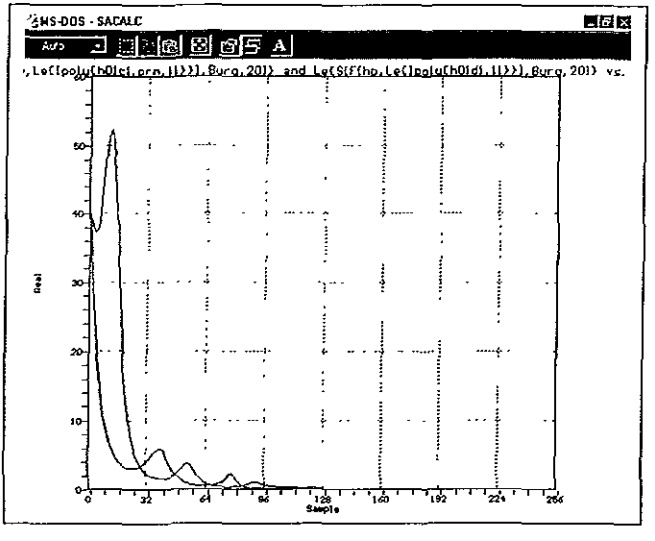

Thus, PSD between 100-250 hz was avialable, all values were pooled in a new file to be read in Excel program. All values were used to create a new data base to analyse into SPSS program.

5). Three-dimensional graphs were constructed from data obtained at each ortogonal lead, thus the changes ocassionated by ischemia were evident.

Case Positive

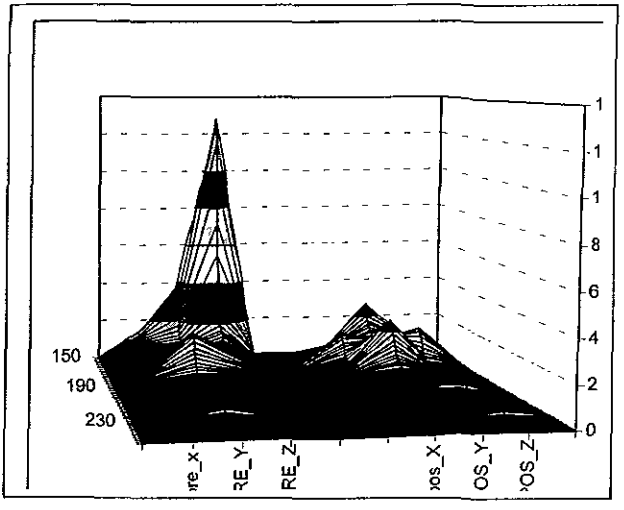

Case Negative

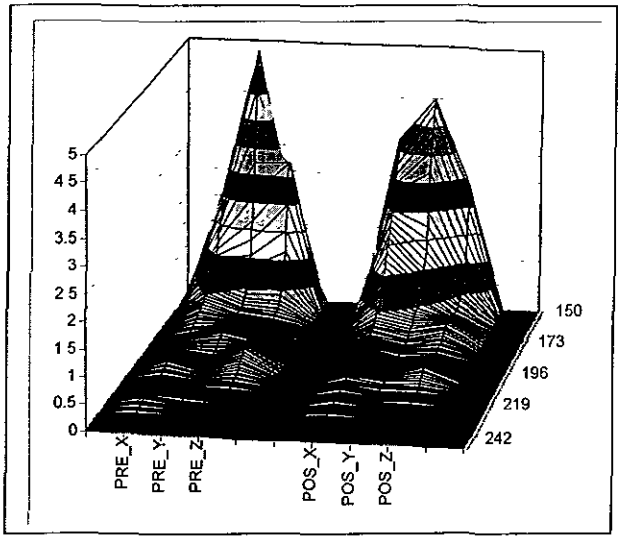

All power spectral density values were recorded at each msec, the sum of that values permitted calculating the areas for each interval of Hz. The total of PSD was calculated for each orthogonal lead and then, these totals were divided into three areas. One area from 100 to 120 Hz termed as very low frequency (VLF), next area from 120 to 150 Hz termed low frequency (LF), and the last one from 150 to 250 Hz, termed high frequency (HF). After the value of each spectral density was obtained, all values were converted to natural logarithm.

III. Justification

The foregoing information let us to establish a clear fundamental to make a study for analyzing the behavior of the electrical activity from the human heart using a noninvasive method. The impact of this model on clinical practice could be relevant as an alternative method to detect earlier myocardial ischemia with several advantages, which are cost-benefit related.

In addition, the use of this system will permit the possibility to explore the ECG recording to open a new way to understand the cardiac physiology, specifically the *contraction phenomena*. Until now, the documentation of high frequency disorders intra-QRS during an episode of ischemia has been very problematic and certainly, it is another justification to make this project. However, the most important justification would be the opportunity to have a new approach for earlier diagnoses of myocardial ischemia that could be applied at any medical room without sophisticated and expensive equipment.

IV. Objectives:

IV.1. Principal.

This study was designed in order 1) to assess the accuracy of a novel noninvasive frequency analysis method to QRS complex for identifying patients with myocardial ischemia during a pharmacological stress test. 2) to determine if the spectral temporal-mapping method on the QRS complex could be used for the location, extension and severity level to the myocardial ischemia. 3). To assess the role of FFT in identifying the frequency changes due to ischemia. 4) to assess the role of a parametric model (Burg's method) to identify the frequency sub-populations intra-QRS and to compare with those obtained after a pharmacological challange (dypiridamole).

IV.2. *Particular.*

To known the changes in frequency content on the signal-averaged QRS complex in both pre and post-application of dipyridamole (Pharmacological stress).

To determine the power spectral density in each orthogonal lead and its correlation with presence or absence of myocardial ischemia.

To develop a computer program in order to analyze in an automatic and accessible way the spectral-temporal mapping. Besides, to determine the sensitivity, specificity and predictive accuracy of the different parameters to analyze the spectrocardiogram in relation to presence of myocardial ischemia.

To determine if an autoregressive model is possible to be applied, if so, shows the changes in the frequency populations intra-QRS.

V. Hypothesis

1. The spectrocardiogram recording is an alternative method for detection of myocardial ischemia whose predictive accuracy is higher than stress-ECG conventional recording.

2. The spectral-temporal mapping allows detecting the extension and severity of an ischemic process.

3. During an episode of ischemia in human myocardium the electrical propagation wave change in the depolarization phase and it can be demonstrated by spectroanalysis.

VI. PATIENTS AND METHODS

The research protocol was approved by the Research and Ethics Committee of the National Heart Institute from México city. The study was performed in two groups of subjects. **Group 1** conformed by patients with a clinical history of precordial pain suggestive of angor and/or with risks factors for coronary disease, such as, smoking, hypercholesterolemia, hypertension, obesity, and familial history of ischemic cardiopathies, submitted recently to a stress test (2 weeks before) yielding doubtful results for the diagnosis of ischemic cardiopathy. **Group 2** comprised by healthy subjects without pathological antecedents in the cardiovascular sphere and a normal ECG-exercise test. In phase II were included patients with spectrum of ischemic cardiopathy.

Patients were collected from the outpatient ward from June 1996 to August 1998. A complete clinical history will be made for each subject, focused on risk factors for arteriosclerosis, past events related to coronary disease, characteristics of the pain, and previous medication. Physical examination was performed by a competent cardiologist. All patients were submitted to an ECG recording in resting position, an echocardiogram, a chest X-ray, and laboratory tests, which will include, complete blood tests, i.e., blood count and blood chemistry with lipid profile.

VI.1.1. Inclusion criteria.

1) Less than 70 years of age, 2) with or without previous infarct, 3) surface ECG in resting position showing normal characteristics (sinusal rhythm, no conduction disorders), 4) suspected ischemic cardiopathy or doubtful ECG-exercise test, 5) living in the metropolitan area of Mexico City, 5) written consent to participate in the study. 6) Without contraindications to make a nuclear medicine study. If phase I was completed the validation of our system would continue with

Phase II. During Phase II of this study we accepted patients with history of Myocardial ischemia or previous angor, recent Myocardial infarction underwent or not to thrombolysis to see if the myocardial ischemia can be anyway detected.

VI.1.2. Exclusion criteria.

1) Extreme obesity which did not allow to lay down the patient in the gammagraphy, 2) cancer or severe systemic disease, 3) hypertension with severe mismanage, 4) suspicion of any other associated cardiopathy, 5) allergy to dipyridamole or iodized materials.

VI.1.3. Elimination criteria.

Those patients that developed disorders in the rhythm, frequent extrasystoles or bundle branch block at the moment of performing the high fidelity ECG with pharmacological stress will be eliminate from the study.

VI.2. Data Collection.

Demographic data, risk factors, and history of ischemic cardiopathy, as well as its evolution, angiographic data, characteristics of the coronary lesions and of the high fidelity ECG will be stored in a computer on special predesigned formats to ease their analysis with the statistics software for social sciences (SPSS-X)*.

VI.3. High fidelity electrocardiogram.

VI.3.1. Orthogonal leads.

We performed a signal averaged surface ECG and another while challenging pharmacologically using the commercial computerized system from del Mar Avionics, Model 183-CEWS. The electrical signals were time-domain analyzed as

described previously by Simson et al. (44), the high sensitivity electrodes (silver chloride) were placed according to the bipolar and orthogonal configuration (X, Y, Z) at the level of V5 on the left and right medial clavicular line (X+, X-), respectively; in the left infraclavicular parasternal line (Y+) and its corresponding (Y-) on the same line at the level of the xyphoid appendix, and finally the last pair of electrodes will be placed in the area of the heart apex (Z+) and its corresponding (Z-) area on the posterior chest. At least 300 beats should be averaged simultaneously on all three leads to limit the noise to <5 uV. A vector magnitude V = (X + Y +Z) will be obtained after high-pass bi-directional filtering. This is the universally accepted system to study late potentials (45-46). Once the filtered QRS had been obtained, we analyzed its duration in each lead, its high frequency and low amplitude components, as well as the spectrotemporal mapping features described by Kellen et al. (47). Our analysis differed from the above technique in that we searched for the spectral turbulence occurring in the 130 to 260 Hz band. This bandwidth will be chosen based on previous studies made at our institute, in which the vectocardiographic traces accompanied by the surface traces in the thoracic circle suggested changes in these frequencies. These observations have been confirmed by other authors (48-50).

VI.3.2. Limiting the region of interest. Once the QRS image has been established on the monitor, the starting mark is placed 25 msec before the start of the QRS complex (termed start mark or T1), and the ending mark is placed 100 msec after the end of the QRS complex (T2).

VI.3.3. Spectrocardiographic calculations. Calculation was performed independently for each orthogonal lead in the terminal region and in the whole QRS. The QRS complex was divided in 24-msec intervals between the T1 and T2 marks, each of these segments was separated from the next one by 2 msec, and the end of the last segment must coincide with the T2 mark.

VI.3.4. Differentiation. Each 24-msec segment was differentiated according to the following formula

$$y(t) = ((x(t+1)) - (x(t-1)) + ((x(t+2)) - (x(t-2) - x(t-2)/8)$$

where **y(t)** is the new (differentiated) value of the signal at a given time; **X(t)** is the original amplitude of the signal from leads **X, Y, or Z** at a given time.

All calculations are made on the basis of the velocity and not the amplitude of the electrical wave front. Hence, each differentiation step is critical for the rest of the analysis. It should be noted that:

a) It is the clear drop (>30%) in the velocity of the wave front which is correlated to the possible presence of ischemia.

b)Differentiation allows to exchange frequency contents of the signal progressively following a precise mathematical path. Fourier analysis of relatively short segments provides sufficient frequency resolution to allow its use.

VI.3.5. Mean Subtraction. The arithmetic mean of the differentiated signal segments is next calculated and subtracted from each (differentiated) data point to remove the effect of direct-current offset.

VI.3.6. Window assignment. After differentiation and subtraction of the general mean from each 24-msec segment, these are each multiplied by a 4th-level Blackman-Harris window of equivalent duration. Window selection is based on the excellent concentration at its central lobe and low structure in the lateral lobe.

VI.3.7. Fast Fourier transform. After window assignment, each 24-msec segment is placed on the beginning of the data arrangement at 64 points, zeros are used to fill from point 25 to 60, and then a fast Fourier transform is performed at a double precision to 64 points. The spectral power density of each frequency

of harmonics is standardly calculated as the sum of the squares of the corresponding real and imaginary Fourier coefficients.

VI.3.8. Normalization. After calculating separately the power of the spectral density for each segment of each of the orthogonal leads (X, Y, Z), the maximum spectral power density for any frequency at any lead is arbitrarily designated as 100% of power in decibels, and the rest of the frequencies are calculated in proportion to this maximal peak.

VI.3.9. Graphic representation of the spectrum. The CEWS equipment's software generates automatically three dimensional plots for each lead, and due to the tridimensional nature of the spectral information multiple views can be obtained.

VI.3.10. Numerical calculations. The power of the normalized spectral density for each segment in each orthogonal lead is recorded on a separate table, rows contain the spectral power density of the 24-msec segments, which varies with frequency. Columns contain the spectral power density at a given frequency which varies with time during the whole QRS complex. The corner stone of normality is that time transition is generally homogeneous from one segment to the next. Calculations are based on the correlation of spectral power density among the different segments.

We chose four spectral turbulence parameters to identify the different variations in abnormality observed visually on the spectrocardiogram. In some subjects spectral turbulence is very intense but with a relatively short duration, whereas in others it might be not as intense but more prolonged. The four spectral turbulence parameters are: 1) Mean interslice correlation (MISC), that is, the average level at which one segment correlates with the preceding one. 2) Standard deviation of the interslice correlation (SDISC). 3) Low interslice correlation rate (LISCR) corresponding to the percentage of paired segments

that correlated below 0.985; 4) Spectral entropy (SE), which is the mean discordance (1 - correlation coefficient) of each segment with respect to a mean imaginary segment, multiplied by 100. The average segment by which each actual segment is correlated corresponds to the arithmetic mean of the spectral power density for each frequency over the entire QRS complex. Our hypothesis was based on the assumption that a crossed correlation index, measured through a determination coefficient (r) > 90%, must be kept when comparing the basal state vs. the pharmacological challenge.

The other two forms to analyze the high frequency ECG were described in the section 'developmnet of our system'.

VI.4. Coronary angiography. All patients with coronary ischemia evidenced by nuclear medicine studies will be submitted to a coronography within two weeks after ischemic cardiopathy had been diagnosed. We will be recorded the number and location of arteries with a greater than 75% obstruction, as well as the TIMI flow classification (51). All coronographies were assessed by two of the authors, whom will not know the results found in the high fidelity spectrocardiogram.

VI.5. Nuclear medicine Study. A Sesta-MIBI study was performed in all patients using the international criteria (rest and stress). Dypiridamol was selected as the challenge drug because of multiple evidence had demonstrated its high utility to provoke myocardial ischemia by the horizontal stole mechanism. The incidence of high-risk collateral effects are minimal and rapidly reverted by aminofilina.

VII. Design.

VII.1. The principal Axis of this study were:

VII.1.1. **Purpose**. The characteristics of this study permit to define it as a comparative study.

that correlated below 0.985; 4) Spectral entropy (SE), which is the mean discordance (1 - correlation coefficient) of each segment with respect to a mean imaginary segment, multiplied by 100. The average segment by which each actual segment is correlated corresponds to the arithmetic mean of the spectral power density for each frequency over the entire QRS complex. Our hypothesis was based on the assumption that a crossed correlation index, measured through a determination coefficient (r) > 90%, must be kept when comparing the basal state vs. the pharmacological challenge.

The other two forms to analyze the high frequency ECG were described in the section 'developmnet of our system'.

VI.4. Coronary angiography. All patients with coronary ischemia evidenced by nuclear medicine studies will be submitted to a coronography within two weeks after ischemic cardiopathy had been diagnosed. We will be recorded the number and location of arteries with a greater than 75% obstruction, as well as the TIMI flow classification (51). All coronographies were assessed by two of the authors, whom will not know the results found in the high fidelity spectrocardiogram.

VI.5. Nuclear medicine Study. A Sesta-MIBI study was performed in all patients using the international criteria (rest and stress). Dypiridamol was selected as the challenge drug because of multiple evidence had demonstrated its high utility to provoke myocardial ischemia by the horizontal stole mechanism. The incidence of high-risk collateral effects are minimal and rapidly reverted by aminofilina.

VII. Design.

VII.1. The principal Axis of this study were:

VII.1.1. **Purpose.** The characteristics of this study permit to define it as a comparative study.

VII.1.2. **Type of Agent**. Due to the principal endpoint is to validate a novel diagnostic marker test the central agent is a process. Despite the possible controversy secondary to the use of a maneuver (dypiridamole), we need keep in mind that we don't want to demonstrate the efficiency of dypiridamole to provoke myocardial ischemia. We want to compare our new tool for identifying myocardial ischemia compared with that tool that is considered as a "gold Standard" of noninvasive testing

VII.1.3. **Assignment of agent**. We decided what patients would be included for this study.

VII.1 4. **The temporal direction**. The temporal direction is defined as transversal.

VII.1.5. **Population of study.** The last axis of this study was defined by the type of population selected. This is an homodemic study.

VII.2. Sequence of study.

All patients included in this study will be evaluated at the same time (8.00 a.m.); after the high fidelity ECG had been recorded in the computer, a copy of the signal-averaged recording from each lead will be saved on diskettes. Immediately thereafter, the radiolabeled tracer (MIBI) will be administered for the basal recordings taken in the gammagraphy. Afterwards, to empty the gallbladder and bile ducts, the patients will take milk (0.5 l) and natural yogurt to reduce false negatives. The patient will be then returned to the high fidelity EKG recording room, here the patient received a doses of Dipyridamole (0.56 mg/kg body weight, administered iv. for 6 min.). During administration of the drug, the 12-leads surface EKG will be continuously monitored and recorded every 2 min Infusion will be suspended if either precordial pain suggestive of angina or clear electrocardiographic signs of subendocardic lesion appeared. Immediately after

the infusion, a second doses of MIBI (Isonitrile) will be administered and another high fidelity ECG will be taken. If precordial pain to persist or a progression to the ischemia is electrocardiographically evidenced one doses of aminophiline (200 mg, iv.) will be administered. It should be noted that this is the current standard protocol used in all nuclear medicine wards (7), so we took advantage of this protocol to make our recordings.

VIII. STATISTICS.

VIII.1. Sample size.

Estimating sample size was based on the binary groups. [Campbel Mj, Julious SA, Altman DG. BMJ 1995;311:1145-48.] Thus, although several contriversies have been discussed in relation to the importance of rigorous methods to assess equivalence studies the fundamental are essentially the same. Using notation found in Pocock [refer] we define 'p' to be the overall percentage of successes to be expected if the treatments are equivalent and use to define the range of equivalence for the difference in percentage success rates. Other notation is *unchanged. The required* size of each treatment group and the power can be calculated as follows.

The overall percentage of successes reported for detecting myocardial ischemia by Nuclear Medicine study (SESTA-MIBI-Dypiridamol) is ~ 95% in high selected population. The minimum expected to be considered equivalent by High fidelity espectrocardiogram *is 85%, (for conventional* exercise-ECG test has been informed in ~ 75%). Thus, 'p'= 90. The maximum variation around 'p' (delta) was estimated in ±15%. Using: $n = \frac{2p(100-p)x2(Zalfa+Zbeta)^2}{Delta^2}$;

Were alfa=.05 and beta=.2 , therefore n=33 patients by group.

the infusion, a second doses of MIBI (Isonitrile) will be administered and another high fidelity ECG will be taken. If precordial pain to persist or a progression to the ischemia is electrocardiographically evidenced one doses of aminophiline (200 mg, iv.) will be administered. It should be noted that this is the current standard protocol used in all nuclear medicine wards (7), so we took advantage of this protocol to make our recordings.

VIII. STATISTICS.

VIII.1. Sample size.

Estimating sample size was based on the binary groups. [Campbel Mj, Julious SA, Altman DG. BMJ 1995;311:1145-48.] Thus, although several contriversies have been discussed in relation to the importance of rigorous methods to assess equivalence studies the fundamental are essentially the same. Using notation found in Pocock [refer] we define 'p' to be the overall percentage of successes to be expected if the treatments are equivalent and use to define the range of equivalence for the difference in percentage success rates. *Other notation is* unchanged. The required size of each treatment group and the power can be calculated as follows.

The overall percentage of successes reported for detecting myocardial ischemia by Nuclear Medicine study (SESTA-MIBI-Dypiridamol) is ~ 95% in high selected population. The minimum expected to be considered equivalent by High fidelity espectrocardiogram is 85%, (for conventional exercise-ECG test has been informed in ~ 75%). Thus, 'p'= 90. The maximum variation around 'p' (delta) was estimated in ±15%. Using: $n = \frac{2p(100-p)x2(Zalfa+Zbeta)^2}{Delta^2}$;

Were alfa=.05 and beta=.2 , therefore n=33 patients by group.

VIII.2. Continuous variables.

Continuous variables were expressed as average ± SD, comparisons between independent *groups was made* using unpaired T-test or U-Mann/Whitney if the distribution of that variables were not Gaussian's. To explore the change in a same variable before and after the Dypiridamole challange, paried t-test was used. The high fidelity espectrocardiogram parameters, measured as continuous form were analyzed in a similar form, however, due to our principal aim was to campare the differences between those subjects with a *nuclear medicine positive* vs those patients with a negative NM study, a two-way ANOVA for repeated measures was used.

VIII.3. Categorical Variables.

Conventional X^2 of pearson or Fisher exact test were used to identify significant independent differences. The differences between 2 categorical variables with a commun factor was explored by McNemar Test.

Concordance *indexes* were obtained to evaluate the NM study vs the new tool of analysis.

VIII.4. End points.

The principal end point was to compare the usefulness of our system with that obtained by NM study in similar circumstances. However, other points such as pathophysiological mechanisms of ischemic injury in heart were also very important.

VIII.5. Dichotomization of continuous variables. After identifying continuos parameters highly related to an event of myocardial ischemia, they were

evaluated in a univariate form to estimating the probability of having ischemia using a logistic model, then a ROC plot was constructed and then, we selected the best cutoff point to discriminate groups.

VIII.6. Autoregressive model.

To identify frequency populations intra-QRS, before and after dypiridamole challenge we use an autoregressive model (Burg's model), then the área under curve was determined and this permitted to compare the differences in the frequency populations measured by Power Spectral Density (PSD expressed on ms^2/Hz). The whole area under curve was then divided in an arbitrary form as follow:

a) High Frequency : PSD localized beyond of 150 Hz.

b). Very Low Frequency (VLF): PSD localized between 100 and 120 Hz.

c). Low Frequency: 120 to 150 Hz.

We would construct ROC tables to find the best frequency band for the detection of ischemia, according to the Tugwell method (52). Differences in proportions will be calculate based on the value of Z. To avoid possible spurious associations we accepted an alpha error (error type I) of 0.05.

IX. Results

From the initial 72 subjects included in this study, 12 were excluded; 6 (8.3%) due to incomplete information on ECG recordings, and 6 due to technical problems in the nuclear medicine study. The remaining 60 patients were included in the analysis. There were 50 (83%) men and 10 (17%) women. The mean age at ECG recording was 54.8 ± 6.94 (range, 43 to 68 years). They were divided into two groups: Group 1 [n= 31] (patients with myocardial ischemia demonstrated in the nuclear medicine study); Group 2 [n=29] (non-ischemic group) patients without any evidence of cardiovascular disease.

All patients who met the inclusion criteria were studied without any major complication due to Dypiridamole's testing. It was tolerated and only in 6 cases (10%) was reported a moderate episode of headache, which disappeared into the first hour later. The clinical demographic and QRS characteristics are showed in Table 1. There were not differences between both groups on the total averaged QRS duration nor in each orthogonal lead. Four patients in group 1 had left bundle branch block, but they were not excluded because of the high frequency analysis was possible without any difficulty. The mean of RR interval confirmed that the heart rate was similar in both groups. However, and even the mentioned foregoing we did the analysis adjusting to this parameter.

[In order to make all the sequence of steps so that a new diagnostic test should undertaken. Our work was designed in according with the mentioned by Alvan R. Feinstein[7] *. Thus, Phase I basically consisted in the comparison of subjects with vs without high risk to development the endpoint, which in this case

[7] Feinstein AR Clinical Epidemiology. The Architecture of Clinical Research. Philadelphia. WB Saundres Co 1985.

is myocardial ischemia. Furthermore we presented that results to the scientific committee to obtain the permission to continue with phase II in which we included a wide spectrum of patients in order to verify the stability of our results

IX 1 Phase I

Following this point we present a brief sumary of that study and the results shown only this aspect. 25 patients were studied. Group A (healthy controls) consisted of 15 subjects, average age of 50 3 +-7.1 years; 13 men, 2 women. Group B (suspected ischemic cardiopathy, with doubtful stress test) consisted of 10 patients, average age of 54.3 +-9.8 years. Four of these patients had a history of diabetes and eight coursed with hypertension.According to our inclusion criteria, significant differences existed among the risk factors for ischemic cardiopathy (diabetes, hypertension, hyperlipidemia, and smoking).

High fidelity ECG. Comparison of the parameters obtained in the high fidelity ECG recorded from both groups in basal (resting) position showed no significant differences among them. However, under pharmacological challenge, in-group B patients the length of the entire QRS complex reached was not statistically significant difference when submitted to paired test analysis.

Dispersion of the changes in the different orthogonal axes avoided reaching significance when comparing QRS duration with the different X, Y, Z axes Although a tendency for a longer duration of QRS in the positive-patients for ischemia demonstrated in the nuclear medicine evaluations, this was not a good predictive parameter.

Qualitative analysis (comparison of spectrocardiograms). Variations in spectral turbulence occurred at around 200 Hz, this region showed the main changes. The comparison among different bandwidth intervals, the interval with the clearest sensitivity and specificity was between 130 and 260 Hz. Comparing the determination coefficients recorded before and after the pharmacological challenge with Dipyridamole in groups A and B yielded clear significant differences. ($p < 0.001$)

Assessing whether the location of myocardial ischemia was correlated with the anormalities of any specific orthogonal axis we did not found any correlation However, due to it was documented the principal endpoint (demostrating changes on the frequency content intra-QRS during an ischemic insult) the phase II was continued (wide spectrum of patients). Intentionally we included patients with history of infarction (recent and old) to demostrate that the interval of frequency

changes produced by ischemia is no influenced by other structural alterations (fibrosis). The kappa index was excellent (.87) between High frequency analysis of QRS using FFT (Fast Fourier *Transform) and* Nuclear Medicine. These findings revitalized our enthusiasm because we were the first group that demonstrated with a novel approach the suspected by other authors since 1950's. However, several pragmatic difficulties were identified and a new software was required. (see "development of our system" *in the section of methods*).]

HIGH FREQUENCY ELECTROCARDIOGRAPHY.

Because of the analysis of QRS complex in terms of *frequency domain* was analyzed by 3 different approaches, the results will be presented following the findings in each method.

IX.2. Phase II. (Patients from Phase I are included)

IX.2.1. High Frequency ECG

IX.2.1.1. Spectral-Temporal Mapping.

Using the *Simpson's method* we obtained the QRSd (magnitude vector or averaged QRS). It represents a squared summation of the three different *orthogonal* leads: $QRSd = \sqrt{X^2 + Y^2 + Z^2}$

Thus, an automated process identified the exactly duration of QRS, which was of 92.5 ± 5.5 in group 1 vs 93.6 ± 5.4 milliseconds *in group* 2 (*p*=NS). As mentioned the QRS duration was different in according with the orthogonal lead, but there was not any significant *difference between* groups.

IX.2.1.1.1. The root mean squared (RMS40) of high frequencies in the last 40 milliseconds, which is used as a marker of late potentials, was similar if the analysis was done using the row data. However if they were classified in accordance with the presence or absence of late potentials, the prevalence of LP's was more elevated in the group 1 (as expected).

IX.2.1.1.3. Power spectral density (PSD) using FFT was determined by each orthogonal lead. The baseline values between both groups of study were similar. (Table 2) Notably it was identified as the most specific parameter to differentiate the impact of an ischemic insult, this point will be detailed later.

IX.2.1.1.4. Mean Peaks per Slice (MPS). The maneuver occasioned changes in the mean peaks per slice. In the X lead, the mean of MPS changed from 26.5 ± .5 to 26.0 ± .5 after dypiridamole, which reached statistical significance, but it was not related with the group of study as it was demonstrated by two-way repeated measures ANOVA. (F .388, p= .536). Similar findings were found in Y and Z lead (Table 8, 8B, 8C).

IX.2.1.1.5. Low Slice Correlations Ratio (LSCR). There were clearly changes in X lead of this important ratio, which means that significant disturbances in the signal propagation have occurred. However, despite the changes were more important in Group 1 (mean difference of –3.3 ± 2.4), the stochastic difference was not reached. The same behavior was observed in Y and Z leads. (Table 9, 9B, 9C).

IX.2.1.1.6. Inter-slice Correlation Mean (ISCM). Dypiridamole's test modified in the same way to X (mean ± sd, before 94.5 ± .31, after 93.0 ± .16, Δ=-1.561 ± .33, p=.001); Y(mean ± sd, before 93.5 ± .31, after 93.0 ± .16, Δ=-.376 ± .12,

p=.003); and Z lead(mean ± sd, before 92.9 ± .31, after 93.6 ± .2, Δ=.61 ± .33, p=.001), which was statistically significant, however it was not related with the groups of analysis (tables 10, 10b, 10c).

IX.2.1.1.7. Inter-slice correlation standard deviation.(ISCSD) The changes in this parameters were clearly showed. In all cases the changes were to increase, it means that a dispersion of the signal process after dypiridamole testing occurred, however these changes were very heterogeneous. (Tables 11, 11b, 11c). The same was observed in the spectral entropy.

The foregoing data demonstrated that important changes occur on the electrical signal after a challenge as dypiridamole testing. However, excepting to the PSD, the obtained values were unable to differentiate ischemic vs no ischemic. The possible reasons for this finding were widely explained into the section of methods, and will be discussed later.

IX.2.2. FFT signal processing.

Using Turbo C++ Pascal language for PC we developed a system that is capable to convert the electrical signal of the QRS from time domain to frequency domain using the Fast Fourier Transform. A comparison of the high frequency components intra-QRS before and after dypiridamole challenge was possible into the two groups of study using a trend index (correlation coefficient, CC). Thus, the mean CC ± SD in group 1 were .33 ± .27; .33 ± .28, and .42 ± .23 for X, Y and Z lead respectively, while in group 2 were .66 ± .27; .66 ± .28, and .71 ± .23. Significant differences between group 1 and 2 were clearly established. (Table 17).

After of knowing this clear differences we used a ROC model to create a predictive estimation to have myocardial ischemia and we found:

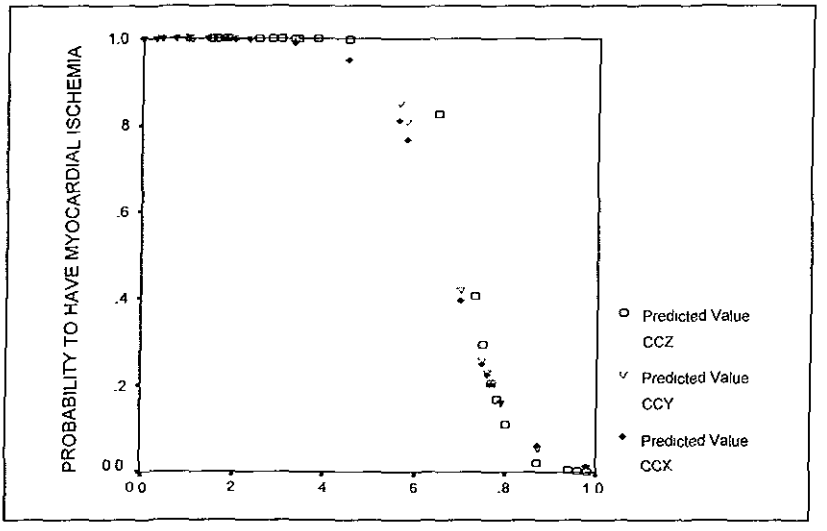

Because of the disturbances in the frequency content intra-QRS at each orthogonal lead are not independent variables a combination of the three parameters was not realized, however we can observe that the risk of ischemia was similar for the three leads.

This finding let us to define the cutoff point to separate subjects at high risk to have myocardial ischemia. The selected point was 0.75. Thus, patients with CC $\geq$ 0.75 at any orthogonal lead were catalogued as negative to have ischemia, and those with a CC < 0.75 as positive for ischemia. After this, we compare the results from FFT with that obtained by Nuclear Medicine. The sensitivity was .90, specificity of .83, PPV of .84 and NPV of .82 and the concordance index was .732 (kappa). The likelihood ratio was 36.2. (Table 18.)

IX.2.3. High Frequency QRS analysis: Autoregressive model.

For reasons explained from page 28 to 43, we developed a new approach of analysis using an autoregressive model (Burg's Method), which let us to know in a very exact manner how the frequency sub-populations intra-QRS are *distributed. Thus the whole area* under curve was possible of analyzing. There were not differences in the baseline values at any orthogonal lead, however after the dypiridamole challence inmediatly occured changes that clearly separates the group 1 from the group 2. All three orthogonal leads were very sensible to change. *All group 1 except 4 cases presented a* sudden drop of delta (mean of change) in the PSD after dypiridamole, by the contrary occurred in group 2. (Tables 13 to 13C). The next graphic shows this finding. The three model curves were estimated according with the obtained delta at each orthogonal lead.

Notably, delta = zero differenciated clearly the High an Low risk of having myocardial ischemia.

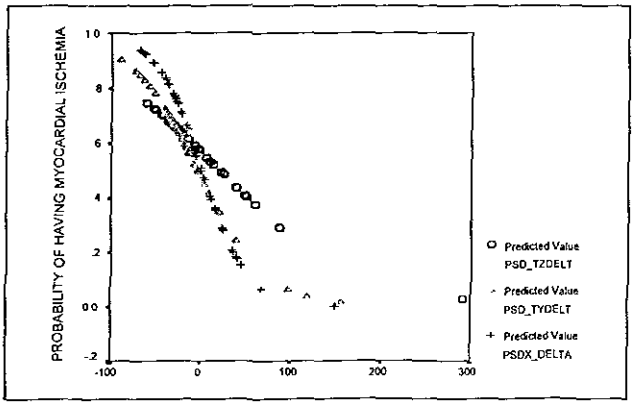

After this we classified in positive vs negative for myocardial ischemia using the zero value as cutoff point. Although the sensitivity was similar to FFT, the specificity was lesser, However, an extraordinary manifestation was that 4 of the 9 supposed false positive presented a major event of myocardial ischemia at six months of follow-up.

Finally we analyzed the behavior of the frequency subpopulations at each orthogonal lead. Thus we discovered, that the principal changes occurred at 100-150 Hz interval because of the ischemic group reduced this area and the contrary occurred in controls.

All values expressed in Ln, as will as the mean differences are showed in tables 14 to 16. Crosstabs between FFT, PSD and Nuclear medicine are showed in tables 17-19.

IX.2.4. Crosstabs.

X. Clinical implications.

Coronary artery disease (CAD) is one of the most common causes of death in the world. In Mexico, each year ~400,000 people are suffering an acute coronary syndrome. Although the mortality in-hospital has been importantly reduced in the last three decades (~8-15%); the mortality rate before arriving to hospital is so far to be resolved. Around 60% of patients with an acute myocardial infarction die while they are carried out to the hospital. Most of them as a consequence of an arrhythmic event.

Therefore, the main challenge to be approach should be aimed to the possibility to detect earlier this catastrophic disease.

After this we classified in positive vs negative for myocardial ischemia using the zero value as cutoff point. Although the sensitivity was similar to FFT, the specificity was lesser, However, an extraordinary manifestation was that 4 of the 9 supposed false positive presented a major event of myocardial ischemia at six months of follow-up.

Finally we analyzed the behavior of the frequency subpopulations at each orthogonal lead. Thus we discovered, that the principal changes occurred at 100-150 Hz interval because of the ischemic group reduced this area and the contrary occurred in controls.

All values expressed in Ln, as will as the mean differences are showed in tables 14 to 16. Crosstabs between FFT, PSD and Nuclear medicine are showed in tables 17-19.

IX.2.4. Crosstabs.

X. Clinical implications.

Coronary artery disease (CAD) is one of the most common causes of death in the world. In Mexico, each year ~400,000 people are suffering an acute coronary syndrome. Although the mortality in-hospital has been importantly reduced in the last three decades (~8-15%); the mortality rate before arriving to hospital is so far to be resolved. Around 60% of patients with an acute myocardial infarction die while they are carried out to the hospital Most of them as a consequence of an arrhythmic event.

Therefore, the main challenge to be approach should be aimed to the possibility to detect earlier this catastrophic disease.

Currently, multiple efforts are being performed in order to detect risk markers such as age, gender, lipid's profile, smoking, genetic factors, etc. However, even though all of this is important and means advances in fighting, the mortality rate has changed just a little bit. In addition, the increased survival of patients with coronary artery disease has enhanced this problem.

There is no doubt that as earlier a patient arrives to the hospital greater the probability to improve the survival. In addition the prognosis to long-term will be increased to.

The electrocardiography has been the most important method to approach and establish a diagnosis of ischemic cardiopathy. Its utility has been proved through many years, and it is not only because of detecting but also permits to evaluate the extension and severity of an ischemic injury in the myocardium. In addition it gives the great opportunity to monitorize on screen the rhytm. RR interval is a significant way to evaluate the sympathovagal balance which is a prognosis marker. The morphology of ECG waves is a guide for therapeutic approaches.

Previous observations have suggested the most of the underlying cardiac pathology is present in ECG. Unfortunately, the basic principles in which is based the ECG were underestimated as the time goes by. Due to the fantastic manner to discover abnormalities in heart using graphical patterns, finally the ECG was enclosed to that 'patterns'. Thus the ECG analysis was restricted to certain band-filters. Step by step, the physiological principles of ECG are being forgotten. Our central point to develop a new approach to analyze the ECG recording is based on that principles.

The Mexican Electrocardiography school has defended that ECG recording is not only a graphical representation of the electrical activity from heart, but also

is essentially the electro-mechano-metabolic state in and out of the myocites. It is a mirror of an electrical phenomenon occasioned by the molecular ionic movement throughout the cellular membrane[De Micheli et al: ¿Que debemos entender por isquemia, lesion y necrosis? Arch Inst Cardiol Mex 1994;64:205-221].

Transmembrane ionic fluxes are responsible for voltage differences between activated and resting tissues. The ionic fluxes reflected as the transmembrane action potential (TAP), the cellular counterpart of TAP are QRS complex, ST segment and T wave. The synchronization and velocity of the electrical wave propagation are crucial to the mechanical efficiency from heart as a blood bomb. Therefore all the vectorial changes in both velocity and magnitude should be present in ECG. If we were able to analyze in a different manner the ECG recording, probably we will discover many information that is masked with the conventional systems.

At any instant, the cardiac generator can be viewed as a dipole consisting of a positive and negative charge, separated by a small distance. Since the dipole generates a force that has magnitude, velocity and direction, it can be expressed as a vector.

The electrical surface with is boundary projected at a given point (P) results in a cone and defines the solid angle subtended by the area in question [see appendix E]. The segment of a sphere inscribed by a radius of unity drawn about point 'P', with P as a center of the sphere and its border delineated by the cone, is proportional to the area of electrical activity. Taking into account that the variables sucha as tissue resistance and geometry being constant, the voltage of 'P' can be expressed as $EP=\phi \times \Omega$, where ϕ is the voltage per unit of solid angle (Ω). In other words, the magnitude and direction of the movements in the

electrical field depends on both the electrochemical phenomena itself that is occurring at any time, and the perspective by which it is recording.

On another hand, the TAP is directly related with the ionic concentration in and out (gradient) of the cellular membrane. The electronegativity potential in cell is crucial, because of it is a determinant to the velocity of the initial ionic movement (Phase 0 of PAT). Thus, as more negative the potential in cell higher, faster and vertical will be inscribed the phase 0. Conversely, if the negative potential in cell is lesser, the PAT will be different. The phase 0 will be slower, oblicue, and the voltage will be also reduced. In other words the electrical propagation is slower.

Different causes have been detected to be responsible of this PAT modification. One of the most important and unfortunately common causes is the ischemic injury. However, any increase in demand or deficiency in support of oxygen and nutrients from the blood flux into the coronaries may cause this damage. A metabolic change, is the first step, initially the cell compensate by several mechanisms but sooner or later the anaerobic metabolism is necessary. However, this mechanism will be insufficient and then a cumulate of protons will transform to the medium in cell. The K+ efflux is obligated as an intent to maintain the equilibrium, but this will call a reaction of transient hyperpolarization. Rapidly, this state is changed to an unstable ionic movement, the cumulate of protons in cell stimulates other membrane-structures to promote the ionic movement. Thus calcium is changed by hydrogenous 2:1 and the over saturation in cell of calcium is obligated. Consequently, the normal electronegativity in cell is changed and the membrane polarization in resting is reduced (termed diastolic depolarization). The diastolic depolarization is the principal marker of 'lesion' in terms of Electrophysiology This depolarization makes to the contractility machinery inefficient, slower and unstable. An important point to be considered is as greater the diastolic depolarization greater also the injury in myocardium.

Thus the difference between lesion and necrosis in terms of pathology is directly related with the magnitude of the diastolic depolarization. We must emphasize that all mentioned changes can be described in terms of vectorial theory.

As the diastolic depolarization increases the resultant vector is lesser and slower. It means that the electrical wave propagation will be torpid, and the frequency of movement is reduced. It can be reflected in terms of frequency content of the electrical field.

In accordance with Dr. Abbud et al, the changes in frequency content in QRS complex permits to discover the changes on electrical propagation in myocardium. Our study support this and enhance the scientific principle in which is based the electrocardiography. We demonstrated that the 'diastolic depolarization changes the frequency content intra-QRS secondary to deficit of oxygen and nutrients by coronary artery disease. Interestingly, the magnitude of changes perhaps is related with the magnitude of diastolic depolarization (lesion). Further studies are necessary to corroborate this tremendous feature that we found. Our study supports the hypothesis that frequency domain analysis is better than time domain to detect myocardial damage secondary to ischemia. The wide spectrum of changes in myocites can be studied in a better and exact form. Part of the limitations occasioned by solid angle may be overcome by this novel approach of the ECG that we have termed 'High Fidelity Spectrocardiography'. We feel and believe that this is the reborn of an old basic principle that could have the similar o may be better impact on clinical practice that had the conventional ECG recording.

XI. Conclusions.

1. The high frequency electrocardiogram is able to detect changes in the frequency content of the QRS complex that otherwise is no detected by the conventional ECG of surface and it is a mirror the magnitude of the *diastolic* depolarization from myocardial cells.

2. The characteristics of the signal propagation in the human myocardium can be detected by spectral analysis. The magnitude of microvectorial changes *occasioned* by an acute damage in the myocardium of humans can be detected and quantified.

3. The hypothesis that an ischemic event can be detected since the depolarization phase in the QRS complex was sustained. The speculations did in the 1950's decade were confirmed.

4. The sensitivity and specificity and concordance of high frequency analysis measured by FFT and PSD were good and similar to that obtained by the Nuclear Medicine Study. However and perhaps, it might be better because of ECG-HF is a mirror of the metabolic and ionic movement throughout the membrane of cell and not only *its capability of the isotope capture.*

5 Spectral turbulence analysis in QRS complex using slice of 24 milliseconds was not able to define an ischemic event, however let us to discover that PSD is the best parameter to analyze.

6 High frequency ECG using FFT and PSD-autoregressive model are alternative techniques to detect myocardial ischemia.

7. The ischemic phenomenon is an event that can be studied between 100-250 Hz.

8. The orthogonal system was unable to define the location of a ischemic process, however as the PSD drop, the extension of myocardial ischemia increase.

9. The novel approach (High frequency analysis) to detect myocardial ischemia in humans has been validated.

XII.1. APPENDIX A

ELECTROCARDIOGRAPHIC FINDINGS DURING THE EXERCISE TEST.

NORMAL MORPHOLOGICAL RESPONSES

During exercise, the P-wave vector tends to become more vertical and the P-wave magnitude increases in the inferior leads. The interval PR shortens and slope downward in the inferior leads. The change, which has been attributed to the atrial repolarization (Ta wave), may cause false positive or indeterminate ST depression in the inferior leads. Changes in R-wave amplitude are noted near maximal effort with a decrease in the R wave in the lateral leads at maximal exercise and 1 min into recovery. In the lateral and vertical leads, the S wave becomes greater depth, showing a greater deflection at maximal exercise, and then gradually returning to resting values in recovery. The J junction is depressed in the lateral precordial leads at a maximum exercise. A dramatic increase in J-junctional depression may be observed in all leads and may be greatest at 1 min into recovery. Subjects with resting J-junction elevation may develop an isoelectric J junction with exercise as a normal finding. These changes revert in recovery. The normal ST segment vector response to both tachycardia and exercise is a shift rightward and upward in the frontal plane; however, there appears to be considerable biological variation in the degree of this shift. A gradual decrease in T-wave amplitude is observed in all leads during early exercise. At maximum exercise the T wave begins to increase, and at 1-min recovery the amplitude is equivalent to resting values in the lateral leads.

ABNORMAL MORPHOLOGICAL RESPONSES

The ST-segment level is measured relative to the PR segment, for with the increased HR during the exercise, the U-P segment is usually unclear, but a clear new manifestation of U wave should be considered as an early sign of ischemia (observation from Dr. De Micheli et al: Instituto Nacional de Cardiología). ST elevation is measured as the deviation from the baseline ST level. If the baseline ST segment is depressed, the deviation from that level to the level during exercise or recovery is measured. The point to the ST level is the J junction; point 60 or 80 ms beyond this are usually used when the ST-segment slope is horizontal or dowsloping. Considering a rapidly upsloping

ST depression to be abnormal increases test sensitivity but decreases specificity. Various ST scores have been recommended but not have been validated as superior to standard "visual" measurements. Exercise-induced myocardial ischemia can result in one of three ST-segment changes on the surface ECG: depression, elevation, and normalization.

ST-segment depression is the most common manifestation of exercise-induced myocardial ischemia. It usually reflects diffuse subendocardial ischemia, with vector direction determined largely by the area of ischemia and the position of heart in the thoracic cavity Classically it is explained by an increase in the wall stress. The standard criterion for this abnormal response is horizontal or downsloping ST segment depression of 0.1 millivolts (1 0 mm) or more for 80 ms in at least 3 consecutive isoelectric or level complexes. As shown in the next figure, however, other criteria have been considered.

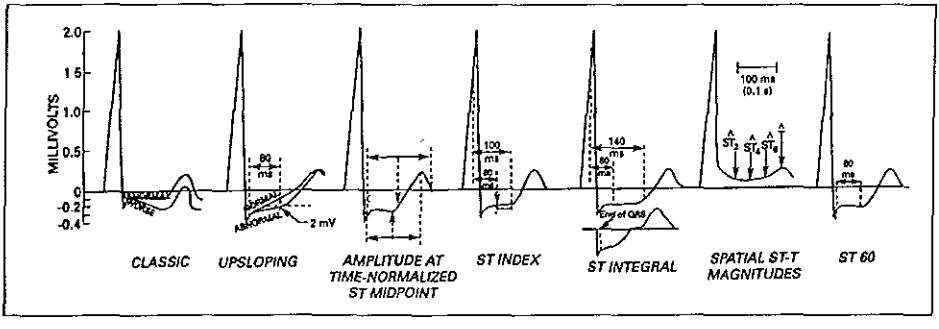

Downsloping (divergent) ST-segment depression usually reflects more ischemia than horizontal depression. In the presence of baseline abnormalities (especially in-patients on digitalis), exercise-induced ST-segment depression becomes more difficult for establishing myocardial ischemia. The lower the workload and the double product at which the ST change occurs, the worse the prognosis and the more likely the presence of multivessel CAD. ST elevation must be judged by whether or not it occurs in the presence of Q waves from a previous myocardial infarction. ST-segment elevation is more frequently observed in anterior leads (V1 and V2) with Q waves.

Previous myocardial infarction is the most frequent cause of ST-segment elevation during exercise and seems to be related to dyskinetic areas or ventricular aneurysms. Approximately 50% of patients with recent anterior and 15 % with previous inferior

myocardial infarction exhibit this finding during exercise. These changes may result in reciprocal ST depression simulating ischemia in other leads. The development of both ST-segment depression and elevation during the same test may indicate multivessel CAD.

In-patients without previous infarct a severe elevation of ST-segment frequently reflects severe transient ischemia resulting from significant proximal CAD or spasm.

XII.2. APPENDIX B

Complications Secondary to Exercise Tests.

Cardiac

Bradyarrhythmias

*** Sinus**

*** *Atrioventricular Junction***

*** Ventricular**

*** Atrioventricular block**

*** Asystole**

Sudden death (ventricular tachycardia/fibrillation)

Myocardial Infarction

Congestive heart failure

Hypotension and shock.

NONCARDIAC

Musculoskeletal trauma.

Miscellaneous

Severe fatigue, dizziness, fainting, general malaise, body aches, delayed *ill* feelings and fatigue sometimes persisting for days.

XII.3. Appendix C

General indications for Exercise Testing

Class I

Condition for which there is general agreement that exercises testing is justified to assist in the diagnosis of coronary artery disease (CAD) in male patients with symptoms that are atypical for myocardial ischemia.

To assess functional capacity and to aid in assessing the prognosis of patients with know CAD.

To evaluate the prognosis and functional capacity of patients with CAD soon after an uncomplicated myocardial infarction.

To evaluate patients after of revascularization chirurgic.

To evaluate patients with symptoms consistent with recurrent, exercise-induced cardiac arrhythmia.

To evaluate functional capacity of selected patients with congenital heart disease.

To evaluate patients with rate-responsive pacemakers.

XII.4. Appendix D

Absolute and Relative Contraindications to Exercise Testing

Absolute	*Relative*
Acute Myocardial Infarction	Less serious noncardiac disorder
Active Unstable Angina	Pulmonary Hypertension severe
Serious cardiac arrhythmias	Tachyarrhythmia or Bradyarrhythmias light
Endocarditis	Drug Effects or electrolytic abnormality.
Severe, dysfunction LV	Hyperthophic Cardiomyopathy
Embolism Pulmonary	
Serious Systemic Disease	
Severe physical handicap or disability.	

XII.5. APPENDIX E

SOLID ANGLE THEORY AND THE ELECTROCARDIOGRAM.[53]

The concept of the solid angle is not new, rather, it has been neglected. Nearly 300 yr. ago, Newton formulated the first expression incorporating the concept of the solid angle in his classic studies on gravitation (55).

The solid angle Ω is defined as the area of spherical surface cut off a unit sphere (inscribed about a point P) by the cone formed by drawing lines from P to every point at a boundary of interest:

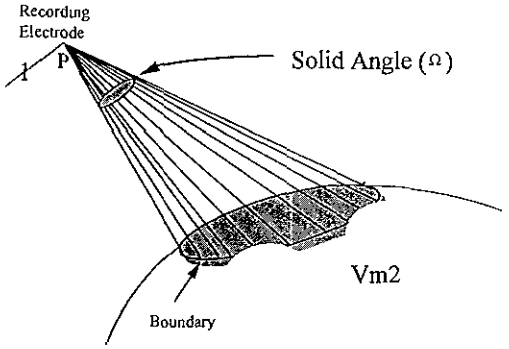

The boundary is a source of current flow established by portions of the heart having different transmembrane voltages (Vm1 and Vm2). The potential recorder at point P can be described by the following relationship:

$$\varepsilon = \frac{\kappa \Delta V m \Omega}{4 \pi}$$

where Ω is the solid angle constructed at point P by the limits of the boundary, ΔVm is the difference in transmembrane potential between the two regions, and K is a term correcting for differences in intracellular and extracellular conductivity and the occupancy of much of the heart muscle by interstitial tissue and space. The electrocardiographically recorded potential is then directly proportional to both ΔVm and Ω. The polarity of Ω is positive or negative depending on whether an observer at point P views first the positive or negative side of the surface enclosed by the boundary.

Although rather easy to visualize, actual computation of the solid angle is often only possible with computer assistance. Here the boundary defines a disc, with the point P directly overlying its center. Ω is then given by:

$$\Omega = 2\prod (1 - \cos\alpha) = 2\prod (1 - D / (R_2 + D_2)\frac{1}{2})$$

Where **R** is the radius of the disc, **D** is the distance from **P** to the disc, and α the polar angle. The examination of this equation and the curve is showing below:

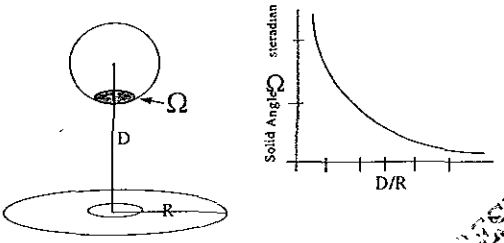

Fig. Computation of the solid angle

In the ischemia, the transmembrane voltages of the cells ischemics (Vmi) differ from those of the normal cells (Vmn):

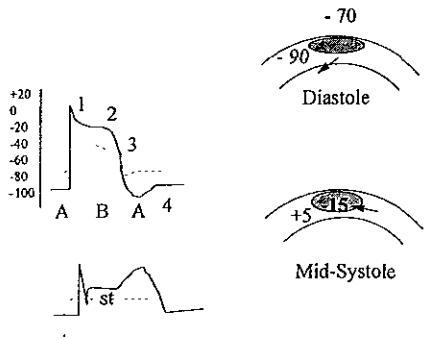

Fig. Genesis of ST and TQ segment

During diastole the ischemic cells have a lower (less negative) Vm than do normal cells. This potential difference establishes a boundary resulting in the flow of the electrical currents from the ischemic to the normal tissue. During the repolarization portion of systole (phases 2 and 3), Vm1 becomes negative earlier than Vmn, either because of incomplete depolarization and/or early repolarization due primarily to the shortening of phase 2.

In electrode leads overlying the ischemic area, diastolic current flow causes TQ segment depression and the midsystolic electron flow causes ST segment elevation. The so-called "ST segment elevation", then, is actually the summation of TQ depression and ST elevation. In addition, precordial and epicardial locations have its differences, so, the boundary of epicardium can be identified as those positions where the polarity of Ω quickly changes. Anothermore, the TQ-ST segment deflection is also a function of the difference in the transmembrane voltage (Δ Vm) that exists between the ischemic and

normal tissues during both systole and diastole. In this situation the equation can be adjusted:

$$\varepsilon T Q = \Omega (V m n - V m i) \frac{K}{4 \prod}.$$

where ETQ equals the magnitude of the TQ segment deflection.

XII.6. Appendix F

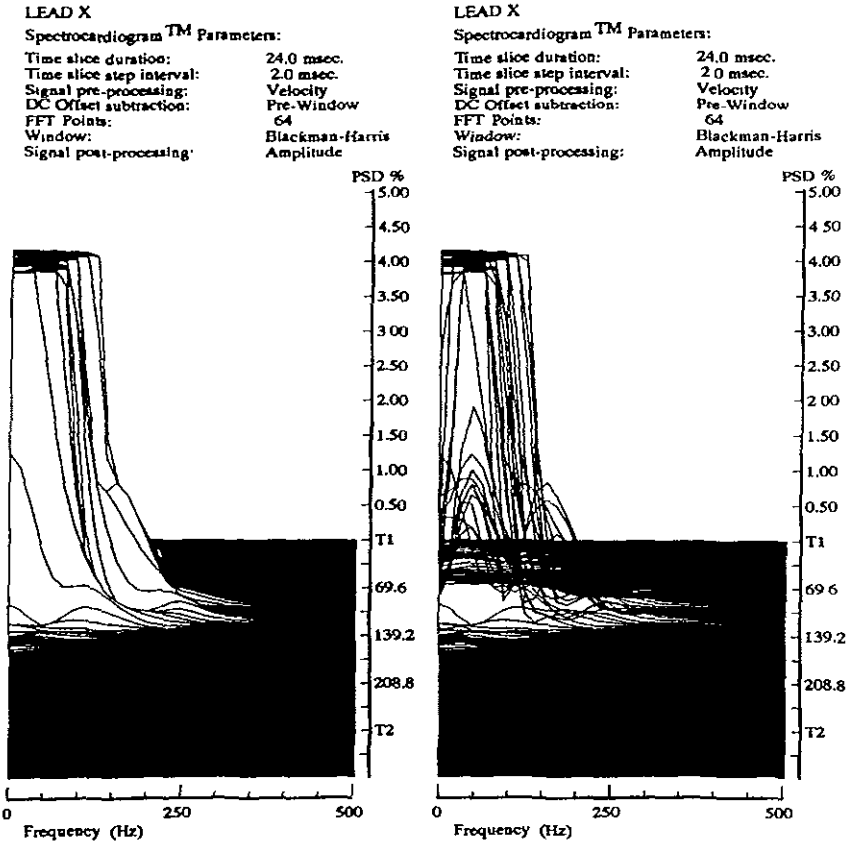

Fig. 3 Spectral mapping, model 3-dimensions for an orthogonal X lead.

XIV. References.

1. **Gillum FR:** Trends in Acute Myocardial Infarction and Coronary Heart Disease Death in the United States. *J Am Coll Cardiol 1993;23.1273-7.*

2. **Organización Panamericana de la Salud. Publicación científica No. 524.** Las condiciones de salud en las Americas. *1990;II:217.*

3. **Ross R, Harker LA:** Hyperlipidemia and Atherosclerosis. *Science 1976; 193:1094-1100*

4. **Aguirre FV.** The cost of Open Infarct-Related Artery: Comparison of Treatment Modalities in the Reperfusion Era. *Mayo Clin Proc 1994;69:87-89.*

5 **Sheffield LT, Maloof JA, Sawyer JA, Roitman D:** Maximal Heart Rate and treadmill performance of healthy women in relation to age. *Circulation 1978; 57:79-84.*

6 **Gianrossi R, Detrano R, Mulvihill D, Leheman K, Dubach P, Colombo A, et al:** Exercise-induced ST depression in the diagnosis of coronary artery disease: A meta-analysis. *Circulation 1989;80:87-98*

7 **Lucarini AR, Picano E, Lattanzi F, Camici P, Marini C:** Dipyridamole-echocardiography stress testing in hypertensives: targets and tools. *Circulation 1991,83(suppl III)·68-72.*

7a. **Armstrong FW:** Stress Echocardiography. Clinical Influence and Future Role *Mayo Clin Proc 1995;70:95-96.*

8. **Fortin DF, Califf RM.** Long-Term survival from acute myocardial infarction: Salutary effect of open coronary vessel. *Am J Med 1990;88:9N-15N.*

9. **Cigarroa RG., Lange RA., Hills LD.** Prognosis after acute myocardial infarction in Patients with and without residual anterograde coronary blood flow. *Am J Cardiol 1989;64:155-160.*

10. **Simoons ML, Vos J., Tijssen Jan GP Vermeer F., Freek WA., Krauss XH., Manger CV.** Long-Term Benefit of Early Thrombolytic Therapy in Patients With Acute Myocardial Infarction: 5 Year Follow-Up of a Trial Conducted by the Interuniversity Cardiology Institute of Netherlands. *J Am Coll Cardiol 1989;14:1609-15.*

11. **Infante-Vazquez O:** Electrocardiografia digital. *Principia Cardiol 1994,9:20-28*

12. **Infante-Vazquez O, Hernandez Gonzalez J, Rodriguez-Rossini G, Garcia Moreira C**: QRS complex identification through an artificial neural network. *Physics in Medicine and Biology 1994;39a·473-77.*

13. **Gomes JA, Stephen LW, IP J:** Signal averaging of surface QRS complex: Practicals Applications. *J Cardiovasc Electrophysiol 1991;2:316-330.*

14. **Novak P, Li Z, Novak V, Hatala R:** Time frequency Mapping of the QRS complex in normal Subjects and postmyocardial infarction patients. *J Electrocardiol 1994; 27:49-60*

15. **Cain ME, Ambos HD:** Quantification of differences in frecuency content of signal averaged electrocardiogramseg in patients with copared to those without sustained ventricular tachycardia. *Am J cardiol 1985; 55:1500-1505.*

16 **Durrer D, Van Dam R. TH., Freud G.E., Janse M.J. et al.**: Total Exitation of the Isolated Human Heart. *Circulation 1970;XLI(June): 899-911.*

17 **Durrer D, Bûller J, Graaff P, et al**: Epicardial excitation pattern as observed in the isolated revived and perfused fetal human heart. *Circulation Research 1961;9:29-34.*

18. **Sodi -Pallares D, Rodriguez MJ, Chait LO, et al**: The activation of the intraventricular Septum. *Am Heart J 1951;41:569-573.*

19. **Barbato E, Pileggi F, Debes AC, et al**: Study of the sequence of ventricular activation and QRS complex of the normal human heart using direct epicardial leads. *Am Heart J 1958,55:867-73.*

20 **Madison SS, Barr RC, Lanning CH, Tucek PC**: Origin of Body surface QRS and T wave potentials from epicardial potential distributions in the intact chimpanzee. *Circulation 1977;55(2):268-278.*

21. **Marcus ML**: The coronary circulation in health and disease. *Mc Graw Hill, New York, 1983: 65-155.*

22. **Epstein SE, Cannon RD**: Site of increased resistance to coronary flow in patients with angina pectoris and normal epicardial coronary arteries. *J Am Coll Cardiol 1986,8:459-61.*

23. **Boyle B, Carson P, Hamer J**: High Frequency electrocardiography in ischemic heart disease. *Br Heart J 1966;28·539.*

24. **Reynolds EW, Muller BD, Anderson GJ, Muller BT:** High-frequency components in the electrocardiogram: a comparative study of normals and patients with myocardial disease. *Circulation 1967;35:195-199*

25. **Kienzle MG, Falcone RA, Simson MB**: Alterations in the initial portion of the signal-averaged QRS complex in acute myocardial infarction with ventricular tachycardia. *Am J Cardiol 1988;61:99-103*

26. **Langner PH, Jr**: The value of high fidelity electrocardiography using the cathode ray oscillograph and expanded time scale. *Circulation 1952;5.249-256*

27. **Goldberger AL, Bhargava V, Froelicher V, et al**: Effect of myocardial infarction on high frequency ECG potentials. *Circulation 1981;63:34-42*

28 **Abboud S**: High-Frequency Electrocardiogram Analysis of the Entire QRS in the Diagnosis and Assessment of Coronary Artery Disease. *Prog Cardiovasc Dis 1993;5.311-328.*

29. **Abboud S**: High Frequency ECG--A new method to examine depolarization changes by transient myocardial ischemia. *IEEE computer Society. Computers in Cardiology 1989: 105-106.*

30. **Prinzmental M, Toyoshima H, Ekmekci A**: Myocardial Ischemia: Nature of ischemic electrocardiographic patterns in the mammalian ventricles as determined by intracelular electrocardiographic and metabolic changes. *Am J Cardiol 1961;8:493-99.*

31. **Wilson FN**: On the choice of a reference point for the study of the electrical field of a tissue immerse in a vulume conduction. En: *Libro homenaje al Dr. Ignacio Chavez. México 1945, 503-516*

32. **Kienzle MG, Falcone RA, Simson MB**: Alterations in the initial portion of the signal-averaged QRS complex in acute myocardial infarction with ventricular tachycardia. *Am J Cardiol 1988;61·99-103*

33. **Novak P., Li Z., Novak V., Hatala R:** Time frequency Mapping of the QRS complex in normal Subjects and postmyocardial infarction patients. *J Electrocardiol 1994; 27:49-60.*

34. **Wigner EP**: On the quantum correction for thermodinamic equilibrium. *Physiol Rev 1932,40·749-59.*

35. **Simson WE and Scher AM**: Mechanism of ST segemnt alteration during acute myocardial injury. *Circ Res 1960;8:780-88.*

36. **Prinzmental, M., Toyoshima H., Ekmekci A.**: Myocardial Ischemia: Nature of *ischemic electrocardiographic patterns in the* mammalian ventricles as determined by intracelular electrocardiographic and metabolic changes. *Am J Cardiol 1961;8:493-99.*

37. **Wilson, FN., MacLeod AG., and Barker PS**: The distribution of the currents of Action and Injury displayed by Heart muscle and other exitable tissues. *University of Michigan Press, Scientific Series, Ann Arbor, Vol X, 1933.*

38. **Bayley RH**: Biophysical Principles of Electrocardiography. *Hoeber 1958;X:184-9.*

39. **Sodi-Pallares D., Calder RM.:** New bases of electrocardiography. *Third edition St. Louis, CV Mosby, 1956, p 378-383.*

40. **de Micheli A.:** Enseñanza y aprendizaje racionales en cardiología. *Arch Inst Cardiol Méx 1990;60:435-438*

41. **Pruit RD., and Valencia F**: The immediate electrocardiographic effects of circumscribed myocardial injuries: An experimental Study. *Am Heart J 1948;35:161-7*

42. **Hellerstein HK., Katz LN**: The electrical effects of injury at various myocardial locations. *Am Heart J 1948;36:184-88*

43. **Smith GT., Geary GG., Blanchard W., Roelofs TH., et al**: An Electrocardiographic Model of Myocardial Ischemic Injury. *J Electrocardiol 1983;16(3):223-234.*

44. **Simson MB, Untereker WJ, Spielman SR, Horwitz LN, et al**: Relations between late potentials on body surface and directly recorded fragmented electrogramseg in patients with ventricular tachycardia. *Am J Cardiol 1983;57:105-12*

45. **El-Sherif Nabil**. Electrophysiologic Basis of Ventricular Late Potentials. Prog Cardiovasc Dis 1993;XXXV(6):417-27.

46. **El-Sherif N., Domes JAC., Restivo M., et al.** Late Potentials and Arrhytmogenesis. PACE 1985;5:440-462.

47. **Kelen GJ., Henkin R., Starr AM., Caref EB., Bloomfield D., El-Sherif N**. Spectral Turbulence Analysis of the Signal-Averaged Electrocardiogram and Its Predictive Accuracy for Inducible Sustained Monomorphic Ventricular Tachycardia. *Am J Cardiol 1991;67:965-75.*

48. **Haberl R., Jilge CA., Pulter R., Steinbeck G.** Spectral Mapping of the Electrocardiogram in the Fourier transform for identification of Patients with ventricular tachycardia and coronary disease. *Eur Heart J 1989;10:316-322.*

49. **Faugere G., Savard P., Nadeau RA., et al.** Characterization of the spatial distribution of late ventricular potentials by body surface potential mapping in patients with ventricular arrhytmia. *Circulation 1986,74:1323.*

50 **Gomes JA., Winters SL., Stewart D., Targonski A., Barreca Philip.** Optimal Banpass Filters for Time-Domain Analysis oh The Signal-Averaged Electrocardiogram. *Am J Cardiol 1987;60:1290-1298.*

51. **The TIMI Study Group.** The Trombolysis in Myocardial Infarction(TIMI) trial: phase I findings. *N Engl J Med 1985,312:923-26.*

52. **Tugwell P.X.** Interpretation of diagnostic data: How to do it with a more complex table. *Can Med Assoc J. 1983;129·832-835.*

53. **Holland RP., and Arnsdorf MF**: Solid angle theory an the electrocardiogram: Physiologic and quantitative Interpretations *Prog Cardiovasc Dis 1977;6·431-474.*

54. **Newton I:** Philosophiae Naturalis Principia Mathematica. *Book 1, sect,12, Theorem 30 London, S. Pepys, 1686*

XIV. TABLES

Table 1. Characteristics of Patients.

Variable	Group 1 (Ischemic)	Group 2 (healthy)	p Value
Number	31	29	
Male(%)	26 (83)	24 (83)	.883
Age	55 4 ± 5 6	54 1 ± 8 1	.446
Diabetes (%)	4 (11)	0	.087
Hypertension (%)	9 (25)	0	.045
Smoking (%)	15 (31)	3 (11)	.032
CTR	0 51 ± 0.09	0.48 ± 0 06	.157
LBBB (%)	4 (11)	0	.087
EF %	57.6 ± 3.1	60 1 ± 9.3	.889
IRTLV msec	100 0 ± 10 3	95.3 ± 6.2	.045
QRSd msec	93.6 ± 5 4	92.5 ± 5.5	.424
QRSx msec	88.9 ± 6 7	90 4 ± 11.0	.522
QRSy msec	100.3 ± 7 6	98 8 ± 9.2	.500
QRSz msec	97 9 ± 10.2	98.4 ± 11.2	844
RMS40	38.4 ± 11.7	32.7 ± 12.1	.070
LAS40	26.0 ± 6.3	25.4 ± 6.7	.732
Qtc msec	330 ± 60.5	410 ± 99.7	.001
LP+ (%)	10 (32)	3 (10)	.765
RRm msec	870.2 ± 174 9	963.7 ± 52.4	.804

Data are showed as mean ± standard deviation or n (%). CTR cardiothoracic ratio, LBBB, left bundle branch block; EF, ejection fraction expressed in percentages, IRTLV isovolumetric relaxation time of left ventricle, QRSd, mean of QRS complex from XYZ leads, QRSx, QRS duration in X lead, QRSy, QRS duration in Y lead, QRSz, QRS duration in Z lead RMS40, root mean square value from last 40 milliseconds of the QRSd complex, LAS40, duration of low amplitude signals from last 40 milliseconds of the QRSd complex (QRSd, RMS40, and LAS40 were calculated using a filter of 40-250 Hz). Qtc, corrected Qt interval duration, RRm, mean duration of RR interval

TABLE 2.

Power Spectral Density (PSD) at each Ortoghonal Lead T-Test (Group 1 vs Group 2)

Group Statistics

	PACIENTE	N	Mean	Std. Deviation	Std. Error Mean
PSDX	1	31	1 784	1 510	.271
	2	29	1.614	1 504	.279
PSDY	1	31	490	311	5 591E-02
	2	29	.683	587	.109
PSDZ	1	31	1.652	1 886	339
	2	29	2.048	2 075	.385

Independent Samples Test

		Levene's Test for Equality of Variances		t-test for Equality of Means						
									95% Confidence Interval of the Difference	
		F	Sig.	t	df	Sig. (2-tailed)	Mean Difference	Std. Error Difference	Lower	Upper
PSDX	Equal variances assumed	.124	726	.437	58	.664	170	.389	- 609	949
	Equal variances not assumed			.437	57.766	.664	.170	.389	-.609	949
PSDY	Equal variances assumed	10 82	.002	-1.601	58	.115	- 192	.120	- 433	4 8E-02
	Equal variances not assumed			-1 571	41 969	124	-.192	.122	- 440	5 5E-02
PSDZ	Equal variances assumed	1 455	233	-.776	58	441	-.397	.511	-1.420	627
	Equal variances not assumed			-.773	56 506	443	- 397	513	-1 424	.631

TABLE 3.

SPECTRAL TURBULENCE
MEAN PEAK PER SLICE
ANALYSIS OF TOTAL QRS COMPLEX
(GROUP 1 VS GROUP 2)
T-Test

Group Statistics

	PACIENTE	N	Mean	Std. Deviation	Std Error Mean
MPSXT	1	31	26.139	4.277	768
	2	29	26.855	4.146	770
MPSYT	1	31	29 216	2.530	454
	2	29	29 624	3 309	614
MPSZT	1	31	30 332	2.731	.490
	2	29	30 703	2.964	550

Independent Samples Test

		Levene's Test for Equality of Variances		t-test for Equality of Means						
									95% Confidence Interval of the Difference	
		F	Sig	t	df	Sig (2-tailed)	Mean Difference	Std. Error Difference	Lower	Upper
MPSXT	Equal variances assumed	.021	884	-.658	58	513	-.716	1 089	-2 896	1.463
	Equal variances not assumed			- 659	57.922	513	-.716	1 088	-2 894	1 461
MPSYT	Equal variances assumed	546	463	- 539	58	592	- 408	757	-1 924	1 108
	Equal variances not assumed			- 534	52 375	596	-.408	764	-1 941	1 125
MPSZT	Equal variances assumed	593	.445	- 505	58	616	- 371	735	-1 843	1 101
	Equal variances not assumed			-.503	56 733	617	- 371	737	-1 848	1 105

TABLE 4.

SPECTRAL TURBULENCE ANALYSIS OF TOTAL QRS COMPLEX (BASAL)
PARAMETER: LOW SLICE CORRELATIONS RATIO (LSCR)
GROUP 1 VS GROUP 2
T-Test

Group Statistics

	PACIENTE	N	Mean	Std Deviation	Std Error Mean
TCSBXT	1	31	62.558	10.477	1.882
	2	29	65.855	11.152	2.071
TCSBYT	1	31	71.081	6.292	1.130
	2	29	70.834	4.412	.819
TCSBZT	1	31	70.094	7.378	1.325
	2	29	67 597	6.568	1.220

Independent Samples Test

		Levene's Test for Equality of Variances		t-test for Equality of Means						
									95% Confidence Interval of the Difference	
		F	Sig	t	df	Sig. (2-tailed)	Mean Difference	Std Error Difference	Lower	Upper
TCSBXT	Equal variances assumed	.150	.700	-1 181	58	242	-3 297	2.792	-8.886	2 292
	Equal variances not assumed			-1 178	57 035	244	-3 297	2.798	-8.900	2 306
TCSBYT	Equal variances assumed	2.861	.096	.174	58	862	.246	1 412	-2.580	3 073
	Equal variances not assumed			.176	53 876	861	.246	1.396	-2 552	3 045
TCSBZT	Equal variances assumed	3.322	074	1.381	58	173	2 497	1 808	-1 122	6 116
	Equal variances not assumed			1 387	57 865	171	2 497	1 801	-1.108	6.102

TABLE 5.

SPECTRAL TURBULENCE ANALYSIS OF TOTAL QRS COMPLEX (BASAL)
PARAMETER: INTER-SLICE CORRELATION MEAN (ISCM)
X Y Z LEADS
GROUP 1 VS GROUP 2
T-Test

Group Statistics

	PACIENTE	N	Mean	Std. Deviation	Std Error Mean
MCISXT	1	31	94.790	2.556	.459
	2	29	94.459	2.224	.413
MCISYT	1	31	93.465	1.679	.302
	2	29	93.414	1.319	.245
MCISZT	1	31	92 974	2 352	.422
	2	29	92 876	2 083	.387

Independent Samples Test

		Levene's Test for Equality of Variances		t-test for Equality of Means						
									95% Confidence Interval of the Difference	
		F	Sig	t	df	Sig. (2-tailed)	Mean Difference	Std. Error Difference	Lower	Upper
MCISXT	Equal variances assumed	.980	.326	.535	58	.595	.332	.620	-.910	1 573
	Equal variances not assumed			.537	57 710	.593	332	.617	-.904	1 568
MCISYT	Equal variances assumed	1.214	.275	130	58	.897	.051	.392	-.733	835
	Equal variances not assumed			131	56 363	.897	.051	389	- 727	829
MCISZT	Equal variances assumed	.899	.347	.171	58	865	098	575	-1.053	1 249
	Equal variances not assumed			172	57.833	864	098	573	-1 048	1 245

TABLE 6.

SPECTRAL TURBULENCE ANALYSIS OF TOTAL QRS COMPLEX (BASAL)
PARAMETER: INTER-SLICE CORRELATION STANDARD DEVIATION (decis)
X Y Z LEADS
GROUP 1 VS GROUP 2

T-Test

Group Statistics

	PACIENTE	N	Mean	Std. Deviation	Std. Error Mean
DECISXT	1	31	62.897	34.631	6.220
	2	29	69.045	32.155	5.971
DECISYT	1	31	86.632	19 645	3 528
	2	29	84 807	17.456	3.242
DECISZT	1	31	98.065	44.608	8.012
	2	29	105.579	45.297	8.411

Independent Samples Test

		Levene's Test for Equality of Variances		t-test for Equality of Means						
									95% Confidence Interval of the Difference	
		F	Sig.	t	df	Sig. (2-tailed)	Mean Difference	Std. Error Difference	Lower	Upper
DECISXT	Equal variances assumed	000	992	-.711	58	480	-6 148	8 644	-23.450	11 154
	Equal variances not assumed			-.713	57.998	479	-6 148	8.622	-23.407	11 111
DECISYT	Equal variances assumed	.604	.440	.379	58	.706	1.825	4.811	-7.804	11 455
	Equal variances not assumed			.381	57.855	.705	1.825	4.791	-7 766	11.417
DECISZT	Equal variances assumed	155	.696	- 647	58	520	-7.515	11.610	-30.756	15.726
	Equal variances not assumed			-.647	57 602	.520	-7 515	11 616	-30 771	15 742

TABLE 7.

SPECTRAL TURBULENCE ANALYSIS OF TOTAL QRS COMPLEX (BASAL)
PARAMETER: SPECTRAL ENTROPY (ee).
X Y Z LEADS
GROUP 1 VS GROUP 2

T-Test

Group Statistics

	PACIENTE	N	Mean	Std Deviation	Std. Error Mean
EEXT	1	31	8 339	3 291	.591
	2	29	10.434	4 575	.850
EEYT	1	31	12.606	4.094	735
	2	29	12.731	3 636	.675
EEZT	1	31	12.900	3 594	645
	2	29	13.428	3.524	.654

Independent Samples Test

		Levene's Test for Equality of Variances		t-test for Equality of Means						
									95% Confidence Interval of the Difference	
		F	Sig.	t	df	Sig. (2-tailed)	Mean Difference	Std. Error Difference	Lower	Upper
EEXT	Equal variances assumed	7.455	.008	-2.047	58	.045	-2 096	1.024	-4 145	-5 E-02
	Equal variances not assumed			-2 025	50 596	048	-2.096	1.035	-4 174	-2 E-02
EEYT	Equal variances assumed	310	.580	- 124	58	902	- 125	1.002	-2 131	1 882
	Equal variances not assumed			-.125	57 852	.901	- 125	998	-2.123	1 874
EEZT	Equal variances assumed	035	852	-.574	58	568	- 528	.920	-2 369	1 314
	Equal variances not assumed			- 574	57.865	568	-.528	919	-2.368	1 313

TABLE 8
SPECTRAL TURBULENCE ANALYSIS OF TOTAL QRS COMPLEX
TWO-WAY REPEATED MEASURES ANOVA
GROUP1 VS GROUP 2
(MEAN PEAKS PER SLICE) X-LEAD

Descriptive Statistics

	PACIENTE	Mean	Std. Deviation	N
MPSXT	1	26 139	4 277	31
	2	26 855	4 146	29
	Total	26.485	4.194	60
MPSXT_D	1	25.803	4.355	31
	2	26 314	3.949	29
	Total	26 050	4 136	60

Tests of Within-Subjects Contrasts

Measure: *MEASURE_1*

Source	MPS	Type III Sum of Squares	df	Mean Square	*F*	*Sig.*
MPS	Linear	5 760	1	5.760	7.039	.010
MPS * PACIENTE	Linear	.318	1	.318	.388	.536
Error(MPS)	Linear	47.461	58	.818		

Tests of Between-*Subjects Effects*

Measure MEASURE_1

Transformed Variable: Average

Source	Type III Sum of Squares	df	Mean Square	*F*	*Sig*
Intercept	82770 192	1	82770.192	2414.547	.000
PACIENTE	11 279	1	11.279	.329	568
Error	1988.229	58	34 280		

1. PACIENTE

Estimates

Measure MEASURE_1

PACIENTE	Mean	Std. Error	95% Confidence Interval	
			Lower Bound	Upper Bound
1	25 971	.744	24.483	27.459
2	26.584	.769	25 046	28 123

Pairwise Comparisons

Measure MEASURE_1

(I) PACIENTE	(J) PACIENTE	Mean Difference (I-J)	Std. Error	Sig.[a]	95% Confidence Interval for Difference[a]	
					Lower Bound	Upper Bound
1	2	-.614	1.070	568	-2 754	1 527
2	1	.614	1.070	.568	-1 527	2.754

Based on estimated marginal means

a Adjustment for multiple comparisons: Bonferroni

2. MPS

Estimates

Measure MEASURE_1

MPS	Mean	Std. Error	95% Confidence Interval	
			Lower Bound	Upper Bound
1	26.497	.544	25.407	27 587
2	26 059	538	24.982	27.135

Pairwise Comparisons

Measure. MEASURE_1

(I) MPS	(J) MPS	Mean Difference (I-J)	Std. Error	Sig.[a]	95% Confidence Interval for Difference[a]	
					Lower Bound	Upper Bound
1	2	.438*	.165	.010	108	769
2	1	- 438*	165	.010	- 769	-.108

Based on estimated marginal means

* The mean difference is significant at the .05 level.

a. Adjustment for multiple comparisons. Bonferroni

3. PACIENTE * MPS

Measure: MEASURE_1

PACIENTE	MPS	Mean	Std Error	95% Confidence Interval	
				Lower Bound	Upper Bound
1	1	26.139	757	24 624	27 654
	2	25 803	748	24 306	27.300
2	1	26 855	783	25 289	28 422
	2	26 314	773	24.766	27.861

TABLE 8 B
SPECTRAL TURBULENCE ANALYSIS OF TOTAL QRS COMPLEX
TWO-WAY REPEATED MEASURES ANOVA
GROUP1 VS GROUP 2
(MEAN PEAKS PER SLICE) Y-LEAD

Descriptive Statistics

	PACIENTE	Mean	Std Deviation	N
MPSYT	1	29.216	2 530	31
	2	29.624	3 309	29
	Total	29 413	2 914	60
MPSYT_D	1	30 219	3.088	31
	2	30.410	3.060	29
	Total	30.312	3.050	60

Tests of Within-Subjects Contrasts

Measure: MEASURE_1

Source	MPS_Y	Type III Sum of Squares	df	Mean Square	F	Sig.
MPS_Y	Linear	23 989	1	23 989	12.067	001
MPS_Y * PACIENTE	Linear	.353	1	.353	.177	.675
Error(MPS_Y)	Linear	115 302	58	1.988		

Tests of Between-Subjects Effects

Measure: MEASURE_1
Transformed Variable: Average

Source	Type III Sum of Squares	df	Mean Square	F	Sig.
Intercept	106929.105	1	106929 105	6657.613	.000
PACIENTE	2.688	1	2.688	167	.684
Error	931.548	58	16 061		

1. PACIENTE

Estimates

Measure: MEASURE_1

PACIENTE	Mean	Std. Error	95% Confidence Interval	
			Lower Bound	Upper Bound
1	29.718	.509	28 699	30 737
2	30.017	526	28 964	31 071

Pairwise Comparisons

Measure MEASURE_1

(I) PACIENTE	(J) PACIENTE	Mean Difference (I-J)	Std. Error	Sig.[a]	95% Confidence Interval for Difference[a]	
					Lower Bound	Upper Bound
1	2	-.299	.732	.684	-1.765	1 166
2	1	299	732	684	-1.166	1 765

Based on estimated marginal means

a. Adjustment for multiple comparisons: Bonferroni

2. MPS_Y

Estimates

Measure: MEASURE_1

MPS_Y	Mean	Std. Error	95% Confidence Interval	
			Lower Bound	Upper Bound
1	29.420	.379	28.662	30.178
2	30.315	.397	29.520	31 110

Pairwise Comparisons

Measure MEASURE_1

(I) MPS_Y	(J) MPS_Y	Mean Difference (I-J)	Std. Error	Sig.[a]	95% Confidence Interval for Difference[a]	
					Lower Bound	Upper Bound
1	2	- 895*	.258	.001	-1.410	-.379
2	1	.895*	258	.001	.379	1.410

Based on estimated marginal means

* The mean difference is significant at the .05 level.

a. Adjustment for multiple comparisons: Bonferroni.

3. PACIENTE * MPS_Y

Measure MEASURE_1

PACIENTE	MPS_Y	Mean	Std. Error	95% Confidence Interval	
				Lower Bound	Upper Bound
1	1	29.216	.527	28 162	30.270
	2	30.219	.552	29.114	31.325
2	1	29.624	.544	28.534	30.714
	2	30 410	.571	29.268	31 553

TABLE 8 C
SPECTRAL TURBULENCE ANALYSIS OF TOTAL QRS COMPLEX
TWO-WAY REPEATED MEASURES ANOVA
GROUP1 VS GROUP 2
(MEAN PEAKS PER SLICE) Z-LEAD

Descriptive Statistics

	PACIENTE	Mean	Std Deviation	N
MPSZT	1	30 332	2.731	31
	2	30.703	2 964	29
	Total	30.512	2 828	60
MPSZT_D	1	31.287	2 589	31
	2	31.066	2 522	29
	Total	31.180	2 538	60

Tests of Within-Subjects Contrasts

Measure: MEASURE_1

Source	MPS_Z	Type III Sum of Squares	df	Mean Square	F	Sig
MPS_Z	Linear	12.992	1	12 992	5.647	.021
MPS_Z * PACIENTE	Linear	2.632	1	2 632	1.144	.289
Error(MPS_Z)	Linear	133 433	58	2.301		

Tests of Between-Subjects Effects

Measure: MEASURE_1
Transformed Variable: Average

Source	Type III Sum of Squares	df	Mean Square	F	Sig.
Intercept	114058.210	1	114058.210	9244 191	.000
PACIENTE	.168	1	168	.014	.908
Error	715.625	58	12.338		

1. PACIENTE

Estimates

Measure: MEASURE_1

PACIENTE	Mean	Std Error	95% Confidence Interval	
			Lower Bound	Upper Bound
1	30.810	446	29 917	31 703
2	30.884	461	29 961	31 808

Pairwise Comparisons

Measure: MEASURE_1

(I) PACIENTE	(J) PACIENTE	Mean Difference (I-J)	Std. Error	Sig.[a]	95% Confidence Interval for Difference[a]	
					Lower Bound	Upper Bound
1	2	-7.481E-02	.642	.908	-1.359	1.210
2	1	7.481E-02	.642	.908	-1.210	1.359

Based on estimated marginal means

a. Adjustment for multiple comparisons: Bonferroni.

2. MPS_Z

Estimates

Measure: MEASURE_1

MPS_Z	Mean	Std. Error	95% Confidence Interval	
			Lower Bound	Upper Bound
1	30.518	.368	29.782	31.254
2	31.176	.330	30.515	31.837

Pairwise Comparisons

Measure: MEASURE_1

(I) MPS_Z	(J) MPS_Z	Mean Difference (I-J)	Std. Error	Sig.[a]	95% Confidence Interval for Difference[a]	
					Lower Bound	Upper Bound
1	2	-.658*	.277	.021	-1.213	-.104
2	1	.658*	.277	.021	.104	1.213

Based on estimated marginal means

* The mean difference is significant at the .05 level.

[a] Adjustment for multiple comparisons: Bonferroni.

3. PACIENTE * MPS_Z

Measure: MEASURE_1

PACIENTE	MPS_Z	Mean	Std. Error	95% Confidence Interval	
				Lower Bound	Upper Bound
1	1	30.332	.511	29.309	31.355
	2	31.287	.459	30.368	32.206
2	1	30.703	.529	29.646	31.761
	2	31.066	.475	30.115	32.016

TABLE 9
SPECTRAL TURBULENCE ANALYSIS OF TOTAL QRS COMPLEX
TWO-WAY REPEATED MEASURES ANOVA
GROUP1 VS GROUP 2
(LOW SLICE CORRELATONS RATIO) X-LEAD

Descriptive Statistics

	PACIENTE	Mean	Std Deviation	N
TCSBXT	1	62.558	10 477	31
	2	65.855	11 152	29
	Total	64.152	10 844	60
TCSBXT_D	1	59.032	8 281	31
	2	62 624	9 149	29
	Total	60 768	8 824	60

Tests of Within-Subjects Contrasts

Measure. MEASURE_1

Source	LSCR	Type III Sum of Squares	df	Mean Square	F	Sig.
LSCR	Linear	342.031	1	342.031	18 321	000
LSCR * PACIENTE	Linear	651	1	.651	.035	.853
Error(LSCR)	Linear	1082 811	58	18.669		

Tests of Between-Subjects Effects

Measure· MEASURE_1
Transformed Variable: Average

Source	Type III Sum of Squares	df	Mean Square	F	Sig.
Intercept	468490.036	1	468490 036	2692.099	000
PACIENTE	355 541	1	355.541	2 043	.158
Error	10093.397	58	174 024		

1. PACIENTE

Estimates

Measure MEASURE_1

PACIENTE	Mean	Std Error	95% Confidence Interval	
			Lower Bound	Upper Bound
1	60 795	1.675	57 442	64.149
2	64 240	1 732	60 772	67.707

Pairwise Comparisons

Measure: MEASURE_1

(I) PACIENTE	(J) PACIENTE	Mean Difference (I-J)	Std. Error	Sig.[a]	95% Confidence Interval for Difference[a]	
					Lower Bound	Upper Bound
1	2	-3.444	2 410	.158	-8.268	1 379
2	1	3.444	2 410	.158	-1.379	8.268

Based on estimated marginal means

a. Adjustment for multiple comparisons: Bonferroni.

2. PACIENTE * LSCR

Measure: MEASURE_1

PACIENTE	LSCR	Mean	Std. Error	95% Confidence Interval	
				Lower Bound	Upper Bound
1	1	62.558	1.941	58.672	66.444
	2	59.032	1.564	55.901	62.164
2	1	65.855	2.007	61.838	69.873
	2	62.624	1.618	59.386	65.862

2. LSCR

Estimates

Measure: MEASURE_1

LSCR	Mean	Std. Error	95% Confidence Interval	
			Lower Bound	Upper Bound
1	64 207	1.396	61.412	67.001
2	60.828	1.125	58 576	63.080

Pairwise Comparisons

Measure MEASURE_1

(I) LSCR	(J) LSCR	Mean Difference (I-J)	Std. Error	Sig.[a]	95% Confidence Interval for Difference[a]	
					Lower Bound	Upper Bound
1	2	3.378*	789	000	1.798	4.958
2	1	-3.378*	789	.000	-4 958	-1.798

Based on estimated marginal means

* The mean difference is significant at the .05 level

a. Adjustment for multiple comparisons: Bonferroni.

TABLE 9 B
SPECTRAL TURBULENCE ANALYSIS OF TOTAL QRS COMPLEX
TWO-WAY REPEATED MEASURES ANOVA
GROUP1 VS GROUP 2
(LOW SLICE CORRELATONS RATIO) Y-LEAD

Descriptive Statistics

	PACIENTE	Mean	Std. Deviation	N
TCSBYT	1	71 081	6.292	31
	2	70 834	4.412	29
	Total	70 962	5.420	60
TCSBYT_D	1	67 745	4.465	31
	2	67 276	4.262	29
	Total	67.518	4.337	60

Tests of Within-Subjects Contrasts

Measure: MEASURE_1

Source	LSCR	Type III Sum of Squares	df	Mean Square	F	Sig.
LSCR	Linear	356.069	1	356.069	22.982	.000
LSCR * PACIENTE	Linear	.373	1	.373	.024	.877
Error(LSCR)	Linear	898.621	58	15.493		

Tests of Between-Subjects Effects

Measure: MEASURE_1
Transformed Variable: Average

Source	Type III Sum of Squares	df	Mean Square	F	Sig.
Intercept	574563.126	1	574563 126	17173.561	.000
PACIENTE	3.835	1	3.835	.115	.736
Error	1940.463	58	33 456		

1. PACIENTE

Estimates

Measure: MEASURE_1

PACIENTE	Mean	Std. Error	95% Confidence Interval	
			Lower Bound	Upper Bound
1	69.413	735	67.942	70.883
2	69 055	759	67.535	70.575

Pairwise Comparisons

Measure MEASURE_1

(I) PACIENTE	(J) PACIENTE	Mean Difference (I-J)	Std. Error	Sig.[a]	95% Confidence Interval for Difference[a]	
					Lower Bound	Upper Bound
1	2	.358	1.057	.736	-1.757	2 473
2	1	-.358	1.057	736	-2 473	1.757

Based on estimated marginal means

a Adjustment for multiple comparisons: Bonferroni.

2. LSCR

Estimates

Measure MEASURE_1

LSCR	Mean	Std. Error	95% Confidence Interval	
			Lower Bound	Upper Bound
1	70.958	.706	69.544	72.371
2	67 511	564	66.381	68.640

Pairwise Comparisons

Measure. MEASURE_1

(I) LSCR	(J) LSCR	Mean Difference (I-J)	Std. Error	Sig.[a]	95% Confidence Interval for Difference[a]	
					Lower Bound	Upper Bound
1	2	3 447*	.719	000	2.008	4.886
2	1	-3.447*	719	.000	-4.886	-2.008

Based on estimated marginal means

*. The mean difference is significant at the 05 level

a Adjustment for multiple comparisons: Bonferroni.

3. PACIENTE * LSCR

Measure MEASURE_1

PACIENTE	LSCR	Mean	Std. Error	95% Confidence Interval	
				Lower Bound	Upper Bound
1	1	71.081	.982	69.116	73.046
	2	67 745	.784	66 175	69.316
2	1	70.834	1.015	68.803	72.866
	2	67 276	.811	65 652	68 899

TABLE 9 C
SPECTRAL TURBULENCE ANALYSIS OF TOTAL QRS COMPLEX
TWO-WAY REPEATED MEASURES ANOVA
GROUP1 VS GROUP 2
(LOW SLICE CORRELATONS RATIO) Z-LEAD

Descriptive Statistics

	PACIENTE	Mean	Std. Deviation	N
TCSBZT	1	70 094	7.378	31
	2	67 597	6.568	29
	Total	68.887	7 052	60
TCSBZT_D	1	71 416	7 608	31
	2	69 117	7.347	29
	Total	70 305	7.509	60

Tests of Within-Subjects Contrasts

Measure. MEASURE_1

Source	LSCR	Type III Sum of Squares	df	Mean Square	F	Sig
LSCR	Linear	60.564	1	60.564	3.328	.073
LSCR * PACIENTE	Linear	294	1	.294	.016	.899
Error(LSCR)	Linear	1055 431	58	18 197		

Tests of Between-Subjects Effects

Measure MEASURE_1
Transformed Variable Average

Source	Type III Sum of Squares	df	Mean Square	F	Sig
Intercept	579917 177	1	579917.177	6682.772	.000
PACIENTE	172.312	1	172 312	1.986	.164
Error	5033 121	58	86 778		

1. PACIENTE

Estimates

Measure: MEASURE_1

PACIENTE	Mean	Std. Error	95% Confidence Interval	
			Lower Bound	Upper Bound
1	70 755	1.183	68 387	73.123
2	68 357	1.223	65 908	70.805

Pairwise Comparisons

Measure: MEASURE_1

(I) PACIENTE	(J) PACIENTE	Mean Difference (I-J)	Std. Error	Sig.[a]	95% Confidence Interval for Difference[a]	
					Lower Bound	Upper Bound
1	2	2 398	1 702	.164	-1.008	5.804
2	1	-2.398	1 702	164	-5 804	1.008

Based on estimated marginal means

a. Adjustment for multiple comparisons: Bonferroni.

2. LSCR

Estimates

Measure MEASURE_1

LSCR	Mean	Std. Error	95% Confidence Interval	
			Lower Bound	Upper Bound
1	68.845	904	67.036	70.655
2	70.267	967	68.332	72.202

Pairwise Comparisons

Measure. MEASURE_1

(I) LSCR	(J) LSCR	Mean Difference (I-J)	Std Error	Sig.[a]	95% Confidence Interval for Difference[a]	
					Lower Bound	Upper Bound
1	2	-1.422	779	073	-2.981	.138
2	1	1.422	.779	073	- 138	2.981

Based on estimated marginal means

a Adjustment for multiple comparisons: Bonferroni

3. PACIENTE * LSCR

Measure MEASURE_1

PACIENTE	LSCR	Mean	Std Error	95% Confidence Interval	
				Lower Bound	Upper Bound
1	1	70.094	1 257	67 578	72 610
	2	71.416	1 344	68 726	74.106
2	1	67 597	1 300	64.995	70.198
	2	69 117	1 390	66 336	71 899

TABLE 10
SPECTRAL TURBULENCE ANALYSIS OF TOTAL QRS COMPLEX
TWO-WAY REPEATED MEASURES ANOVA
GROUP1 VS GROUP 2
(INTER-SLICE CORRELATON MEAN) X-LEAD

Descriptive Statistics

	PACIENTE	Mean	Std Deviation	N
MCISXT	1	94 790	2.556	31
	2	94.459	2 224	29
	Total	94.630	2 387	60
MCISYT_D	1	92.906	1.433	31
	2	93.221	1 157	29
	Total	93 058	1 305	60

Tests of Within-Subjects Contrasts

Measure· MEASURE_1

Source	ISCM	Type III Sum of Squares	df	Mean Square	F	Sig.
ISCM	Linear	73.011	1	73.011	22.238	000
ISCM * PACIENTE	Linear	3.126	1	3.126	.952	.333
Error(ISCM)	Linear	190 425	58	3.283		

Tests of Between-Subjects Effects

Measure MEASURE_1
Transformed Variable: Average

Source	Type III Sum of Squares	df	Mean Square	F	Sig.
Intercept	1055629.81	1	1055629 81	251920 97	.000
PACIENTE	2.285E-03	1	2 285E-03	.001	981
Error	243.039	58	4 190		

1. PACIENTE

Estimates

Measure· MEASURE_1

PACIENTE	Mean	Std Error	95% Confidence Interval	
			Lower Bound	Upper Bound
1	93 848	260	93 328	94.369
2	93 840	269	93 302	94.378

Pairwise Comparisons

Measure: MEASURE_1

(I) PACIENTE	(J) PACIENTE	Mean Difference (I-J)	Std. Error	Sig.[a]	95% Confidence Interval for Difference[a]	
					Lower Bound	Upper Bound
1	2	8.732E-03	374	.981	-.740	757
2	1	-8.732E-03	374	981	- 757	.740

Based on estimated marginal means

a Adjustment for multiple comparisons. Bonferroni.

2. PACIENTE * ISCM

Measure: MEASURE_1

PACIENTE	ISCM	Mean	Std. Error	95% Confidence Interval	
				Lower Bound	Upper Bound
1	1	94.790	.431	93.927	95.654
	2	92.906	235	92 437	93.376
2	1	94.459	.446	93.566	95.351
	2	93.221	243	92 735	93.706

2. ISCM

Estimates

Measure: MEASURE_1

ISCM	Mean	Std. Error	95% Confidence Interval	
			Lower Bound	Upper Bound
1	94.624	.310	94.004	95 245
2	93.064	169	92.726	93.401

Pairwise Comparisons

Measure: MEASURE_1

(I) ISCM	(J) ISCM	Mean Difference (I-J)	Std. Error	Sig.[a]	95% Confidence Interval for Difference[a]	
					Lower Bound	Upper Bound
1	2	1.561*	331	000	898	2.223
2	1	-1.561*	331	.000	-2.223	-.898

Based on estimated marginal means

* The mean difference is significant at the 05 level

a. Adjustment for multiple comparisons: Bonferroni

TABLE 10 B
SPECTRAL TURBULENCE ANALYSIS OF TOTAL QRS COMPLEX
TWO-WAY REPEATED MEASURES ANOVA
GROUP1 VS GROUP 2
(INTER-SLICE CORRELATON MEAN) Y-LEAD

Descriptive Statistics

	PACIENTE	Mean	Std Deviation	N
MCISYT	1	93.465	1 679	31
	2	93 414	1 319	29
	Total	93 440	1.503	60
MCISYT_D	1	92.906	1.433	31
	2	93 221	1.157	29
	Total	93.058	1.305	60

Tests of Within-Subjects Contrasts

Measure: MEASURE_1

Source	ISCM_Y	Type III Sum of Squares	df	Mean Square	F	Sig.
ISCM_Y	Linear	4.227	1	4.227	9.765	.003
ISCM_Y * PACIENTE	Linear	.998	1	.998	2.305	.134
Error(ISCM_Y)	Linear	25 107	58	.433		

Tests of Between-Subjects Effects

Measure: MEASURE_1
Transformed Variable. Average

Source	Type III Sum of Squares	df	Mean Square	F	Sig
Intercept	1042338.55	1	1042338.55	291683.23	.000
PACIENTE	.520	1	.520	146	.704
Error	207 265	58	3 574		

1. PACIENTE

Estimates

Measure MEASURE_1

PACIENTE	Mean	Std Error	95% Confidence Interval	
			Lower Bound	Upper Bound
1	93 185	240	92 705	93.666
2	93.317	.248	92.820	93.814

Pairwise Comparisons

Measure MEASURE_1

(I) PACIENTE	(J) PACIENTE	Mean Difference (I-J)	Std. Error	Sig.[a]	95% Confidence Interval for Difference[a]	
					Lower Bound	Upper Bound
1	2	-.132	.345	.704	- 823	559
2	1	.132	345	704	-.559	823

Based on estimated marginal means

a Adjustment for multiple comparisons: *Bonferroni*

2. PACIENTE * ISCM_Y

Measure: MEASURE_1

PACIENTE	ISCM_Y	Mean	Std. Error	95% Confidence Interval	
				Lower Bound	Upper Bound
1	1	93.465	.272	92 919	94.010
	2	92.906	235	92 437	93.376
2	1	93.414	.282	92.850	93.977
	2	93 221	243	92.735	93.706

3. ISCM_Y

Estimates

Measure: MEASURE_1

ISCM_Y	Mean	Std. Error	95% Confidence Interval	
			Lower Bound	Upper Bound
1	93 439	.196	93 047	93.831
2	93.064	169	92.726	93.401

Pairwise Comparisons

Measure. MEASURE_1

(I) ISCM_Y	(J) ISCM_Y	Mean Difference (I-J)	Std. Error	Sig.[a]	95% Confidence Interval for Difference[a]	
					Lower Bound	Upper Bound
1	2	.376*	120	.003	135	.616
2	1	-.376*	120	003	- 616	- 135

Based on estimated marginal means

*. The mean difference is significant at the .05 level

a Adjustment for multiple comparisons. Bonferroni.

TABLE 10 C
SPECTRAL TURBULENCE ANALYSIS OF TOTAL QRS COMPLEX
TWO-WAY REPEATED MEASURES ANOVA
GROUP1 VS GROUP 2
(INTER-SLICE CORRELATON MEAN) Z-LEAD

Descriptive Statistics

	PACIENTE	Mean	Std. Deviation	N
MCISZT	1	92.974	2 352	31
	2	92.876	2 083	29
	Total	92 927	2 208	60
MCISZT_D	1	93.416	1 814	31
	2	93 734	1.540	29
	Total	93 570	1.681	60

Tests of Within-Subjects Contrasts

Measure. MEASURE_1

Source	ISCM_Z	Type III Sum of Squares	df	Mean Square	F	Sig.
ISCM_Z	Linear	12.672	1	12.672	13 577	.001
ISCM_Z * PACIENTE	Linear	1.301	1	1.301	1.394	.243
Error(ISCM_Z)	Linear	54 133	58	933		

Tests of Between-Subjects Effects

Measure. MEASURE_1
Transformed Variable: Average

Source	Type III Sum of Squares	df	Mean Square	F	Sig
Intercept	1042311.82	1	1042311.82	151724.28	.000
PACIENTE	.363	1	.363	.053	.819
Error	398 447	58	6 870		

1. PACIENTE

Estimates

Measure MEASURE_1

PACIENTE	Mean	Std Error	95% Confidence Interval	
			Lower Bound	Upper Bound
1	93 195	.333	92 529	93 861
2	93 305	.344	92 616	93 994

Pairwise Comparisons

Measure: MEASURE_1

(I) PACIENTE	(J) PACIENTE	Mean Difference (I-J)	Std. Error	Sig.[a]	95% Confidence Interval for Difference[a]	
					Lower Bound	Upper Bound
1	2	-.110	.479	819	-1 068	848
2	1	110	479	819	-.848	1 068

Based on estimated marginal means

a Adjustment for multiple comparisons: Bonferroni

2. ISCM_Z

Estimates

Measure: MEASURE_1

ISCM_Z	Mean	Std. Error	95% Confidence Interval	
			Lower Bound	Upper Bound
1	92.925	.288	92 349	93.501
2	93.575	.218	93 139	94 012

Pairwise Comparisons

Measure. MEASURE_1

(I) ISCM_Z	(J) ISCM_Z	Mean Difference (I-J)	Std. Error	Sig [a]	95% Confidence Interval for Difference[a]	
					Lower Bound	Upper Bound
1	2	- 650*	176	001	-1 004	-.297
2	1	.650*	176	001	.297	1 004

Based on estimated marginal means

* The mean difference is significant at the 05 level.

a. Adjustment for multiple comparisons Bonferroni

3. PACIENTE * ISCM_Z

Measure: MEASURE_1

PACIENTE	ISCM_Z	Mean	Std Error	95% Confidence Interval	
				Lower Bound	Upper Bound
1	1	92 974	400	92.174	93.775
	2	93 416	303	92.809	94.023
2	1	92 875	413	92 048	93 703
	2	93 734	313	93 107	94 362

TABLE 11
SPECTRAL TURBULENCE ANALYSIS OF TOTAL QRS COMPLEX
TWO-WAY REPEATED MEASURES ANOVA
GROUP1 VS GROUP 2
(INTER-SLICE CORRELATON SD) X-LEAD

Descriptive Statistics

	PACIENTE	Mean	Std Deviation	N
DECISXT	1	62 897	34 631	31
	2	69 045	32.155	29
	Total	65 868	33.318	60
DECISXT_D	1	70 226	41.040	31
	2	73 548	35.321	29
	Total	71.832	38.096	60

Tests of Within-Subjects Contrasts

Measure: MEASURE_1

Source	ISCSD	Type III Sum of Squares	df	Mean Square	F	Sig.
ISCSD	Linear	1048 890	1	1048.890	1.937	.169
ISCSD * PACIENTE	Linear	59.813	1	59.813	.110	.741
Error(ISCSD)	Linear	31407.737	58	541.513		

Tests of Between-Subjects Effects

Measure MEASURE_1
Transformed Variable: Average

Source	Type III Sum of Squares	df	Mean Square	F	Sig.
Intercept	569510 046	1	569510.046	277.618	000
PACIENTE	671.934	1	671.934	328	.569
Error	118982.156	58	2051.416		

1. PACIENTE

Estimates

Measure: MEASURE_1

PACIENTE	Mean	Std. Error	95% Confidence Interval	
			Lower Bound	Upper Bound
1	66.561	5 752	55 047	78.075
2	71 297	5.947	59 392	83 201

Pairwise Comparisons

Measure: MEASURE_1

(I) PACIENTE	(J) PACIENTE	Mean Difference (I-J)	Std. Error	Sig.[a]	95% Confidence Interval for Difference[a]	
					Lower Bound	Upper Bound
1	2	-4.735	8.274	569	-21.297	11.827
2	1	4.735	8.274	569	-11.827	21.297

Based on estimated marginal means

a. Adjustment for multiple comparisons: Bonferroni.

2. PACIENTE * ISCSD

Measure: MEASURE_1

PACIENTE	ISCSD	Mean	Std. Error	95% Confidence Interval	
				Lower Bound	Upper Bound
1	1	62.897	6.009	50.868	74.926
	2	70.226	6.894	56.425	84.026
2	1	69.045	6.213	56.608	81.482
	2	73.548	7.128	59.280	87.817

3. ISCSD

Estimates

Measure: MEASURE_1

ISCSD	Mean	Std. Error	95% Confidence Interval	
			Lower Bound	Upper Bound
1	65.971	4.322	57.320	74.622
2	71.887	4.958	61.962	81.812

Pairwise Comparisons

Measure: MEASURE_1

(I) ISCSD	(J) ISCSD	Mean Difference (I-J)	Std. Error	Sig.[a]	95% Confidence Interval for Difference[a]	
					Lower Bound	Upper Bound
1	2	-5.916	4.251	.169	-14.425	2.593
2	1	5.916	4.251	.169	-2.593	14.425

Based on estimated marginal means

a. Adjustment for multiple comparisons: Bonferroni.

TABLE 11 B
SPECTRAL TURBULENCE ANALYSIS OF TOTAL QRS COMPLEX
TWO-WAY REPEATED MEASURES ANOVA
GROUP1 VS GROUP 2
(INTER-SLICE CORRELATON SD) Y-LEAD

Descriptive Statistics

	PACIENTE	Mean	Std Deviation	N
DECISYT	1	86.632	19 645	31
	2	84 807	17 456	29
	Total	85 750	18.485	60
DECISYT_D	1	101 645	29.221	31
	2	94 403	27 517	29
	Total	98.145	28 404	60

Tests of Within-Subjects Contrasts

Measure: MEASURE_1

Source	ISCSD_Y	Type III Sum of Squares	df	Mean Square	F	Sig
ISCSD_Y	Linear	4537.143	1	4537.143	17.021	.000
ISCSD_Y * PACIENTE	Linear	219.782	1	219.782	.824	.368
Error(ISCSD_Y)	Linear	15461.002	58	266 569		

Tests of Between-Subjects Effects

Measure. MEASURE_1
Transformed Variable Average

Source	Type III Sum of Squares	df	Mean Square	F	Sig
Intercept	1011729.03	1	1011729 03	1140.180	.000
PACIENTE	615.904	1	615.904	694	408
Error	51465 811	58	887 342		

1. PACIENTE

Estimates

Measure MEASURE_1

			95% Confidence Interval	
PACIENTE	Mean	Std Error	Lower Bound	Upper Bound
1	94 139	3.783	86.566	101 711
2	89 605	3 911	81 776	97.435

Pairwise Comparisons

Measure: MEASURE_1

(I) PACIENTE	(J) PACIENTE	Mean Difference (I-J)	Std. Error	Sig.[a]	95% Confidence Interval for Difference[a]	
					Lower Bound	Upper Bound
1	2	4.534	5.442	408	-6 359	15 426
2	1	-4 534	5 442	408	-15.426	6 359

Based on estimated marginal means

a Adjustment for multiple comparisons Bonferroni

2. ISCSD_Y

Estimates

Measure MEASURE_1

ISCSD_Y	Mean	Std. Error	95% Confidence Interval	
			Lower Bound	Upper Bound
1	85.720	2 405	80.905	90 534
2	98.024	3.670	90.678	105.370

Pairwise Comparisons

Measure: MEASURE_1

(I) ISCSD_Y	(J) ISCSD_Y	Mean Difference (I-J)	Std. Error	Sig.[a]	95% Confidence Interval for Difference[a]	
					Lower Bound	Upper Bound
1	2	-12.305*	2 983	.000	-18.275	-6.335
2	1	12.305*	2.983	.000	6.335	18.275

Based on estimated marginal means

* The mean difference is significant at the .05 level.

a. Adjustment for multiple comparisons Bonferroni.

3. PACIENTE * ISCSD_Y

Measure: MEASURE_1

PACIENTE	ISCSD_Y	Mean	Std. Error	95% Confidence Interval	
				Lower Bound	Upper Bound
1	1	86.632	3 344	79 938	93 327
	2	101 645	5.103	91 431	111 859
2	1	84 807	3.458	77 885	91 728
	2	94.403	5.276	83 843	104 964

TABLE 11 C
SPECTRAL TURBULENCE ANALYSIS OF TOTAL QRS COMPLEX
TWO-WAY REPEATED MEASURES ANOVA
GROUP1 VS GROUP 2
(INTER-SLICE CORRELATON SD) Z-LEAD

Descriptive Statistics

	PACIENTE	Mean	Std Deviation	N
DECISZT	1	98 065	44 608	31
	2	105 579	45.297	29
	Total	101 697	44 720	60
DECISZT_D	1	89 258	30 869	31
	2	83.376	27 983	29
	Total	86.415	29.410	60

Tests of Within-Subjects Contrasts

Measure MEASURE_1

Source	ISCSD_Z	Type III Sum of Squares	df	Mean Square	F	Sig.
ISCSD_Z	Linear	7204.091	1	7204.091	11 459	.001
ISCSD_Z * PACIENTE	Linear	1344.601	1	1344.601	2.139	.149
Error(ISCSD_Z)	Linear	36465.174	58	628.710		

Tests of Between-Subjects Effects

Measure. MEASURE_1
Transformed Variable Average

Source	Type III Sum of Squares	df	Mean Square	F	Sig.
Intercept	1060707.23	1	1060707 23	468.928	.000
PACIENTE	19 968	1	19 968	009	.925
Error	131195 033	58	2261.983		

1. PACIENTE

Estimates

Measure MEASURE_1

PACIENTE	Mean	Std Error	95% Confidence Interval	
			Lower Bound	Upper Bound
1	93 661	6 040	81 571	105 752
2	94.478	6 245	81.977	106 978

Pairwise Comparisons

Measure MEASURE_1

(I) PACIENTE	(J) PACIENTE	Mean Difference (I-J)	Std. Error	Sig.[a]	95% Confidence Interval for Difference[a]	
					Lower Bound	Upper Bound
1	2	-.816	8.688	.925	-18 207	16.575
2	1	.816	8.688	.925	-16 575	18 207

Based on estimated marginal means

a. Adjustment for multiple comparisons Bonferroni

2. ISCSD_Z

Estimates

Measure: MEASURE_1

ISCSD_Z	Mean	Std. Error	95% Confidence Interval	
			Lower Bound	Upper Bound
1	101 822	5.805	90.201	113.442
2	86.317	3.812	78.686	93.947

Pairwise Comparisons

Measure. MEASURE_1

(I) ISCSD_Z	(J) ISCSD_Z	Mean Difference (I-J)	Std. Error	Sig.[a]	95% Confidence Interval for Difference[a]	
					Lower Bound	Upper Bound
1	2	15.505*	4.580	.001	6.336	24.674
2	1	-15.505*	4.580	001	-24.674	-6.336

Based on estimated marginal means

* The mean difference is significant at the 05 level

a Adjustment for multiple comparisons: Bonferroni

3. PACIENTE * ISCSD_Z

Measure. MEASURE_1

PACIENTE	ISCSD_Z	Mean	Std. Error	95% Confidence Interval	
				Lower Bound	Upper Bound
1	1	98 065	8 072	81.907	114 222
	2	89 258	5.300	78 648	99.868
2	1	105 579	8.346	88 874	122 285
	2	83 376	5.480	72.406	94.345

TABLE 12
SPECTRAL TURBULENCE ANALYSIS OF TOTAL QRS COMPLEX
TWO-WAY REPEATED MEASURES ANOVA
GROUP1 VS GROUP 2
(SPECTRAL ENTROPY) X-LEAD

Descriptive Statistics

	PACIENTE	Mean	Std Deviation	N
EEXT	1	8 339	3.291	31
	2	10.434	4.575	29
	Total	9 352	4.069	60
EEXT_D	1	7 816	1.591	31
	2	9.662	3.834	29
	Total	8 708	3.021	60

Tests of Within-Subjects Contrasts

Measure: MEASURE_1

Source	EE	Type III Sum of Squares	df	Mean Square	F	Sig.
EE	Linear	12.564	1	12.564	6.594	.013
EE * PACIENTE	Linear	468	1	468	.245	.622
Error(EE)	Linear	110.516	58	1.905		

Tests of Between-Subjects Effects

Measure: MEASURE_1
Transformed Vanable: Average

Source	Type III Sum of Squares	df	Mean Square	F	Sig.
Intercept	9845.273	1	9845.273	443 325	.000
PACIENTE	116.399	1	116.399	5.241	.026
Error	1288 053	58	22.208		

1. PACIENTE

Estimates

Measure· MEASURE_1

PACIENTE	Mean	Std Error	95% Confidence Interval	
			Lower Bound	Upper Bound
1	8 077	.598	6 879	9 275
2	10 048	.619	8 810	11.287

Pairwise Comparisons

Measure: MEASURE_1

(I) PACIENTE	(J) PACIENTE	Mean Difference (I-J)	Std. Error	Sig.[a]	95% Confidence Interval for Difference[a]	
					Lower Bound	Upper Bound
1	2	-1.971*	.861	.026	-3.694	-.248
2	1	1.971*	.861	.026	.248	3.694

Based on estimated marginal means

* The mean difference is significant at the .05 level.

a Adjustment for multiple comparisons: Bonferroni.

2. EE

Estimates

Measure: MEASURE_1

EE	Mean	Std. Error	95% Confidence Interval	
			Lower Bound	Upper Bound
1	9.387	.512	8.362	10.411
2	8.739	.375	7.989	9.489

Pairwise Comparisons

Measure: MEASURE_1

(I) EE	(J) EE	Mean Difference (I-J)	Std. Error	Sig.[a]	95% Confidence Interval for Difference[a]	
					Lower Bound	Upper Bound
1	2	.647*	.252	.013	.143	1.152
2	1	-.647*	.252	.013	-1.152	-.143

Based on estimated marginal means

*. The mean difference is significant at the .05 level.

a Adjustment for multiple comparisons: Bonferroni.

3. PACIENTE * EE

Measure: MEASURE_1

PACIENTE	EE	Mean	Std. Error	95% Confidence Interval	
				Lower Bound	Upper Bound
1	1	8.339	.712	6.914	9.764
	2	7.816	.521	6.774	8.858
2	1	10.434	.736	8.961	11.908
	2	9.662	.538	8.584	10.740

TABLE 12 B
SPECTRAL TURBULENCE ANALYSIS OF TOTAL QRS COMPLEX
TWO-WAY REPEATED MEASURES ANOVA
GROUP1 VS GROUP 2
(SPECTRAL ENTROPY) Y-LEAD

Descriptive Statistics

	PACIENTE	Mean	Std Deviation	N
EEYT	1	12.606	4.094	31
	2	12 731	3 636	29
	Total	12.667	3 847	60
EEYT_D	1	12.910	4.892	31
	2	12.917	3.870	29
	Total	12.913	4.390	60

Tests of Within-Subjects Contrasts

Measure· MEASURE_1

Source	EE_Y	Type III Sum of Squares	df	Mean Square	F	Sig
EE_Y	Linear	1.795	1	1.795	.443	.508
EE_Y * PACIENTE	Linear	.103	1	.103	.025	.874
Error(EE_Y)	Linear	235 142	58	4.054		

Tests of Between-Subjects Effects

Measure: MEASURE_1
Transformed Variable: Average

Source	Type III Sum of Squares	df	Mean Square	F	Sig
Intercept	19611.657	1	19611 657	640.764	.000
PACIENTE	.131	1	.131	.004	948
Error	1775.187	58	30 607		

1. PACIENTE

Estimates

Measure MEASURE_1

PACIENTE	Mean	Std Error	95% Confidence Interval	
			Lower Bound	Upper Bound
1	12 758	.703	11.352	14 164
2	12.824	726	11.370	14 278

Pairwise Comparisons

Measure: MEASURE_1

(I) PACIENTE	(J) PACIENTE	Mean Difference (I-J)	Std. Error	Sig.[a]	95% Confidence Interval for Difference[a]	
					Lower Bound	Upper Bound
1	2	-6.607E-02	1.011	948	-2.089	1 957
2	1	6 607E-02	1 011	.948	-1 957	2.089

Based on estimated marginal means

a. Adjustment for multiple comparisons: Bonferroni.

2. EE_Y

Estimates

Measure: MEASURE_1

EE_Y	Mean	Std. Error	95% Confidence Interval	
			Lower Bound	Upper Bound
1	12.669	.501	11.666	13.672
2	12.913	.572	11.769	14.058

Pairwise Comparisons

Measure: MEASURE_1

(I) EE_Y	(J) EE_Y	Mean Difference (I-J)	Std. Error	Sig.[a]	95% Confidence Interval for Difference[a]	
					Lower Bound	Upper Bound
1	2	-.245	.368	508	-.981	.492
2	1	.245	368	.508	-.492	.981

Based on estimated marginal means

a Adjustment for multiple comparisons: Bonferroni.

3. PACIENTE * EE_Y

Measure: MEASURE_1

PACIENTE	EE_Y	Mean	Std Error	95% Confidence Interval	
				Lower Bound	Upper Bound
1	1	12.606	.697	11.212	14 001
	2	12.910	.795	11.318	14 502
2	1	12.731	.720	11 289	14 173
	2	12.917	822	11.271	14 563

TABLE 12 C
SPECTRAL TURBULENCE ANALYSIS OF TOTAL QRS COMPLEX
TWO-WAY REPEATED MEASURES ANOVA
GROUP1 VS GROUP 2
(SPECTRAL ENTROPY) Z-LEAD

Descriptive Statistics

	PACIENTE	Mean	Std. Deviation	N
EEZT	1	12 900	3.594	31
	2	13.428	3.524	29
	Total	13.155	3.540	60
EEZT_D	1	14 923	5.952	31
	2	13.797	5.772	29
	Total	14.378	5.844	60

Tests of Within-Subjects Contrasts

Measure: MEASURE_1

Source	EE_Z	Type III Sum of Squares	df	Mean Square	F	Sig.
EE_Z	Linear	42.849	1	42.849	3.257	.076
EE_Z * PACIENTE	Linear	20.486	1	20.486	1.557	217
Error(EE_Z)	Linear	763.118	58	13.157		

Tests of Between-Subjects Effects

Measure. MEASURE_1
Transformed Variable: Average

Source	Type III Sum of Squares	df	Mean Square	F	Sig.
Intercept	22700.808	1	22700.808	669.027	000
PACIENTE	2.683	1	2.683	.079	.780
Error	1968 004	58	33 931		

1. PACIENTE

Estimates

Measure: MEASURE_1

PACIENTE	Mean	Std. Error	95% Confidence Interval	
			Lower Bound	Upper Bound
1	13.911	.740	12.430	15.392
2	13.612	765	12.081	15 143

Pairwise Comparisons

Measure: MEASURE_1

(I) PACIENTE	(J) PACIENTE	Mean Difference (I-J)	Std. Error	Sig.[a]	95% Confidence Interval for Difference[a]	
					Lower Bound	Upper Bound
1	2	.299	1.064	.780	-1.831	2.429
2	1	-.299	1.064	.780	-2.429	1.831

Based on estimated marginal means

a. Adjustment for multiple comparisons: Bonferroni.

2. EE_Z

Estimates

Measure: MEASURE_1

EE_Z	Mean	Std. Error	95% Confidence Interval	
			Lower Bound	Upper Bound
1	13.164	.460	12.243	14.084
2	14.360	.758	12.843	15.876

Pairwise Comparisons

Measure: MEASURE_1

(I) EE_Z	(J) EE_Z	Mean Difference (I-J)	Std. Error	Sig.[a]	95% Confidence Interval for Difference[a]	
					Lower Bound	Upper Bound
1	2	-1.196	.663	.076	-2.522	.131
2	1	1.196	.663	.076	-.131	2.522

Based on estimated marginal means

a. Adjustment for multiple comparisons. Bonferroni.

3. PACIENTE * EE_Z

Measure: MEASURE_1

PACIENTE	EE_Z	Mean	Std. Error	95% Confidence Interval	
				Lower Bound	Upper Bound
1	1	12.900	.639	11.620	14.180
	2	14.923	1.054	12.814	17.032
2	1	13.428	.661	12.104	14.751
	2	13.797	1.089	11.616	15.977

TABLE 13
POWER SPECTRAL DENSITY OF TOTAL QRS COMPLEX
100-250 HZ INTERVAL
GROUP 1 VS GROUP 2
PSD(Ln) X LEAD

Descriptive Statistics

	ISQMN	Mean	Std. Deviation	N
PSD_TXB_LN	1	6.550106	1.127510	31
	2	6 219086	1.171648	29
	Total	6.390113	1.151399	60
PSD_TXD_LN	1	6.085932	1.129583	31
	2	6.284610	1.034701	29
	Total	6.181960	1.080232	60

Tests of Within-Subjects Contrasts

Measure: MEASURE_1

Source	PSD_X	Type III Sum of Squares	df	Mean Square	F	Sig.
PSD_X	Linear	1.191	1	1.191	11.661	.001
PSD_X * ISQMN	Linear	2.102	1	2.102	20.588	.000
Error(PSD_X)	Linear	5.922	58	.102		

Tests of Between-Subjects Effects

Measure: MEASURE_1
Transformed Variable: Average

Source	Type III Sum of Squares	df	Mean Square	F	Sig.
Intercept	4734.780	1	4734.780	1976 951	.000
ISQMN	.131	1	.131	.055	.816
Error	138.909	58	2.395		

1. ISQMN

Estimates

Measure: MEASURE_1

ISQMN	Mean	Std. Error	95% Confidence Interval	
			Lower Bound	Upper Bound
1	6.318	197	5 925	6.711
2	6 252	.203	5 845	6.659

Pairwise Comparisons

Measure: MEASURE_1

(I) ISQMN	(J) ISQMN	Mean Difference (I-J)	Std. Error	Sig.[a]	95% Confidence Interval for Difference[a]	
					Lower Bound	Upper Bound
1	2	6.617E-02	.283	.816	-.500	.632
2	1	-6.617E-02	.283	.816	-.632	.500

Based on estimated marginal means

a Adjustment for multiple comparisons. Bonferroni.

2. PSD_X

Estimates

Measure: MEASURE_1

PSD_X	Mean	Std. Error	95% Confidence Interval	
			Lower Bound	Upper Bound
1	6.385	.148	6.087	6.682
2	6.185	.140	5.905	6.466

Pairwise Comparisons

Measure. MEASURE_1

(I) PSD_X	(J) PSD_X	Mean Difference (I-J)	Std. Error	Sig.[a]	95% Confidence Interval for Difference[a]	
					Lower Bound	Upper Bound
1	2	.199*	.058	.001	8.248E-02	.316
2	1	-.199*	.058	.001	-.316	-8.248E-02

Based on estimated marginal means

*. The mean difference is significant at the .05 level.

a Adjustment for multiple comparisons: Bonferroni.

3. ISQMN * PSD_X

Measure: MEASURE_1

ISQMN	PSD_X	Mean	Std. Error	95% Confidence Interval	
				Lower Bound	Upper Bound
1	1	6.550	.206	6.137	6.963
	2	6.086	.195	5.696	6.476
2	1	6.219	.213	5.792	6.646
	2	6.285	.201	5.881	6.688

TABLE 13 B
POWER SPECTRAL DENSITY OF TOTAL QRS COMPLEX
100-250 HZ INTERVAL
GROUP 1 VS GROUP 2
PSD(Ln) Y LEAD

Descriptive Statistics

	ISQMN	Mean	Std. Deviation	N
PSD_TYB_LN	1	6.036303	1.171335	31
	2	6.112631	1.013771	29
	Total	6 073195	1.089429	60
PSD_TYD_LN	1	5.499435	1.375484	31
	2	6.060107	.983533	29
	Total	5.770427	1.225120	60

Tests of Within-Subjects Contrasts

Measure: MEASURE_1

Source	PSD_Y	Type III Sum of Squares	df	Mean Square	F	Sig.
PSD_Y	Linear	2.602	1	2 602	14.772	.000
PSD_Y * ISQMN	Linear	1.757	1	1.757	9.976	.003
Error(PSD_Y)	Linear	10.218	58	.176		

Tests of Between-Subjects Effects

Measure: MEASURE_1
Transformed Variable: Average

Source	Type III Sum of Squares	df	Mean Square	F	Sig.
Intercept	4211.005	1	4211.005	1701.259	.000
ISQMN	3.040	1	3.040	1.228	.272
Error	143 563	58	2.475		

1. ISQMN

Estimates

Measure. MEASURE_1

ISQMN	Mean	Std. Error	95% Confidence Interval	
			Lower Bound	Upper Bound
1	5.768	.200	5 368	6.168
2	6.086	.207	5.673	6 500

Pairwise Comparisons

Measure MEASURE_1

(I) ISQMN	(J) ISQMN	Mean Difference (I-J)	Std. Error	Sig.[a]	95% Confidence Interval for Difference[a]	
					Lower Bound	Upper Bound
1	2	-.318	.287	.272	-.894	.257
2	1	.318	.287	.272	-.257	.894

Based on estimated marginal means

a. Adjustment for multiple comparisons: Bonferroni.

2. PSD_Y

Estimates

Measure: MEASURE_1

PSD_Y	Mean	Std. Error	95% Confidence Interval	
			Lower Bound	Upper Bound
1	6.074	.142	5.791	6.358
2	5.780	.155	5.469	6.091

Pairwise Comparisons

Measure: MEASURE_1

(I) PSD_Y	(J) PSD_Y	Mean Difference (I-J)	Std. Error	Sig.[a]	95% Confidence Interval for Difference[a]	
					Lower Bound	Upper Bound
1	2	.295*	.077	.000	.141	.448
2	1	-.295*	.077	.000	-.448	-.141

Based on estimated marginal means

* The mean difference is significant at the .05 level.

a. Adjustment for multiple comparisons: Bonferroni.

3. ISQMN * PSD_Y

Measure MEASURE_1

ISQMN	PSD_Y	Mean	Std. Error	95% Confidence Interval	
				Lower Bound	Upper Bound
1	1	6.036	.197	5.642	6.431
	2	5.499	.216	5.067	5.932
2	1	6.113	.204	5.704	6.521
	2	6.060	.223	5.613	6.507

TABLE 13 C
POWER SPECTRAL DENSITY OF TOTAL QRS COMPLEX
100-250 HZ INTERVAL
GROUP 1 VS GROUP 2
PSD(Ln) Z LEAD

Descriptive Statistics

	ISQMN	Mean	Std. Deviation	N
PSD_TZB_LN	1	6.265784	.770026	31
	2	6.012621	1 057886	29
	Total	6 143422	921347	60
PSD_TZD_LN	1	6.039377	.710830	31
	2	6.042410	.783433	29
	Total	6 040843	740407	60

Tests of Within-Subjects Contrasts

Measure· MEASURE_1

Source	PSD_Z	Type III Sum of Squares	df	Mean Square	F	Sig.
PSD_Z	Linear	.290	1	.290	2.762	.102
PSD_Z * ISQMN	Linear	.492	1	492	4.690	.034
Error(PSD_Z)	Linear	6.081	58	.105		

Tests of Between-Subjects Effects

Measure. MEASURE_1
Transformed Vanable: Average

Source	Type III Sum of Squares	df	Mean Square	F	Sig.
Intercept	4445 697	1	4445.697	3420.371	.000
ISQMN	.469	1	.469	361	.551
Error	75.387	58	1 300		

1. ISQMN

Estimates

Measure· MEASURE_1

ISQMN	Mean	Std. Error	95% Confidence Interval	
			Lower Bound	Upper Bound
1	6 153	145	5 863	6 442
2	6.028	150	5.728	6 327

Pairwise Comparisons

Measure: MEASURE_1

(I) ISQMN	(J) ISQMN	Mean Difference (I-J)	Std. Error	Sig.[a]	95% Confidence Interval for Difference[a]	
					Lower Bound	Upper Bound
1	2	.125	.208	.551	-.292	.542
2	1	-.125	.208	.551	-.542	.292

Based on estimated marginal means

a. Adjustment for multiple comparisons: Bonferroni

2. PSD_Z

Estimates

Measure: MEASURE_1

PSD_Z	Mean	Std. Error	95% Confidence Interval	
			Lower Bound	Upper Bound
1	6.139	.119	5.901	6.377
2	6.041	.096	5.848	6.234

Pairwise Comparisons

Measure: MEASURE_1

(I) PSD_Z	(J) PSD_Z	Mean Difference (I-J)	Std. Error	Sig.[a]	95% Confidence Interval for Difference[a]	
					Lower Bound	Upper Bound
1	2	9.831E-02	.059	.102	-2.009E-02	.217
2	1	-9.831E-02	.059	.102	-.217	2.009E-02

Based on estimated marginal means

a. Adjustment for multiple comparisons: Bonferroni

3. ISQMN * PSD_Z

Measure: MEASURE_1

ISQMN	PSD_Z	Mean	Std. Error	95% Confidence Interval	
				Lower Bound	Upper Bound
1	1	6.266	.165	5.935	6.597
	2	6.039	.134	5.771	6.308
2	1	6.013	.171	5.671	6.355
	2	6.042	.139	5.765	6.320

TABLE 14
POWER SPECTRAL DENSITY OF TOTAL QRS COMPLEX
Very low Frequency 100-120 HZ INTERVAL
GROUP 1 VS GROUP 2
VLF(Ln) X LEAD

Descriptive Statistics

	ISQMN	Mean	Std. Deviation	N
VLF_XB_LN	1	5.991435	1.322705	31
	2	5.684934	1.262982	29
	Total	5.843293	1 292465	60
VLF_XD_LN	1	5.495135	1 257137	31
	2	5 784562	1 087100	29
	Total	5 635025	1.177162	60

Tests of Within-Subjects Contrasts

Measure MEASURE_1

Source	VLF_X	Type III Sum of Squares	df	Mean Square	F	Sig.
VLF_X	Linear	1.179	1	1.179	5.879	.018
VLF_X * ISQMN	Linear	2 661	1	2 661	13 269	.001
Error(VLF_X)	Linear	11.629	58	.201		

Tests of Between-Subjects Effects

Measure: MEASURE_1
Transformed Variable: Average

Source	Type III Sum of Squares	df	Mean Square	F	Sig.
Intercept	3947 966	1	3947.966	1379 225	000
ISQMN	2 184E-03	1	2.184E-03	.001	978
Error	166.022	58	2 862		

1. ISQMN

Estimates

Measure. MEASURE_1

ISQMN	Mean	Std Error	95% Confidence Interval	
			Lower Bound	Upper Bound
1	5 743	215	5 313	6 173
2	5 735	222	5 290	6 179

Pairwise Comparisons

Measure: MEASURE_1

(I) ISQMN	(J) ISQMN	Mean Difference (I-J)	Std. Error	Sig.[a]	95% Confidence Interval for Difference[a]	
					Lower Bound	Upper Bound
1	2	8.537E-03	.309	.978	-.610	.627
2	1	-8.537E-03	.309	.978	-.627	.610

Based on estimated marginal means

a. Adjustment for multiple comparisons: Bonferroni.

2. VLF_X

Estimates

Measure: MEASURE_1

VLF_X	Mean	Std. Error	95% Confidence Interval	
			Lower Bound	Upper Bound
1	5.838	.167	5.504	6.173
2	5.640	.152	5.335	5.944

Pairwise Comparisons

Measure: MEASURE_1

(I) VLF_X	(J) VLF_X	Mean Difference (I-J)	Std. Error	Sig.[a]	95% Confidence Interval for Difference[a]	
					Lower Bound	Upper Bound
1	2	.198*	.082	.018	3.460E-02	.362
2	1	-.198*	.082	.018	-.362	-3.460E-02

Based on estimated marginal means

* The mean difference is significant at the .05 level.

a. Adjustment for multiple comparisons. Bonferroni.

3. ISQMN * VLF_X

Measure: MEASURE_1

ISQMN	VLF_X	Mean	Std. Error	95% Confidence Interval	
				Lower Bound	Upper Bound
1	1	5.991	.232	5.526	6.457
	2	5.495	.212	5.072	5.919
2	1	5.685	.240	5.204	6.166
	2	5.785	.219	5.347	6.222

TABLE 14 B
POWER SPECTRAL DENSITY OF TOTAL QRS COMPLEX
Very low Frequency 100-120 HZ INTERVAL
GROUP 1 VS GROUP 2
VLF(Ln) Y-LEAD

Descriptive Statistics

	ISQMN	Mean	Std. Deviation	N
VLF_YB_LN	1	5 593052	1.255229	31
	2	5.605990	1.071229	29
	Total	5.599305	1.160080	60
VLF_YD_LN	1	4 900929	1.474348	31
	2	5.505314	1.092556	29
	Total	5.193048	1.328356	60

Tests of Within-Subjects Contrasts

Measure: MEASURE_1

Source	VLF_Y	Type III Sum of Squares	df	Mean Square	F	Sig.
VLF_Y	Linear	4.709	1	4.709	19.060	.000
VLF_Y * ISQMN	Linear	2.621	1	2.621	10 608	002
Error(VLF_Y)	Linear	14.328	58	.247		

Tests of Between-Subjects Effects

Measure MEASURE_1
Transformed Variable: Average

Source	Type III Sum of Squares	df	Mean Square	F	Sig.
Intercept	3497.022	1	3497 022	1238.984	.000
ISQMN	2 855	1	2.855	1 012	319
Error	163 705	58	2.822		

1. ISQMN

Estimates

Measure: MEASURE_1

ISQMN	Mean	Std. Error	95% Confidence Interval	
			Lower Bound	Upper Bound
1	5 247	.213	4 820	5.674
2	5.556	.221	5 114	5 997

Pairwise Comparisons

Measure: MEASURE_1

(I) ISQMN	(J) ISQMN	Mean Difference (I-J)	Std. Error	Sig.[a]	95% Confidence Interval for Difference[a]	
					Lower Bound	Upper Bound
1	2	- 309	.307	.319	-.923	.306
2	1	.309	.307	.319	-.306	.923

Based on estimated marginal means

a. Adjustment for multiple comparisons: Bonferroni

2. VLF_Y

Estimates

Measure: MEASURE_1

VLF_Y	Mean	Std. Error	95% Confidence Interval	
			Lower Bound	Upper Bound
1	5.600	.151	5.297	5.902
2	5.203	.168	4.866	5.540

Pairwise Comparisons

Measure. MEASURE_1

(I) VLF_Y	(J) VLF_Y	Mean Difference (I-J)	Std. Error	Sig.[a]	95% Confidence Interval for Difference[a]	
					Lower Bound	Upper Bound
1	2	.396*	.091	.000	.215	.578
2	1	-.396*	091	.000	-.578	-.215

Based on estimated marginal means

*. The mean difference is significant at the .05 level.

a. Adjustment for multiple comparisons: Bonferroni

3. ISQMN * VLF_Y

Measure: MEASURE_1

ISQMN	VLF_Y	Mean	Std. Error	95% Confidence Interval	
				Lower Bound	Upper Bound
1	1	5.593	.210	5 172	6.014
	2	4.901	.234	4.432	5.370
2	1	5.606	.217	5.171	6.041
	2	5.505	242	5.021	5 990

TABLE 14 C
POWER SPECTRAL DENSITY OF TOTAL QRS COMPLEX
Very low Frequency 100-120 HZ INTERVAL
GROUP 1 VS GROUP 2
VLF(Ln) Z-LEAD

Descriptive Statistics

	ISQMN	Mean	Std. Deviation	N
VLF_ZB_LN	1	5 734903	826967	31
	2	5.583403	1.149932	29
	Total	5.661678	.990512	60
VLF_ZD_LN	1	5 448871	.831894	31
	2	5.553931	.866690	29
	Total	5.499650	.843310	60

Tests of Within-Subjects Contrasts

Measure: MEASURE_1

Source	VLF_Z	Type III Sum of Squares	df	Mean Square	F	Sig.
VLF_Z	Linear	.746	1	.746	4.087	.048
VLF_Z * ISQMN	Linear	.493	1	.493	2.703	106
Error(VLF_Z)	Linear	10.583	58	.182		

Tests of Between-Subjects Effects

Measure: MEASURE_1
Transformed Variable: Average

Source	Type III Sum of Squares	df	Mean Square	F	Sig.
Intercept	3732.587	1	3732.587	2439.251	.000
ISQMN	1.616E-02	1	1.616E-02	.011	.919
Error	88.753	58	1.530		

1. ISQMN

Estimates

Measure: MEASURE_1

ISQMN	Mean	Std. Error	95% Confidence Interval	
			Lower Bound	Upper Bound
1	5.592	.157	5.277	5 906
2	5.569	.162	5.244	5 894

Pairwise Comparisons

Measure: MEASURE_1

(I) ISQMN	(J) ISQMN	Mean Difference (I-J)	Std. Error	Sig.[a]	95% Confidence Interval for Difference[a]	
					Lower Bound	Upper Bound
1	2	2.322E-02	.226	.919	-.429	.476
2	1	-2.322E-02	.226	.919	-.476	.429

Based on estimated marginal means

a Adjustment for multiple comparisons: Bonferroni.

2. VLF_Z

Estimates

Measure: MEASURE_1

VLF_Z	Mean	Std. Error	95% Confidence Interval	
			Lower Bound	Upper Bound
1	5.659	.129	5.402	5.917
2	5.501	.110	5.282	5.721

Pairwise Comparisons

Measure: MEASURE_1

(I) VLF_Z	(J) VLF_Z	Mean Difference (I-J)	Std. Error	Sig.[a]	95% Confidence Interval for Difference[a]	
					Lower Bound	Upper Bound
1	2	.158*	.078	.048	1.556E-03	.314
2	1	-.158*	.078	.048	-.314	-1.556E-03

Based on estimated marginal means

*. The mean difference is significant at the .05 level.

a. Adjustment for multiple comparisons: Bonferroni.

3. ISQMN * VLF_Z

Measure: MEASURE_1

ISQMN	VLF_Z	Mean	Std. Error	95% Confidence Interval	
				Lower Bound	Upper Bound
1	1	5.735	.179	5.377	6.093
	2	5.449	.152	5.144	5.754
2	1	5 583	.185	5.213	5.954
	2	5.554	.158	5 238	5 869

TABLE 15.
POWER SPECTRAL DENSITY OF TOTAL QRS COMPLEX
Low Frequency 120-150 HZ INTERVAL
GROUP 1 VS GROUP 2
LF(Ln) X-LEAD

Descriptive Statistics

	ISQMN	Mean	Std. Deviation	N
LF_XB_LN	1	5.331858	1.047484	31
	2	5.073555	1.121705	29
	Total	5.207012	1.082578	60
LF_XD_LN	1	5 065965	1 128528	31
	2	5.023997	1.170129	29
	Total	5.045680	1.139218	60

Tests of Within-Subjects Contrasts

Measure: MEASURE_1

Source	LF_X	Type III Sum of Squares	df	Mean Square	F	Sig.
LF_X	Linear	.745	1	.745	4.826	.032
LF_X * ISQMN	Linear	.351	1	351	2.270	.137
Error(LF_X)	Linear	8.959	58	.154		

Tests of Between-Subjects Effects

Measure: MEASURE_1
Transformed Variable: Average

Source	Type III Sum of Squares	df	Mean Square	F	Sig.
Intercept	3146.952	1	3146.952	1344.729	.000
ISQMN	.675	1	675	.289	.593
Error	135.732	58	2.340		

1. ISQMN

Estimates

Measure: MEASURE_1

ISQMN	Mean	Std. Error	95% Confidence Interval	
			Lower Bound	Upper Bound
1	5.199	194	4.810	5 588
2	5 049	201	4.647	5.451

Pairwise Comparisons

Measure: MEASURE_1

(I) ISQMN	(J) ISQMN	Mean Difference (I-J)	Std. Error	Sig.[a]	95% Confidence Interval for Difference[a]	
					Lower Bound	Upper Bound
1	2	.150	.279	593	- 409	.710
2	1	- 150	279	.593	-.710	409

Based on estimated marginal means

a. Adjustment for multiple comparisons: Bonferroni.

2. LF_X

Estimates

Measure: MEASURE_1

LF_X	Mean	Std. Error	95% Confidence Interval	
			Lower Bound	Upper Bound
1	5 203	.140	4.922	5.483
2	5.045	148	4 748	5.342

Pairwise Comparisons

Measure. MEASURE_1

(I) LF_X	(J) LF_X	Mean Difference (I-J)	Std. Error	Sig.[a]	95% Confidence Interval for Difference[a]	
					Lower Bound	Upper Bound
1	2	.158*	072	.032	1 401E-02	.301
2	1	-.158*	072	032	- 301	-1.401E-02

Based on estimated marginal means

* The mean difference is significant at the .05 level

a Adjustment for multiple comparisons: Bonferroni

3. ISQMN * LF_X

Measure. MEASURE_1

ISQMN	LF_X	Mean	Std. Error	95% Confidence Interval	
				Lower Bound	Upper Bound
1	1	5 332	.195	4.942	5.722
	2	5 066	206	4.653	5 479
2	1	5.074	201	4 671	5 476
	2	5 024	.213	4 597	5 451

TABLE 15 B
POWER SPECTRAL DENSITY OF TOTAL QRS COMPLEX
Low Frequency 120-150 HZ INTERVAL
GROUP 1 VS GROUP 2
LF(Ln) Y-LEAD

Descriptive Statistics

	ISQMN	Mean	Std Deviation	N
LF_YB_LN	1	4.679165	1.151748	31
	2	4.926797	1 035498	29
	Total	4.798853	1 094963	60
LF_YD_LN	1	4 403423	1 444346	31
	2	4.857886	1.049239	29
	Total	4.623080	1.278929	60

Tests of Within-Subjects Contrasts

Measure: MEASURE_1

Source	LF_Y	Type III Sum of Squares	df	Mean Square	F	Sig.
LF_Y	Linear	.890	1	.890	4.616	.036
LF_Y * ISQMN	Linear	.320	1	.320	1 662	.202
Error(LF_Y)	Linear	11.182	58	.193		

Tests of Between-Subjects Effects

Measure: MEASURE_1
Transformed Variable. Average

Source	Type III Sum of Squares	df	Mean Square	F	Sig
Intercept	2666.838	1	2666.838	1017.303	000
ISQMN	3 693	1	3 693	1.409	240
Error	152 046	58	2 621		

1. ISQMN

Estimates

Measure: MEASURE_1

ISQMN	Mean	Std. Error	95% Confidence Interval	
			Lower Bound	Upper Bound
1	4.541	206	4 130	4 953
2	4 892	.213	4 467	5 318

Pairwise Comparisons

Measure: MEASURE_1

(I) ISQMN	(J) ISQMN	Mean Difference (I-J)	Std. Error	Sig.[a]	95% Confidence Interval for Difference[a]	
					Lower Bound	Upper Bound
1	2	-.351	.296	.240	- 943	.241
2	1	.351	296	.240	-.241	.943

Based on estimated marginal means

a Adjustment for multiple comparisons Bonferroni

2. LF_Y

Estimates

Measure MEASURE_1

LF_Y	Mean	Std. Error	95% Confidence Interval	
			Lower Bound	Upper Bound
1	4.803	.142	4 519	5 087
2	4.631	164	4.303	4.959

Pairwise Comparisons

Measure: MEASURE_1

(I) LF_Y	(J) LF_Y	Mean Difference (I-J)	Std. Error	Sig.[a]	95% Confidence Interval for Difference[a]	
					Lower Bound	Upper Bound
1	2	.172*	.080	036	1.177E-02	333
2	1	-.172*	.080	036	-.333	-1 177E-02

Based on estimated marginal means

*. The mean difference is significant at the 05 level.

a Adjustment for multiple comparisons Bonferroni.

3. ISQMN * LF_Y

Measure: MEASURE_1

ISQMN	LF_Y	Mean	Std. Error	95% Confidence Interval	
				Lower Bound	Upper Bound
1	1	4 679	.197	4 285	5 074
	2	4 403	228	3 947	4 860
2	1	4.927	.204	4 519	5.335
	2	4 858	236	4 386	5 330

TABLE 15 C
POWER SPECTRAL DENSITY OF TOTAL QRS COMPLEX
Low Frequency 120-150 HZ INTERVAL
GROUP 1 VS GROUP 2
LF(Ln) Z-LEAD

Descriptive Statistics

	ISQMN	Mean	Std. Deviation	N
LF_ZB_LN	1	5 160674	842584	31
	2	4.693883	1 021506	29
	Total	4 935058	954743	60
LF_ZD_LN	1	4 872606	885035	31
	2	4.760503	877365	29
	Total	4.818423	.875664	60

Tests of Within-Subjects Contrasts

Measure: MEASURE_1

Source	LF_Z	Type III Sum of Squares	df	Mean Square	F	Sig
LF_Z	Linear	.367	1	.367	1.825	.182
LF_Z * ISQMN	Linear	.942	1	.942	4 682	.035
Error(LF_Z)	Linear	11.675	58	.201		

Tests of Between-Subjects Effects

Measure: MEASURE_1
Transformed Variable. Average

Source	Type III Sum of Squares	df	Mean Square	F	Sig.
Intercept	2845.104	1	2845 104	1966.975	.000
ISQMN	2 511	1	2 511	1.736	.193
Error	83.893	58	1.446		

1. ISQMN

Estimates

Measure: MEASURE_1

ISQMN	Mean	Std. Error	95% Confidence Interval	
			Lower Bound	Upper Bound
1	5 017	153	4 711	5.322
2	4.727	158	4 411	5.043

Pairwise Comparisons

Measure: MEASURE_1

(I) ISQMN	(J) ISQMN	Mean Difference (I-J)	Std. Error	Sig.[a]	95% Confidence Interval for Difference[a]	
					Lower Bound	Upper Bound
1	2	.289	.220	.193	-.150	.729
2	1	-.289	.220	.193	-.729	.150

Based on estimated marginal means

a Adjustment for multiple comparisons: Bonferroni

2. LF_Z

Estimates

Measure. MEASURE_1

LF_Z	Mean	Std. Error	95% Confidence Interval	
			Lower Bound	Upper Bound
1	4.927	.121	4.686	5.169
2	4.817	.114	4.589	5.044

Pairwise Comparisons

Measure: MEASURE_1

(I) LF_Z	(J) LF_Z	Mean Difference (I-J)	Std. Error	Sig.[a]	95% Confidence Interval for Difference[a]	
					Lower Bound	Upper Bound
1	2	.111	.082	.182	-5.333E-02	.275
2	1	-.111	.082	.182	-.275	5.333E-02

Based on estimated marginal means

a. Adjustment for multiple comparisons. Bonferroni.

3. ISQMN * LF_Z

Measure: MEASURE_1

ISQMN	LF_Z	Mean	Std. Error	95% Confidence Interval	
				Lower Bound	Upper Bound
1	1	5.161	.168	4.825	5.496
	2	4.873	.158	4.556	5.189
2	1	4.694	.173	4.347	5.041
	2	4.761	.164	4.433	5.088

TABLE 16
POWER SPECTRAL DENSITY OF TOTAL QRS COMPLEX
High Frequency 150-250 HZ INTERVAL
GROUP 1 VS GROUP 2
HF(Ln) X-LEAD

Descriptive Statistics

	ISQMN	Mean	Std. Deviation	N
HF_XB_LN	1	3 460248	1.035533	31
	2	3 285259	1.030423	29
	Total	3 375670	1.028066	60
HF_XD_LN	1	3.329377	1.095498	31
	2	3.535907	1.123367	29
	Total	3 429200	1 104516	60

Tests of Within-Subjects Contrasts

Measure MEASURE_1

Source	HF_X	Type III Sum of Squares	df	Mean Square	F	Sig.
HF_X	Linear	.107	1	.107	.891	.349
HF_X * ISQMN	Linear	1.090	1	1.090	9.035	004
Error(HF_X)	Linear	7 000	58	.121		

Tests of Between-Subjects Effects

Measure: MEASURE_1
Transformed Variable. Average

Source	Type III Sum of Squares	df	Mean Square	F	Sig.
Intercept	1387 859	1	1387 859	637 652	000
ISQMN	7.452E-03	1	7 452E-03	003	.954
Error	126 238	58	2 177		

1. ISQMN

Estimates

Measure: MEASURE_1

ISQMN	Mean	Std. Error	95% Confidence Interval	
			Lower Bound	Upper Bound
1	3 395	187	3 020	3 770
2	3 411	194	3 023	3 798

Pairwise Comparisons

Measure: MEASURE_1

(I) ISQMN	(J) ISQMN	Mean Difference (I-J)	Std. Error	Sig [a]	95% Confidence Interval for Difference[a]	
					Lower Bound	Upper Bound
1	2	-1.577E-02	.270	.954	-.555	524
2	1	1.577E-02	.270	.954	- 524	555

Based on estimated marginal means

a. Adjustment for multiple comparisons: Bonferroni

2. HF_X

Estimates

Measure MEASURE_1

HF_X	Mean	Std. Error	95% Confidence Interval	
			Lower Bound	Upper Bound
1	3.373	.133	3.106	3 640
2	3 433	143	3.146	3.719

Pairwise Comparisons

Measure: MEASURE_1

(I) HF_X	(J) HF_X	Mean Difference (I-J)	Std. Error	Sig [a]	95% Confidence Interval for Difference[a]	
					Lower Bound	Upper Bound
1	2	-5 989E-02	.063	349	-.187	6.714E-02
2	1	5.989E-02	.063	.349	-6 714E-02	.187

Based on estimated marginal means

a. Adjustment for multiple comparisons: Bonferroni

3. ISQMN * HF_X

Measure. MEASURE_1

ISQMN	HF_X	Mean	Std. Error	95% Confidence Interval	
				Lower Bound	Upper Bound
1	1	3.460	186	3.089	3 832
	2	3 329	.199	2.931	3.728
2	1	3 285	192	2 901	3.669
	2	3 536	206	3 124	3 948

TABLE 16 B
POWER SPECTRAL DENSITY OF TOTAL QRS COMPLEX
High Frequency 150-250 HZ INTERVAL
GROUP 1 VS GROUP 2
HF(Ln) Y-LEAD

Descriptive Statistics

	ISQMN	Mean	Std Deviation	N
HF_YB_LN	1	3.244148	1 243355	31
	2	3.409379	.803119	29
	Total	3 324010	1 048381	60
HF_YD_LN	1	2 962687	1.246854	31
	2	3.636683	.791067	29
	Total	3.288452	1 096743	60

Tests of Within-Subjects Contrasts

Measure MEASURE_1

Source	HF_Y	Type III *Sum of* Squares	df	Mean Square	F	Sig
HF_Y	Linear	2.197E-02	1	2.197E-02	.118	.732
HF_Y * ISQMN	Linear	1.939	1	1.939	10.419	002
Error(HF_Y)	Linear	10 794	58	186		

Tests of Between-Subjects Effects

Measure. MEASURE_1
Transformed Variable: Average

Source	Type III Sum of Squares	df	Mean Square	F	Sig
Intercept	1315 831	1	1315.831	647 835	.000
ISQMN	5 276	1	5.276	2 598	.112
Error	117.805	58	2 031		

1. ISQMN

Estimates

Measure: MEASURE_1

ISQMN	Mean	Std Error	95% Confidence Interval	
			Lower Bound	Upper Bound
1	3 103	.181	2 741	3.466
2	3.523	187	3 148	3 898

Pairwise Comparisons

Measure MEASURE_1

(I) ISQMN	(J) ISQMN	Mean Difference (I-J)	Std. Error	Sig [a]	95% Confidence Interval for Difference [a]	
					Lower Bound	Upper Bound
1	2	-.420	.260	112	- 941	102
2	1	.420	.260	.112	- 102	.941

Based on estimated marginal means

a. Adjustment for multiple comparisons: Bonferroni.

2. HF_Y

Estimates

Measure: MEASURE_1

HF_Y	Mean	Std. Error	95% Confidence Interval	
			Lower Bound	Upper Bound
1	3.327	.136	3.054	3 599
2	3.300	.136	3.028	3 572

Pairwise Comparisons

Measure· MEASURE_1

(I) HF_Y	(J) HF_Y	Mean Difference (I-J)	Std. Error	Sig [a]	95% Confidence Interval for Difference [a]	
					Lower Bound	Upper Bound
1	2	2.708E-02	.079	732	-.131	.185
2	1	-2.708E-02	079	732	-.185	.131

Based on estimated marginal means

a Adjustment for multiple comparisons: Bonferroni

3. ISQMN * HF_Y

Measure· MEASURE_1

ISQMN	HF_Y	Mean	Std. Error	95% Confidence Interval	
				Lower Bound	Upper Bound
1	1	3.244	189	2.865	3.623
	2	2.963	189	2.585	3 341
2	1	3.409	196	3.018	3 801
	2	3 637	195	3.246	4 028

TABLE 16 C
POWER SPECTRAL DENSITY OF TOTAL QRS COMPLEX
High Frequency 150-250 HZ INTERVAL
GROUP 1 VS GROUP 2
HF(Ln) Z-LEAD

Descriptive Statistics

	ISQMN	Mean	Std Deviation	N
HF_ZB_LN	1	3 213865	.843679	31
	2	3.318062	.860419	29
	Total	3.264227	.846183	60
HF_ZD_LN	1	3.339755	.719950	31
	2	3.206369	.865767	29
	Total	3.275285	.789807	60

Tests of Within-Subjects Contrasts

Measure: MEASURE_1

Source	HF_Z	Type III Sum of Squares	df	Mean Square	F	Sig.
HF_Z	Linear	1.510E-03	1	1 510E-03	.011	916
HF_Z * ISQMN	Linear	423	1	423	3 168	.080
Error(HF_Z)	Linear	7.741	58	.133		

Tests of Between-Subjects Effects

Measure: MEASURE_1
Transformed Variable: Average

Source	Type III Sum of Squares	df	Mean Square	F	Sig.
Intercept	1281.340	1	1281.340	1048.518	.000
ISQMN	6.383E-03	1	6.383E-03	005	.943
Error	70 879	58	1 222		

1. ISQMN

Estimates

Measure: MEASURE_1

ISQMN	Mean	Std. Error	95% Confidence Interval	
			Lower Bound	Upper Bound
1	3 277	140	2 996	3 558
2	3 262	145	2.972	3 553

Pairwise Comparisons

Measure MEASURE_1

(I) ISQMN	(J) ISQMN	Mean Difference (I-J)	Std. Error	Sig.[a]	95% Confidence Interval for Difference[a]	
					Lower Bound	Upper Bound
1	2	1.459E-02	.202	.943	-.390	.419
2	1	-1.459E-02	.202	.943	-.419	.390

Based on estimated marginal means

a Adjustment for multiple comparisons: Bonferroni.

2. HF_Z

Estimates

Measure: MEASURE_1

HF_Z	Mean	Std. Error	95% Confidence Interval	
			Lower Bound	Upper Bound
1	3.266	.110	3.046	3.486
2	3.273	.103	3.068	3.478

Pairwise Comparisons

Measure: MEASURE_1

(I) HF_Z	(J) HF_Z	Mean Difference (I-J)	Std. Error	Sig.[a]	95% Confidence Interval for Difference[a]	
					Lower Bound	Upper Bound
1	2	-7.099E-03	.067	.916	-.141	.126
2	1	7.099E-03	.067	.916	-.126	.141

Based on estimated marginal means

a Adjustment for multiple comparisons: Bonferroni

3. ISQMN * HF_Z

Measure: MEASURE_1

ISQMN	HF_Z	Mean	Std. Error	95% Confidence Interval	
				Lower Bound	Upper Bound
1	1	3.214	.153	2.908	3.520
	2	3.340	.143	3.054	3.625
2	1	3.318	.158	3.001	3.635
	2	3.206	.147	2.911	3.501

TABLE 17

CORRELATION COEFFICIENT (r) BEFORE AND AFTER DYPIRIDAMOLE CHALLANGE.
X Y Z LEADS.
GROUP 1 VS GROUP 2

Group Statistics

	ISQMN	N	Mean	Std Deviation	Std. Error Mean
CCX	1	31	331032	276040	4.95783E-02
	2	29	.666207	276682	5.13786E-02
CCY	1	31	.337484	.283798	5.09717E-02
	2	29	.666207	273501	5 07879E-02
CCZ	1	31	.427097	233584	4.19529E-02
	2	29	.716207	.231230	4.29383E-02

Independent Samples Test

		Levene's Test for Equality of Variances		t-test for Equality of Means						
									95% Confidence Interval of the Difference	
		F	Sig.	t	df	Sig (2-tailed)	Mean Difference	Std Error Difference	Lower	Upper
CCX	Equal variances assumed	374	.543	-4.695	58	.000	-.3352	7 1E-02	-.478083	-.192266
	Equal variances not assumed			-4.694	57.716	.000	-.3352	7.1E-02	-.478110	-.192240
CCY	Equal variances assumed	.996	.322	-4.563	58	000	-.3287	7.2E-02	-.472937	-.184509
	Equal variances not assumed			-4.568	57 945	.000	- 3287	7 2E-02	-.472760	-.184686
CCZ	Equal variances assumed	1 565	216	-4.814	58	000	-.2891	6 0E-02	- 409317	- 168903
	Equal variances not assumed			-4.816	57.807	000	- 2891	6.0E-02	-.409284	- 168936

TABLE 18
CROSSTABS BETWEEN FFT ANALYSIS AND NUCLEAR MEDICINE

GPOFFT * ISQMN Crosstabulation

Count

		ISQMN		
		1	2	Total
GPOFFT	1	28	5	33
	2	3	24	27
Total		31	29	60

Chi-Square Tests

	Value	df	Asymp. Sig. (2-sided)	Exact Sig (2-sided)	Exact Sig (1-sided)
Pearson Chi-Square	32 333[b]	1	.000		
Continuity Correction[a]	29 448	1	000		
Likelihood Ratio	36 202	1	.000		
Fisher's Exact Test				000	.000
Linear-by-Linear Association	31 794	1	.000		
N of Valid Cases	60				

a. Computed only for a 2x2 table

b 0 cells (.0%) have expected *count less than 5* The minimum expected count is 13.05.

Symmetric Measures

		Value	Asymp. Std Error[a]	Approx T[b]	Approx. Sig
Nominal by Nominal	Contingency Coefficient	592			.000
Measure of Agreement	Kappa	.732	.088	5.686	.000
N of Valid Cases		60			

a Not assuming the null hypothesis

b Using the asymptotic standard error assuming the null hypothesis

TABLE 19
CROSSTABS BETWEEN PSD(+) ANALYSIS AND NUCLEAR MEDICINE

GPOF * ISQMN Crosstabulation

Count

		ISQMN		
		1	2	Total
psd +	1	28	9	37
	2	3	20	23
Total		31	29	60

Chi-Square Tests

	Value	df	Asymp. Sig. (2-sided)	Exact Sig. (2-sided)	Exact Sig (1-sided)
Pearson Chi-Square	22 280[b]	1	.000		
Continuity Correction[a]	19 843	1	000		
Likelihood Ratio	24 245	1	.000		
Fisher's Exact Test				.000	.000
Linear-by-Linear Association	21.909	1	.000		
N of Valid Cases	60				

a Computed only for a 2x2 table

b 0 cells (.0%) have expected count less than 5 The minimum expected count is 11.12.

Symmetric Measures

		Value	Asymp. Std Error[a]	Approx. T[b]	Approx. Sig
Nominal by Nominal	Contingency Coefficient	.520			000
Measure of Agreement	Kappa	.597	.102	4.720	000
N of Valid Cases		60			

a Not assuming the null hypothesis.

b Using the asymptotic standard error assuming the null hypothesis.

Risk Estimate

	Value	95% Confidence Interval	
		Lower	Upper
Odds Ratio for GPOF (1 / 2)	20 741	4 978	86.417
For cohort ISQMN = 1	5 802	1 988	16.930
For cohort ISQMN = 2	280	155	505
N of Valid Cases	60		